

**UNITED STATES
DEPARTMENT OF THE INTERIOR
GEOLOGICAL SURVEY**

**SOURCEBOOK OF LOCATIONS OF GEOPHYSICAL SURVEYS IN TUNNELS
AND HORIZONTAL HOLES INCLUDING RESULTS OF SEISMIC-REFRACTION SURVEYS,
RAINIER MESA, AQUEDUCT MESA, AND AREA 16, NEVADA TEST SITE**

Open-File Report 83-399

1983

This report is preliminary and has not been reviewed
for conformity with U.S. Geological Survey editorial standards.
Any use of trade names is for descriptive purposes only
and does not imply endorsement by the USGS

**Prepared by the U.S. Geological Survey
for the
Nevada Operations Office
U.S. Department of Energy
Interagency Agreement (DE-AI08-76DP00474)
and the
Defense Nuclear Agency**

*Copies of this Open-file Report
may be purchased from*

*Open-File Services Section
Branch of Distribution
U.S. Geological Survey
Box 25425, Federal Center
Denver, Colorado 80225*

PREPAYMENT IS REQUIRED

*Price information will be published
in the monthly listing
"New Publications of the Geological Survey"*

FOR ADDITIONAL INFORMATION

CALL: Commercial: (303)234-5888

FTS: 234-5888

CONTENTS

	Page
Abstract	1
Introduction.....	1
Acknowledgments.....	5
Location maps.....	5
Horizontal drill-hole measurements.....	6
Seismic-refraction measurements.....	6
Shoshone Mountain.....	15
Area 16 tunnel complex.....	16
U16a.03 (Double Play).....	16
U16a.04 (Ming Vase).....	16
U16a.05 (Diamond Dust).....	16
U16a.06 (Diamond Mine).....	17
Aqueduct and Rainier Mesa tunnel complexes.....	17
T-tunnel complex-Aqueduct Mesa.....	17
U12T.01 (Mint Leaf).....	17
U12t.02 (Diamond Skulls).....	17
U12t.03 (Husky Pup).....	17
B-tunnel complex--Rainier Mesa.....	17
E-tunnel complex--Rainier Mesa.....	18
U12e.10 (Dorsal Fin).....	18
U12e.11 (Diesel Train).....	18
U12e.12 (Hudson Moon).....	18
U12e.14 (Dido Queen).....	19
U12e.15-17 (pre-Mine Dust).....	19
U12e.18 (Dining Car).....	19
U12e.20 (Hybla Gold).....	19
G-tunnel complex--Rainier Mesa.....	19
U12g.05 (Deep Well).....	19
U12g.06 (Red Hot).....	20
U12g.07 (Door Mist).....	20
U12g.09 (Cypress).....	20
U12g.10 (Camphor).....	20
N-tunnel complex--Rainier Mesa.....	22
U12n.02 (Midi Mist).....	22
U12n.03.....	22
U12n.04 (Hudson Seal).....	22
U12n.05 (Misty North).....	22
U12n.06 (Diana Mist).....	25
U12n.07 (Husky Ace).....	25
U12n.08 (Ming Blade).....	25
U12n.09 (Hybla Fair--SPLAT).....	25
U12n.10 (Mighty Epic).....	25
U12n.10A (Diablo Hawk).....	25
U12n.11 (Miners Iron).....	26
Summary of refraction data.....	26
References cited.....	84

ILLUSTRATIONS

[Plates are in pocket]

- Plate 1.--Map of U16a tunnel complex showing locations where geophysical surveys were made.
 2.--Map of U12t tunnel complex showing locations where geophysical surveys were made.
 3.--Map of U12e tunnel complex showing locations where geophysical surveys were made.
 4.--Map of U12g tunnel complex showing locations where geophysical surveys were made.
 5.--Map of U12n tunnel complex showing locations where geophysical surveys were made.

	Page
Figure 1.--Index map of the Nevada Test Site showing locations of main tunnel testing areas.....	2
2.--Index map showing location of tunnel complexes in Rainier and Aqueduct Mesas.....	3
3.--Index map showing location of Area 16 tunnel complex...	4
4.--Graph showing results of seismic shooting in the U12t.03 drift.....	8
5.--Illustrations showing details of explosive source used to generate shear waves.....	9
6.--Photograph of typical shear-wave records obtained in tunnels.....	10
7.--Graph showing results of seismic shooting in the U16a.03 drift.....	33
8.--Graph showing results of seismic shooting in the U16a.04 drift.....	34
9.--Graph showing results of postshot seismic shooting in the U16a.04 reentry drift.....	35
10.--Graph showing results of seismic shooting in the U16a.05 drift.....	36
11.--Graph showing results of seismic shooting in drill holes radial from the cavity in U16a.06 drift.....	37
12.--Graph showing results of seismic shooting in the U12t.01 drift.....	38
13.--Graph showing results of seismic shooting in the U12t.02 drift.....	39
14.--Graph showing results of seismic shooting in the U12e.10 drift.....	40
15.--Graph showing results of seismic shooting in the U12e.11 drift.....	41
16.--Graph showing results of seismic shooting in the U12e.12 drift.....	42
17.--Graph showing results of postshot seismic shooting in the U12e.12 reentry drift.....	43
18.--Graph showing results of seismic shooting in the U12e.14 drift.....	44
19.--Graph showing results of seismic shooting in the U12e.14 HFR drift.....	45
20.--Graph showing results of seismic shooting in the U12e.16 drift.....	46

ILLUSTRATIONS--Continued

	Page
Figure 21.--Graph showing results of seismic shooting in the U12e.17 drift.....	47
22.--Graph showing results of seismic shooting in the U12e.18 drift.....	48
23.--Graph showing results of repeat seismic shooting in the U12e.18 drift.....	49
24.--Graph showing results of seismic shooting in the U12e.20 main drift.....	50
25.--Graph showing results of seismic shooting in the U12e.20 auxiliary drift.....	51
26.--Graph showing results of seismic shooting in the U12g.07 drift.....	52
27.--Graph showing results of combining seismic-refraction data in the U12g.09 drift.....	53
28.--Graph showing results of seismic shooting in the U12g.09 reentry drift.....	54
29.--Graph showing results of seismic shooting in the U12g.10 drift (December 1968).....	55
30.--Graph showing results of seismic shooting in the U12g.10 drift (April 17, 1970).....	56
31.--Graph showing results of seismic shooting in the U12g.10 drift (March 1971).....	57
32.--Graph showing results of postshot seismic shooting in the U12g.10 reentry drift.....	58
33.--Map showing locations where geophysical surveys were made in connection with the U12n.10A (Diablo Hawk) event, U12n tunnel complex.....	23
34.--Graph showing results of seismic shooting in the U12n.02 drift.....	59
35.--Graph showing results of seismic shooting in the U12n.02 hook drift.....	60
36.--Graph showing results of seismic shooting in the U12n.03 drift.....	61
37.--Graph showing results of seismic shooting in the U12n.04 drift.....	62
38.--Graph showing results of seismic shooting in the U12n.05 drift.....	63
39.--Graph showing results of seismic shooting in the U12n.06 drift.....	64
40.--Graph showing results of seismic shooting in the U12n.07 drift.....	65
41.--Graph showing results of seismic shooting in the U12n.08 drift (January 31, 1974).....	66
42.--Graph showing results of additional seismic shooting in the U12n.08 drift (February 16, 1974).....	67
43.--Graph showing results of original seismic shooting in the U12n.10 main drift.....	68
44.--Graph showing results of seismic shooting in the U12n.10 bypass drift.....	69
45.--Graph showing results of seismic shooting in the U12n.10A main drift.....	70

ILLUSTRATIONS--Continued

	Page
Figure 46.--Graph showing results of seismic shooting in the U12n.10A bypass drift (July 1976).....	71
47.--Graph showing results of repeat seismic shooting in the U12n.10A bypass drift (October 1976).....	72
48.--Graph showing results of seismic shooting in the U12n.10A cable access drift.....	73
49.--Graph showing results of seismic shooting in the U12n.10A interface reentry and EMP drifts.....	74
50.--Graph showing results of seismic shooting in the U12n.10A G drift.....	75
51.--Graph showing results of seismic shooting in the U12n.10A AB reentry (Boeing) drift.....	76
52.--Graph showing results of seismic shooting in the U12n.10A interface drift, post-Mighty Epic.....	77
53.--Graph showing results of seismic shooting in the U12n.10A structures reentry drift (June 1980).....	78
54.--Graph showing results of shear-wave recording in the U12n.10A structures reentry drift (June 1980).....	79
55.--Graph showing results of shear (SV)- and compressional-wave survey obtained in the Boeing reentry drift.....	80
56.--Graph showing results of shear-wave (SH) survey obtained in the Boeing reentry drift.....	81
57.--Graph showing results of seismic shooting in the U12n.11 main drift.....	82
58.--Graph showing results of seismic shooting in the U12n.11 bypass drift.....	83
59.--Relative frequency histograms of (a) 23 compressional and (b) 17 shear velocities obtained near the WP of tunnel events.....	29
60.--Relative frequency histograms of Young's and bulk moduli calculated from shear and compressional velocities for 17 tunnel events.....	30
61.--Relative frequency histograms of shear modulus and Poisson's ratio calculated from shear and compressional velocities for 17 tunnel events.....	31

TABLES

Table 1.--Velocities and elastic constants of rock behind low-velocity layer, flat face, Red Hot and Deep Well cavities.....	21
2.--Geophysical surveys made in the U12n.10A complex.....	24
3.--Average velocity and dynamic moduli data obtained near the WP of tunnel events.....	28

**SOURCEBOOK OF LOCATIONS OF GEOPHYSICAL SURVEYS IN TUNNELS AND
HORIZONTAL HOLES INCLUDING RESULTS OF SEISMIC REFRACTION SURVEYS,
RAINIER MESA, AQUEDUCT MESA, AND AREA 16, NEVADA TEST SITE**

By

R. D. Carroll and J. E. Kibler

ABSTRACT

Seismic refraction surveys have been obtained sporadically in tunnels in zeolitized tuff at the Nevada Test Site since the late 1950's. Commencing in 1967 and continuing to date (1982), extensive measurements of shear- and compressional-wave velocities have been made in five tunnel complexes in Rainier and Aqueduct Mesas and in one tunnel complex in Shoshone Mountain. The results of these surveys to 1980 are compiled in this report. In addition, extensive horizontal drilling was initiated in 1967 in connection with geologic exploration in these tunnel complexes for sites for nuclear weapons tests. Seismic and electrical surveys were conducted in the majority of these holes. The type and location of these tunnel and borehole surveys are indexed in this report.

Synthesis of the seismic refraction data indicates a mean compressional-wave velocity near the nuclear device point (WP) of 23 tunnel events of 2,430 m/s (7,970 f/s) with a range of 1,846-2,753 m/s (6,060-9,030 f/s). The mean shear-wave velocity of 17 tunnel events is 1,276 m/s (4,190 f/s) with a range of 1,140-1,392 m/s (3,740-4,570 f/s). Experience indicates that these velocity variations are due chiefly to the extent of fracturing and (or) the presence of partially saturated rock in the region of the survey.

INTRODUCTION

The U.S. Geological Survey (USGS) has been obtaining seismic velocity and electrical resistivity measurements for several years in connection with geologic exploration programs in tunnels and horizontal holes at the Nevada Test Site (NTS), Nye County, Nev. These tunnels, located in Areas 12 and 16 (fig. 1), are primarily used for the siting of nuclear weapon tests. Area 12 has been the more intensely utilized region, consisting of five tunnel complexes in Rainier and Aqueduct Mesas (fig. 2). The Area 16 tunnel complex which is located in Shoshone Mountain, and has not been utilized since 1971, is shown on figure 3.

This report deals chiefly with the measurements made by the senior author dating from the Midi Mist event in 1967 through the Miners Iron event in October 1980. Prior to 1967, events were detonated in the B- and E-tunnel

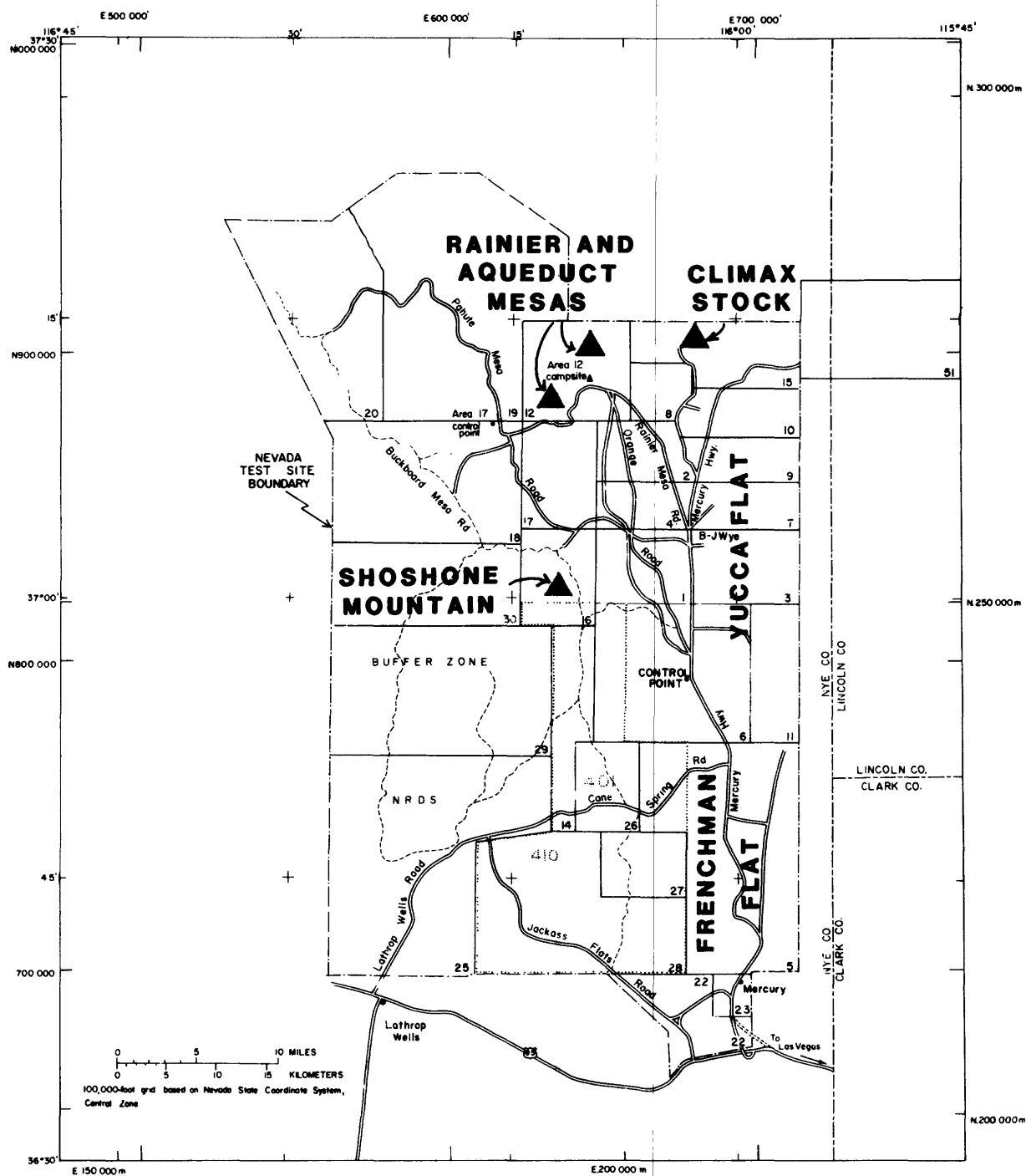


Figure 1.--Index map of the Nevada Test Site showing locations of main tunnel testing areas.

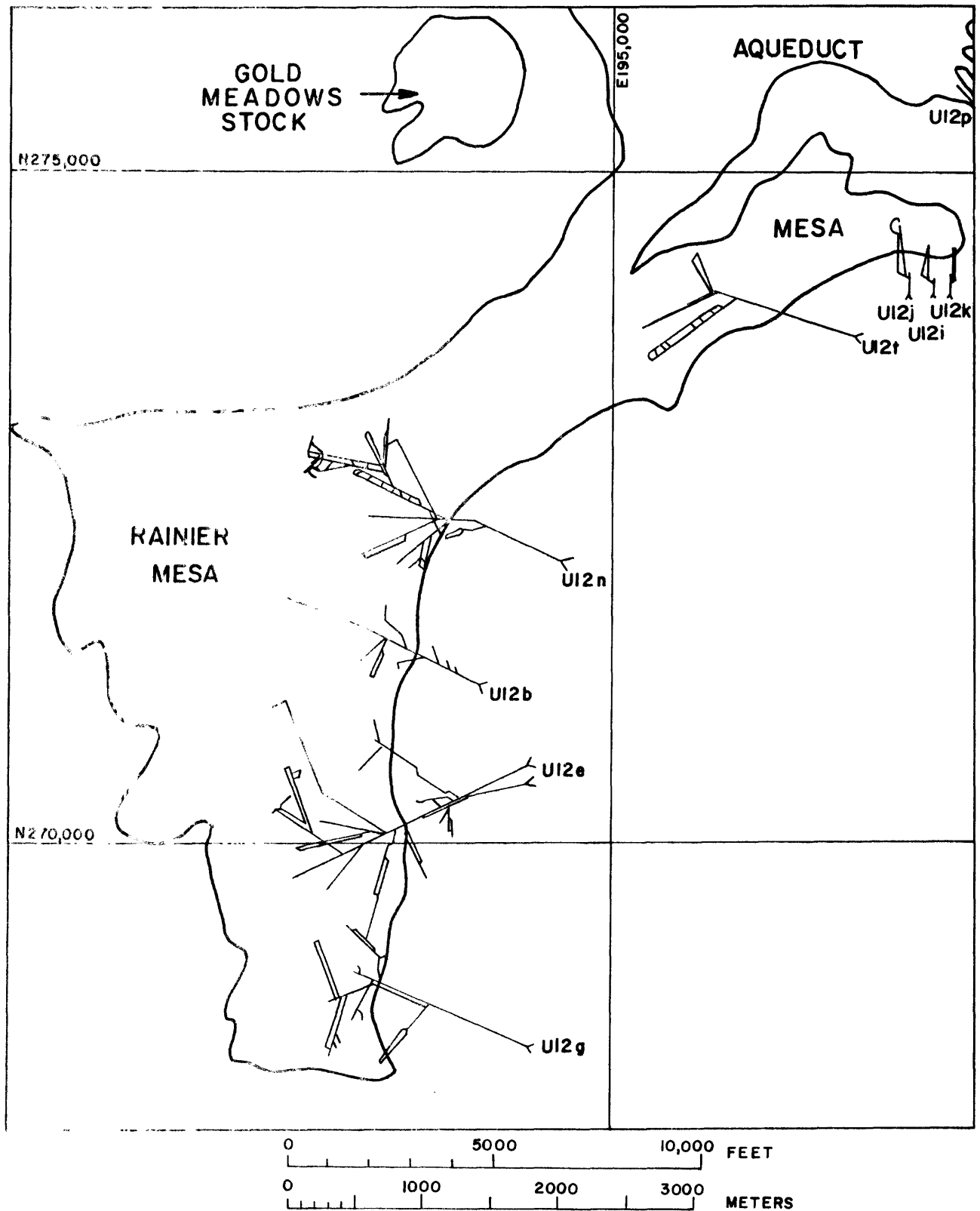


Figure 2 --Index map showing location of tunnel complexes in Rainier and Aqueduct Mesas.

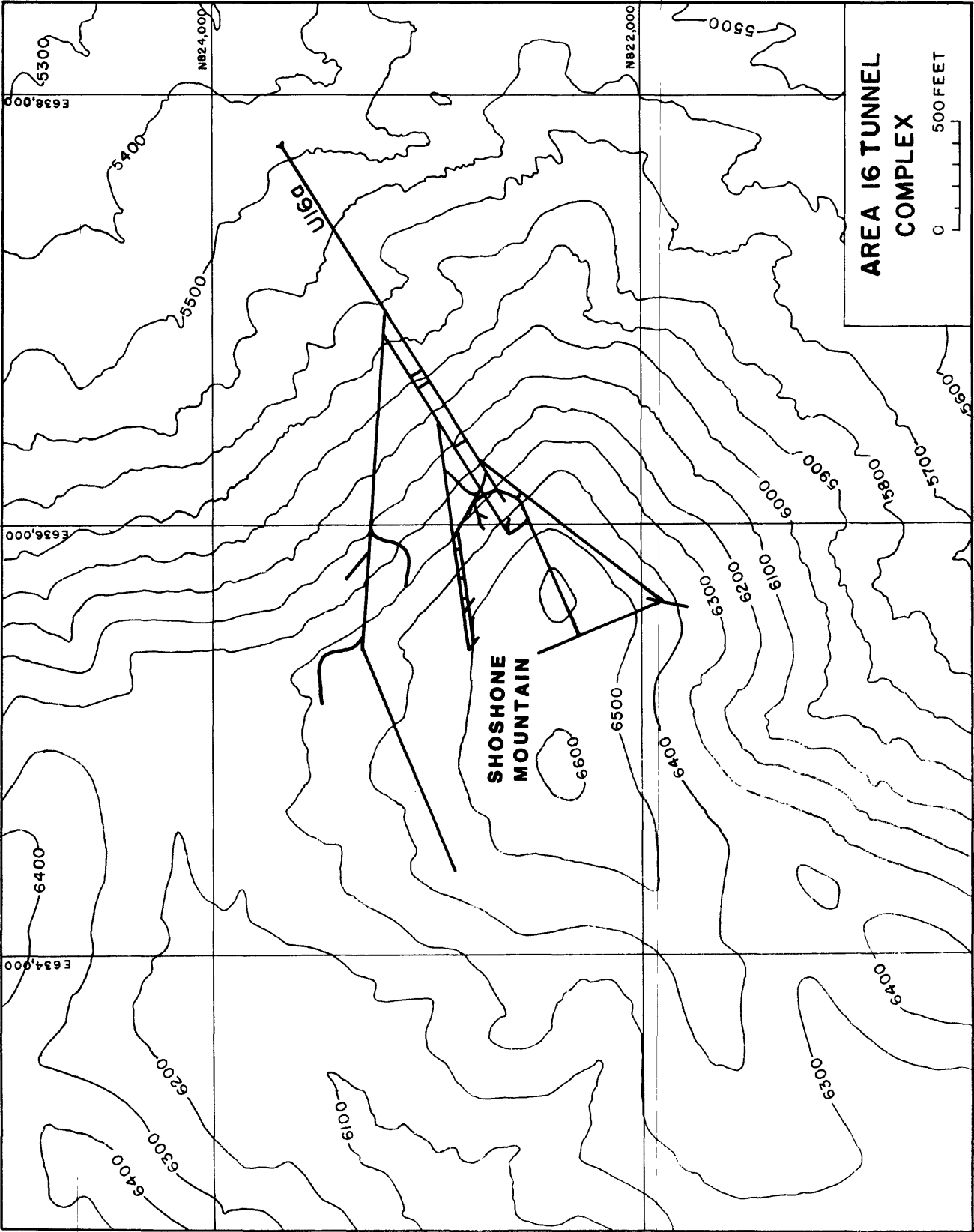


Figure 3.--Index map showing location of Area 16 tunnel complex (contour interval, 100 ft).

complexes in Rainier Mesa and in some Area 16 tunnels. Where pertinent, references to the applicable geophysical surveys obtained for these earlier events will be cited or extracted. In Aqueduct Mesa, four earlier tunnel complexes (I, J, K, P) were driven. Nuclear events in 1962 were located in J and K tunnels. No seismic refraction surveys were performed by the USGS in these tunnels and thus no references to geophysical surveys in those complexes are reported here.

Tunnels in other areas at the NTS are rare and consist of three locations in granite in the Climax stock, Area 15 (Hardhat, Piledriver, and Tiny Tot), and one in tuff in Yucca Flat (Snubber). Data for these locations are not reported here. In addition, a number of special geophysical investigations were made in several of the tunnel complexes and drill holes to be discussed. These will be mentioned where appropriate but the data are not reported here.¹

This report is meant to serve chiefly as an index of type and location of geophysical measurements made in horizontal exploratory holes and seismic refraction measurements made in tunnels. It is further meant to serve as a reference for shear- and compressional-velocity experience acquired in the tunnels and in this regard is directed more toward those in the nuclear testing community than to the general earth science reader. The significance of seismic velocity to containment has been discussed elsewhere (Carroll and Cunningham, 1980). The integration of the geophysical data with other geologic measurements for a typical nuclear event may be found in the literature (U.S. Geological Survey, 1978; 1979; 1982). All of the nuclear events associated with the data in this report were announced events of low yield (less than 20 kt).

Acknowledgments

The majority of the data reported here were collected by the USGS on behalf of the Defense Nuclear Agency. Discussions, support, and encouragement from J. W. LaComb of that agency are gratefully acknowledged. Over the time period discussed in this report, individuals from the Defense Nuclear Agency and Reynolds Electric and Engineering Company (REECO) provided unqualified support. Notable among these were J. Witz of REECO and M. J. Cunningham, formerly of the USGS.

LOCATION MAPS

The locations where geophysical surveys have been made are shown on maps of each tunnel complex (pls. 1-5, in pocket). On these figures, intervals where geophysical surveys were run are shown by dotted lines along individual tunnels (capital letters) or drill holes (lower-case letters). The specifics on the types of surveys run are listed in a table on the map.

¹Such data, where mentioned as not included in this report, are available in the U.S. Geological Survey files in Denver, Colorado.

In several tunnels, acceleration measurements were made by detonating a fixed weight of explosives and measuring amplitudes of arrivals at accelerometers mounted at varying distances on the tunnel rib. These studies attempted to determine the variation of the seismic attenuation in different regions. The locations where such measurements were made are listed in tables on the accompanying plates for each tunnel as "accel." The data for these measurements are not included in this report.

Surveys in drill holes are located and listed chronologically in lower case letters in a separate table on each map. In those horizontal drill holes wherein a sonic logging tool was pumped down the hole to obtain the velocity data, the survey is described as "sonic" in the descriptive column of the table. In those instances where a geophone was pumped down the hole and velocity determined by an explosive source at the hole collar, the survey is described as "seismic" in the descriptive column of the table.

In some areas the density of drill holes is so great that individual holes could not be plotted clearly at the map scales used. Consequently, these areas are shown shaded.

Designations, such as CS 4+45 used in this report, refer to construction stations in the tunnel complexes in accordance with surveying practice and are measured in English units. To convert to meters, multiply 445 by 0.3048.

HORIZONTAL DRILL-HOLE MEASUREMENTS

Horizontal drilling was initiated by DNA for geologic exploration in 1967 in the Area 16 tunnel complex and the first deep hole was drilled to 616.6 m (2,023 ft) in 1968. Since that time there has been an extensive drilling program utilizing horizontal exploratory holes in excess of 300 m (984 ft) to determine the geology and the media properties. Geophysical measurements made in these holes consist of resistivity and sonic logs and seismic surveys utilizing inhole geophones and dynamite or air-gun energy sources detonated at the hole collars. The exploration rationale for those measurements and the techniques of measurement have been reported in detail in the literature (Carroll and Cunningham, 1980).

SEISMIC-REFRACTION MEASUREMENTS

Seismic-refraction measurements in the tunnels in Rainier Mesa have been reported since the initial Rainier event in 1957 (U.S. Geological Survey, 1958). Systematic and extensive measurements were initiated in 1967 when testing in tunnels was accelerated. The initial interest in acquiring seismic velocity was in providing compressional velocity for event measurement instrumentation. Compressional velocity later became highly significant in defining possible zones of rock wherein air-filled voids approach levels considered inadequate for site engineering purposes (Carroll and Cunningham, 1980). The primary area of interest in these measurements is most often the region within a hundred meters or so of the WP.

Prior to, and including, the Cypress event (Feb. 2, 1969), the refraction measurements were made with an Electrotech portable seismic refraction unit (Portaseis, Mod SM-1). Measurements thereafter were made using an SIE RS-4 refraction unit.

The layout of the seismic line has varied depending upon the geometry of the tunnel and the purposes of the studies. The general seismic configuration now used most frequently is illustrated on figure 4. It consists of three spreads of 12 geophones, each spaced on 6.1-m (20-ft) centers. One overlap geophone is used on each line resulting in a total geophone-to-geophone spread length of 201 m (660 ft). Shotpoints are located at both ends of the three-spread line and also at the ends of the individual spreads.

Shot holes are drilled (1.5-2.4 m or 5-8 ft) in the invert with a jackleg drill and charges consisting of one-half to three sticks of dynamite are used to obtain the compressional velocity. The seismic noise level is relatively high in the tunnels due chiefly to ventilation and compressed air lines and construction activity.

Initial attempts to obtain the shear velocity in tunnels were based on obtaining the dynamic moduli of the tuff to further characterize the media. Recent studies indicate that the shear velocity is highly diagnostic of the range of effects near a nuclear explosion in tuff (Carroll, 1982). In 1967, the first attempts were made to obtain shear waves in the tunnels based on a modification of a technique described by Cook (1965). This method involves the use of detonating cord coiled on the back of aluminum plates (fig. 5). The technique has been found to consistently generate excellent shear waves. A typical record is shown on figure 6. The shear waves generated in this fashion have been found to be of the SV type regardless of which side of the trench the plate is located. Shear waves of the SH variety have been generated in the tunnels by transverse hammer impacts. Mechanical impact has not generally been used as an energy source, however, because of the low amplitudes generated at the ranges of interest. Therefore the SV mode has been recorded exclusively in the work reported here with the exception of the survey made in the Boeing drift reentry (fig. 56).

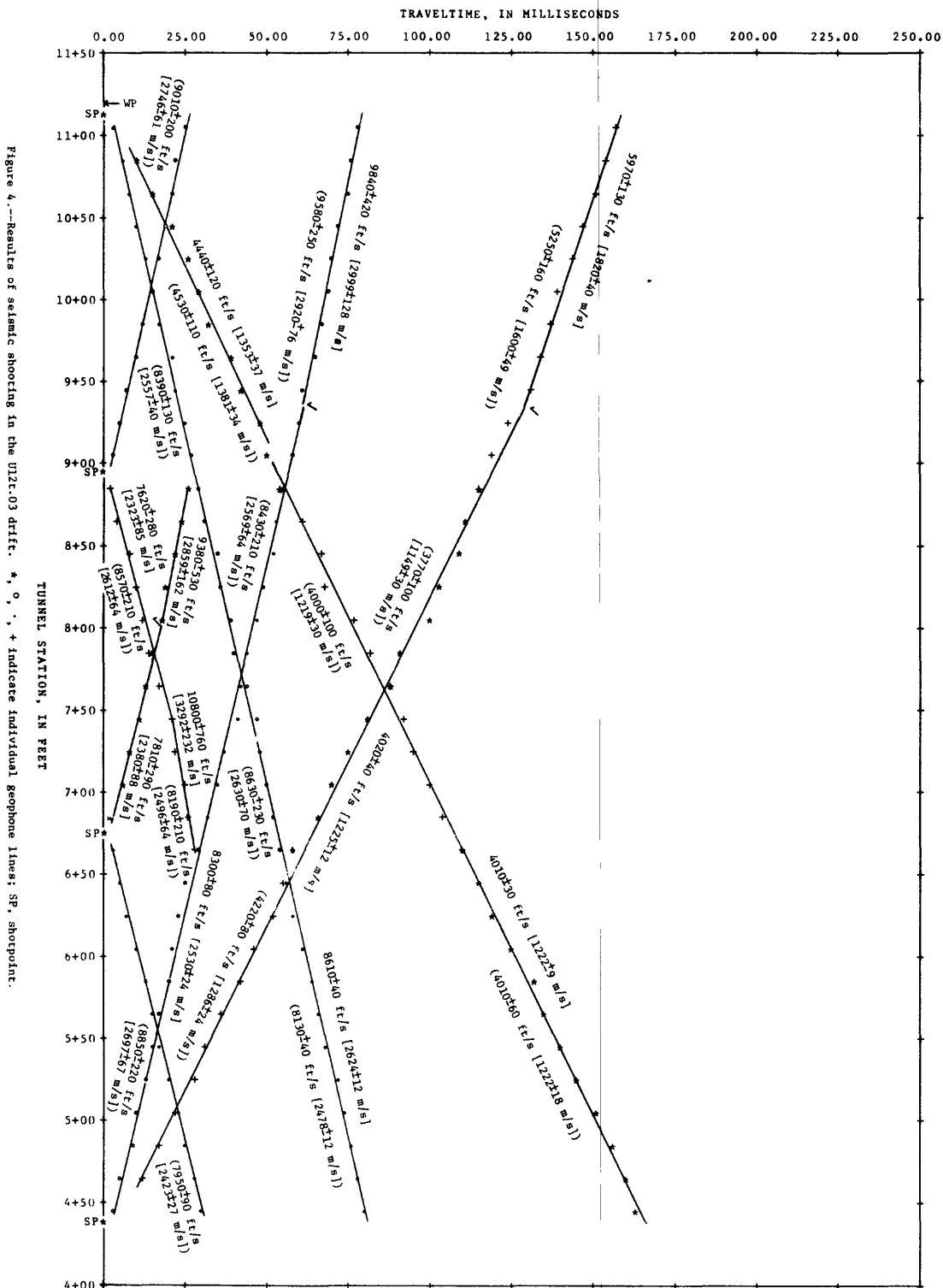
The use of a small dynamite charge taped to the back of a 15-cm (6-in.) square rock-bolt plate has replaced the detonating-cord method because of the greater ease in preparing charges. The shear wave generated by this method is adequate although occasionally not as free of noise as the detonating-cord technique. The shear- and compressional-wave velocities have been used for the calculation of the dynamic moduli listed on the various travel-time plots included in this report. The density assumed in these calculations is $1.9 \pm 0.05 \text{ g/cm}^3$ ($119 \pm 3 \text{ lb/f/s}$), a figure that may be considered fairly representative of the in situ bulk density of the tuff (Brethauer and others, 1980).

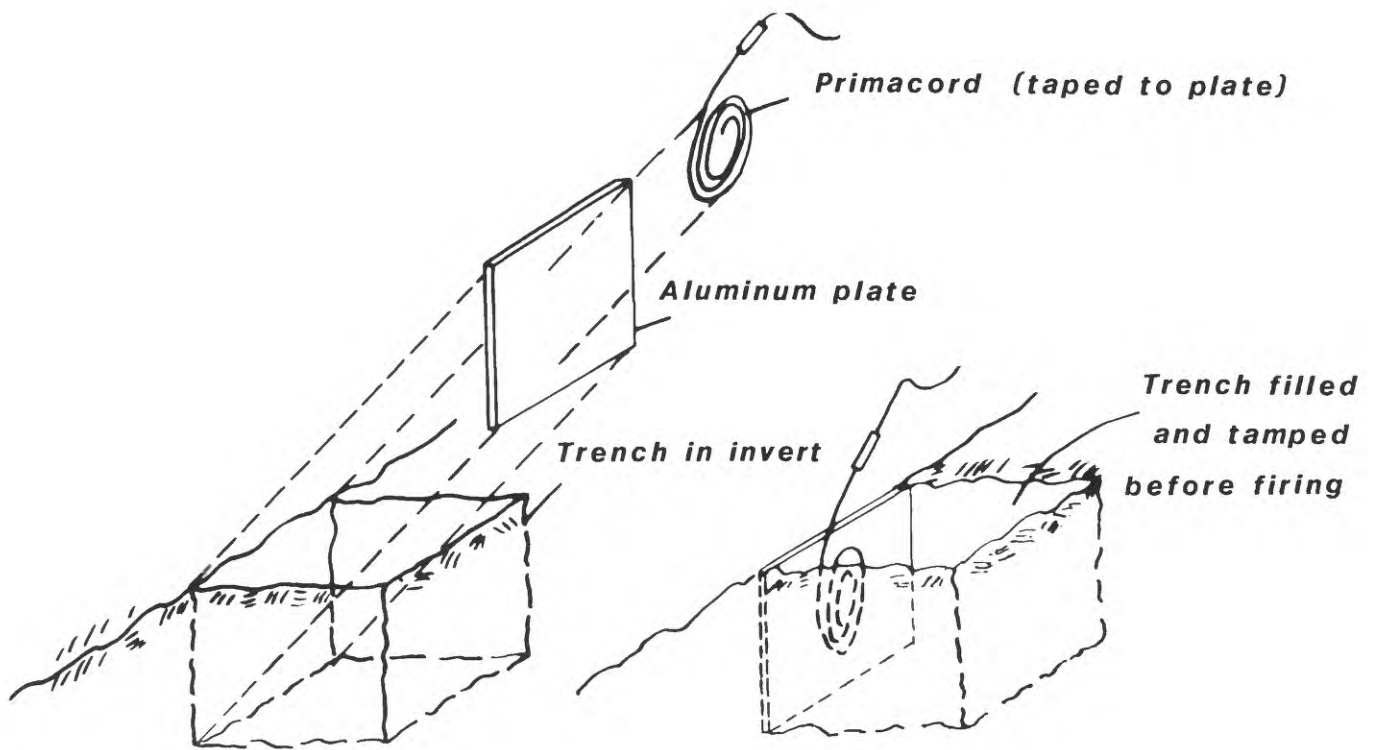
The standard errors of the slope of the regression lines shown on figure 4 are not usually listed in reporting the results of seismic refraction surveys. The procedure was initiated for the refraction surveys in tunnels in an attempt to more fully quantify the velocity data for comparative purposes. This arose because of the need for assessing the meaning of differences in velocity in pre- and postshot studies as well as the need to evaluate velocity in terms of previous experience for containment purposes.

(Based on an assumed rock specific gravity of 1.90±0.05)

INTERVAL (feet) ^{1/}	COMPRESSIONAL VELOCITY (m/s)	SHEAR VELOCITY (m/s)	CHARACTERISTIC COMPRESSIONAL IMPEDANCE (10 ⁶ mks Rayls)	CHARACTERISTIC SHEAR IMPEDANCE (10 ⁶ mks Rayls)	POISSON'S RATIO	YOUNG'S MODULUS (kbar)	BULK MODULUS (kbar)	SHEAR MODULUS (kbar)
11+05 - 9+05	2624± 12	1353± 37	4.99±0.13	2.57±0.10	0.32±0.01	91.8±4.8	84.5±7.7	34.8±2.1
9+05 - 4+45	2624± 12	1222± 9	4.99±0.13	2.32±0.06	0.36±0.00	77.3±2.5	93.0±3.6	28.4±0.9
4+45 - 9+25	2530± 24	1225± 12	4.81±0.13	2.33±0.07	0.35±0.01	76.8±3.1	83.6±4.5	28.5±0.9
9+45 - 11+05	2999±128	1820± 40	5.70±0.29	3.46±0.12	0.21±0.04	152.1±16.3	87.0±16.2	62.9±3.2

1/ meters = 0.3048 x feet



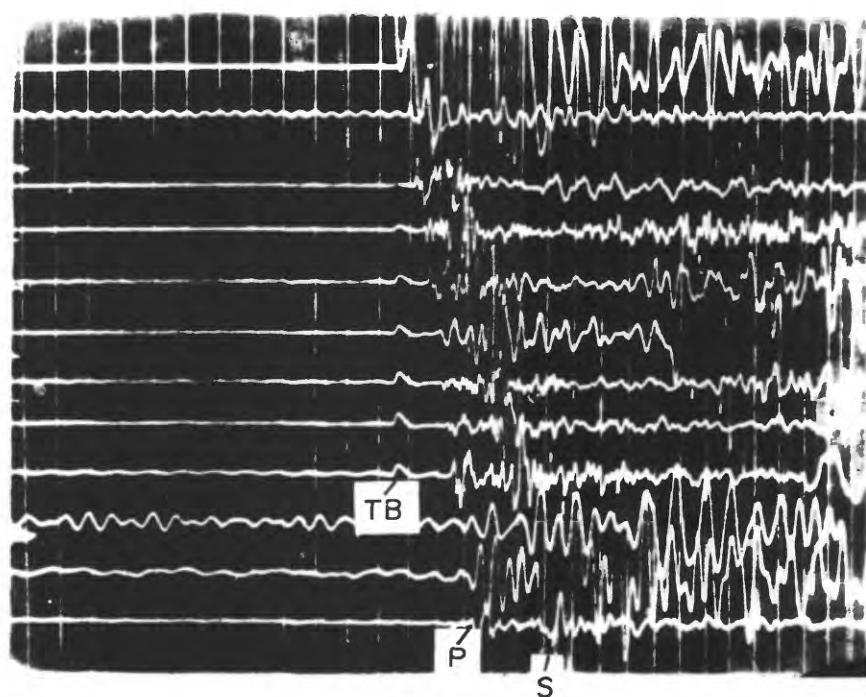


(a)

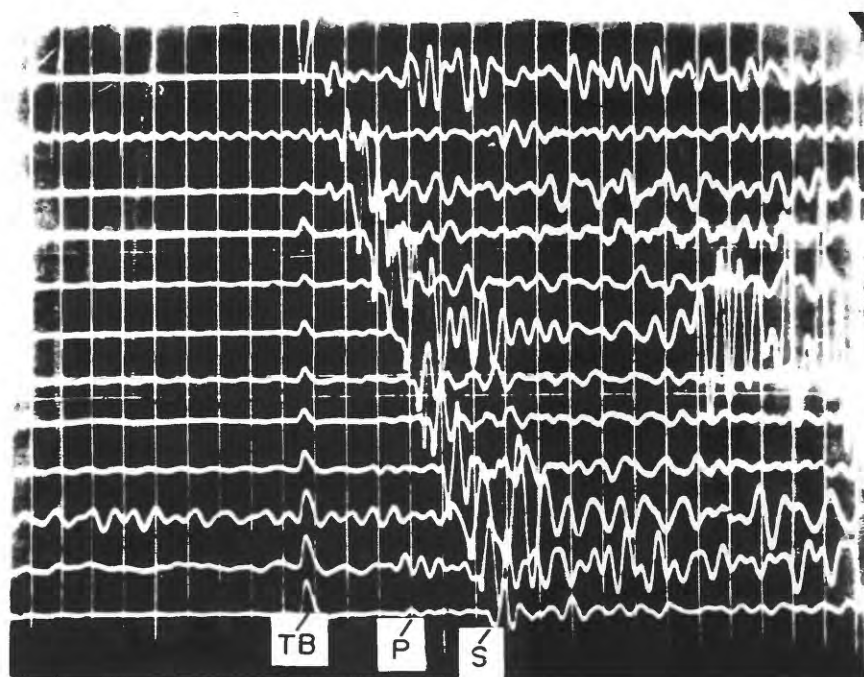


(b)

Figure 5.--Details of explosive source used to generate shear waves. (a) Method of emplacing charges. (b) Expended aluminum plate showing imprint of primacord charge.



(a)



(b)

Figure 6.--Typical shear-wave records obtained in tunnels. (a) Record obtained with dynamite charge, (b) record obtained with shear-wave technique. TB=timebreak, P=compressional wave, S=shear wave, timing lines=10 milliseconds, geophone spacing=6 m (20 ft).

The standard error of the slope (S) is obtained from the equation (Ostle, 1960, p. 127):

$$S^2 = \frac{\sum_{i=1}^n (Y_i - \hat{Y}_i)^2}{(n-2) \sum_{i=1}^n (X_i - \bar{X})^2}$$

where,

Y_i = distance from shotpoint to ith geophone,

\hat{Y}_i = distance to ith geophone calculated from regression equation,

n = number of geophones,

X_i = arrival time at ith geophone, and

\bar{X} = mean of arrival times.

Confidence intervals of estimation of S may be obtained from the t-test with n-2 degrees of freedom. The upper and lower bounds (L) of the velocity (b) at, for example, the 95 percent confidence limit are given by,

$$L = b \pm t_{(0.05)(n-2)} S$$

where,

t follows the t-distribution for (n-2) degrees of freedom.

The above treatment of the refraction data utilizes the traveltime as the independent variable and the geophone offset as the dependent variable. Although this is the reverse of the situation applicable to the usual traveltime plot, additional statistical refinements are not considered warranted given the accuracy involved in the field measurement.

The standard errors listed on the traveltime plots are for an infinite population and do not take into account the reduced sample size occasioned by a finite number of geophones. The differences are not considered significant. The standard error of the velocity is about 10 percent higher for a standard 12 geophone refraction line as opposed to a line with an infinite number of geophones. Thus, using a 12-geophone array, for example, the upper and lower bounds (L) of velocity (b) with standard error (S) using the above equation become:

$L = b \pm 1.18S$ for 68 percent confidence,

$L = b \pm 2.44S$ for 95 percent confidence,

$L = b \pm 2.83S$ for 99 percent confidence.

A further statistic of interest is the comparison of two velocities (b_1 , b_2) which can be made using the t-test (Ostle, 1960, p. 129),

$$t = \frac{b_1 - b_2}{\alpha}$$

where

$$\alpha^2 = \left[\frac{\sum_{i=1}^{n_1} (Y_i - \hat{Y}_i)^2 + \sum_{j=1}^{n_2} (Y_j - \hat{Y}_j)^2}{(n_1 + n_2 - 4)} \right] \left[\frac{1}{\sum_{i=1}^{n_1} (X_i - \bar{X}_1)^2} + \frac{1}{\sum_{j=1}^{n_2} (X_j - \bar{X}_2)^2} \right].$$

The listed variables have their meanings as before except that there are now two data sets (i, j) with probably different means (\bar{X}_1, \bar{X}_2) and possibly a different number of geophones (n_1, n_2). The t-distribution in this case has ($n_1 + n_2 - 4$) degrees of freedom.

Unfortunately, the standard error and associated statistics can frequently be misleading because they represent a measure of the precision of the velocity determination but not necessarily the accuracy of repeated surveys. The standard error of velocity derived from individual seismic lines can occasionally be 1 percent or less, a result that the experienced geophysicist would find highly optimistic as a measure of accuracy. Thus, one must frequently resort to empiricism when a comparison of two velocities by the above equation indicates they are significantly different because of an inordinately low value of S in one or both velocities. Such empiricism frequently consists of examining reverse spreads for consistency in velocity differences on both legs of the traveltime plot when comparing one survey with another, or in requiring the change in velocity be consistently different in a region by some fixed percent before accepting the premise that the velocities differ. It is our present feeling that, given $1/2$ -millisecond timing and adequate care in planting of geophones, repeat surveys of compressional velocity should conservatively be viewed to be no less than 5 percent accurate. Thus, upper and lower bounds (L) on S, taken at the 95-percent confidence limits, which support less than 5 percent uncertainty in velocity should be used with caution in velocity comparisons.

The dynamic moduli listed on each individual survey were derived by the standard equations involving the measured shear- and compressional-wave velocities and assumed density. The errors listed for the velocity data are standard errors of the slope of the least-squares regression line of distance and time-of-arrival. These errors have been propagated through the appropriate sensitivity equations to yield the errors for the individual moduli. The equations utilized in calculating the moduli and impedance are well known (Dobrin, 1976, p. 36):

Young's Modulus

$$E = \frac{V_p^2 (1 - \sigma - 2\sigma^2) \rho}{1 - \sigma}$$

Shear Modulus

$$G = \rho V_s^2$$

Bulk Modulus

$$K = \frac{E}{3(1-2\sigma)}$$

Poisson's Ratio

$$\sigma = \frac{0.5 (V_p/V_s)^2 - 1}{(V_p/V_s)^2 - 1}$$

Shear-wave Impedance

$$I_p = \rho V_p$$

Compressional-wave Impedance

$$I_s = \rho V_s$$

where

E=Young's modulus
 V_p =compressional-wave velocity
 σ =Poisson's ratio
 ρ =density
 G =shear modulus
 V_s =shear-wave velocity
 K =bulk modulus

The equations involving the propagation of error in the measured velocities and density are less frequently used. The propagated errors in the dynamic moduli and impedances are derived from the partial differentiation of the above equation with respect to the two measured velocities and the assumed density. Thus, the errors in the moduli and impedances in the table on figure 4 are given by:

(a) Error in Young's modulus= S_e

$$S_e^2 = \left(\frac{V_p^2 (1-\sigma-2\sigma^2) S_\rho}{1-\sigma} \right)^2 + \left(\frac{2V_p (1-\sigma-2\sigma^2) \rho S_{Vp}}{1-\sigma} \right)^2 + \left(\frac{2V_p^2 \rho \sigma (\sigma-2) S_\sigma}{(1-\sigma)^2} \right)^2$$

(b) Error in bulk modulus= S_k

$$S_k^2 = \left(\frac{S_e}{3(1-2\sigma)} \right)^2 + \left(\frac{2E S_\sigma}{3(1-2\sigma)^2} \right)^2$$

(c) Error in shear modulus= S_g

$$S_g^2 = (V_s^2 S_\rho)^2 + (2\rho V_s S_{Vs})^2$$

(d) Error in Poisson's ratio= S_σ

$$S_\sigma^2 = \left(\frac{(V_p/V_s^2) S_{vp}}{(V_p^2/V_s^2 - 1)^2} \right)^2 + \left(\frac{-(V_p^2/V_s^3) S_{vs}}{(V_p^2/V_s^2 - 1)^2} \right)^2$$

(e) Error in compressional impedance= S_{ip}

$$S_{ip}^2 = (V_p S_\rho)^2 + (\rho S_{vp})^2$$

(f) Error in shear impedance= S_{is}

$$S_{is}^2 = (V_s S_\rho)^2 + (\rho S_{vs})^2$$

where

S_{vp} =standard error of compressional velocity

S_{vs} =standard error of shear velocity

S_ρ =standard error of density (=0.05 g/cm³, 3 lb/ft³).

The above equations for the errors in the Young's and bulk moduli are not strictly the correct equations for propagation of error in these quantities because they involve the use of a calculated value (Poisson's ratio) rather than only measured values. They were originally derived because the derivations were more tractable than the equations using measured values. The equations for propagated error in the Young's and bulk moduli involving only the measured quantities of velocity and the assumed density are given below. For small standard errors they do not yield results significantly different from those obtained using the equations previously given.

$$\begin{aligned} (a) \quad S_e^2 &= \left[\frac{(3V_p^2 V_s^2 - 4V_s^4)}{(V_p^2 - V_s^2)} S_\rho \right]^2 \\ &+ \left[\frac{\rho(V_p^2 - V_s^2) (6V_p V_s^2) - \rho(3V_p^2 V_s^2 - 4V_s^4) 2V_p}{(V_p^2 - V_s^2)^2} \right]^2 S_{vp}^2 \\ &+ \left[\frac{\rho(V_p^2 - V_s^2) (6V_p^2 V_s - 16V_s^3) + 2V_{sp} (3V_p^2 V_s^2 - 4V_s^4)}{(V_p^2 - V_s^2)^2} \right]^2 S_{vs}^2 \end{aligned}$$

$$(b) \quad S_k^2 = (2\rho V_p S_{vp})^2 + \left(\frac{8}{3} \rho V_s S_{vs}\right)^2 + \left[(V_p^2 - \frac{4}{3} V_s^2) S_p \right]^2$$

Some note should also be taken of the method of generally depicting velocities on the time-distance plots accompanying this report. For example, on figure 4 the velocities for each individual refraction line are listed below the line. In addition, where applicable, the least-squares velocity of the composite of the three individual spreads is also listed above and at the end of the line. Where the composite line indicates a break in velocity this is indicated by a "/" and the velocity is listed above the regression line for the segment of line in question. An example of this occurs on the shear-wave velocities derived from 4+50 to 11+00. Velocities derived by least-squares regression are listed in both metric and English units.

The long offset traveltime plots obtained from the shotpoint near 4+40 (fig. 4) suggest refracted arrivals on both the shear and compressional modes. Such refractions are rare in the data presented in this report. The velocity variations generally noted on tunnel traveltime plots are minor and in general suggest that the tuffs at tunnel level are not characterized by the presence of significant refractors over the range of the seismic coverage.

On figure 4 an offset occurs on the traveltime plot for the shear-wave data near station 9+10. This type of response is typical of many of the plots included in this report. It is our experience that such events occur in the vicinity of faults or bedding planes crossing the tunnel in the vicinity of the geophones affected. Offsets are frequently seen on the shear-wave traveltime plots but sometimes occur in compressional-wave data. Although this type of offset is classically associated with faulting it exhibits peculiarities, in that: (a) it is often not seen on all relevant traveltime plots; (b) it is occasionally associated with bedding planes, rather than faults; (c) when associated with faults the fault displacement is generally insignificant (generally less than 3-6 m or 9.8-19.4 ft) compared with the displacement suggested by the offset in the traveltime plot. We have no ready explanation for this phenomenon other than to believe it suggests some form of trapping of the seismic wave in the bedded tuff.

On the figures the shotpoint is indicated by a single designation "SP" to denote the locations of single or multiple drill holes as well as ditches used for the generation of shear waves.

The distance axis indicates the tunnel station in standard surveying usage, that is, 13+00 is equivalent to 1,300 feet (396 m).

SHOSHONE MOUNTAIN

The Area 16 tunnel complex in Shoshone Mountain has not been utilized for nuclear testing since the detonation of the Diamond Mine event in the U16a.06 complex in 1971. The general geologic setting of the region has been mapped by Orkild (1963). The geology at tunnel level in the vicinity of the geophysical survey data is similar to the zeolitized tuff tunnel beds in Rainier Mesa where more extensive testing has been conducted.

Area 16 Tunnel Complex

The plan map of the tunnel-level locations where geophysical surveys have been made is shown on plate 1. The resistivity measurements made in this tunnel are not included in this report. They were made for the purposes of obtaining baseline data on resistivity of the tuff, particularly in those zones containing appreciable amounts of clay. A discussion of the resistivity measurements in the U16a.04 drift with respect to the problems of clay definition has been published in Carroll and Cunningham (1980).

Seismic velocities obtained in the Area 16 tunnels are considerably lower in the region of U16a.03, U16a.04, U16a.04 reentry, and U16a.05 than is the case in the Rainier-Aqueduct complexes where overburden thicknesses are similar. This is possibly due to the larger faults present in the 16-tunnel complex and associated local zones exhibiting high fracture frequency. In addition, physical properties obtained on samples from the U16a.03 drift indicate water saturations less than those typically encountered in the Rainier/Aqueduct Mesa area (J. H. Scott, written commun., 1966). Water saturation has been found to strongly affect compressional velocity values (Carroll and Cunningham, 1980).

The seismic refraction data available for individual tunnel complexes are itemized below.

U16a.03 (Double Play)

Seismic data for U16a.03 are listed on figure 7 (figs. 7-32, 34-58 are in back of the report). Only compressional velocities were obtained. These velocities were obtained by J. H. Scott, USGS (written commun., 1966) and are consistently the lowest obtained in any of the four complexes reported. The Double Play event was detonated on June 6, 1966.

U16a.04 (Ming Vase)

Ming Vase was detonated on November 20, 1968. Preshot compressional velocities obtained are shown on figure 8. A postshot survey, including shear wave, was made in 1969 (fig. 9). However, at the range from the detonation point at which the measurements were made experience indicates it is doubtful explosion effects on the compressional velocity would be encountered. The pre- and postshot surveys do not overlap.

16a.05 (Diamond Dust)

Diamond Dust was detonated on April 12, 1970. Because of the geometry of this drift complex, radial velocities were obtained rather than the standard in-line refraction data. These data are shown on figure 10. The velocity data listed in the table on the figure are the averages of the velocities obtained on radials from the shotpoint to the individual geophones on the two seismic lines. Shear waves were also obtained at this site.

U16a.06 (Diamond Mine)

Diamond Mine was detonated on July 1, 1971. It too was of a geometry such that velocity data were obtained in radial drill holes rather than by in-line techniques. The results of the surveys are shown on figure 11.

AQUEDUCT AND RAINIER MESA TUNNEL COMPLEXES

This area encompasses the major tunnel complexes wherein testing has been recently performed. The geology at tunnel level is chiefly zeolitized ash-fall tuff. The geology in the region has been mapped by Gibbons and others (1963) and extensive physical properties of core have been reported (Brethauer and others, 1980). Published logs for vertical exploratory holes in the area are available (Maldonado and others, 1979); however, published reports on the geology of the drifts discussed in this report are available for only a few sites. Those individual sites having such reports are referenced where applicable.

T-Tunnel Complex--Aqueduct Mesa

Three events have been fielded in the T-tunnel complex. The locations where geophysical surveys were made are shown on plate 2. The results of the seismic surveys are relatively straightforward. Shear and compressional waves were obtained in all three tunnels.

U12t.01 (Mint Leaf)

Mint Leaf was detonated on May 5, 1970. The results of the seismic refraction survey are shown on figure 12.

U12t.02 (Diamond Skulls)

Diamond Skulls was detonated on July 20, 1972. The results of the seismic refraction survey are shown on figure 13. An attempt was made in the Diamond Skulls drift to obtain reflections from the pre-Tertiary dolomite which was within 61 m (200 ft) of the tunnel near the WP. Results were poor, however the attempt was not elaborate. In addition, cross-block shooting was accomplished over limited distances in connection with a high-explosive experiment (SPLAT) performed in the t.02 drift in 1973. The results of these two surveys are not reported here.

U12t.03 (Husky Pup)

Husky Pup was detonated on October 24, 1975. The results of the seismic refraction survey in that drift are shown on figure 4.

B-Tunnel Complex--Rainier Mesa

The B-tunnel complex was the site of the first underground nuclear explosion (Rainier). The device was detonated in 1957. Several nuclear events and high-explosive tests were conducted in the complex through 1963. No data or maps from this complex are included in this report. The seismic refraction data available for this complex have been published (U.S. Geological Survey, 1959; Hazlewood, 1961). The report by Hazlewood also contains an

areal reference map of the B-tunnel complex which portals about 914 m (3,000 ft) north of the E-tunnel portal and approximately 148 m (485 ft) higher in elevation.

E-Tunnel Complex--Rainier Mesa

The E-tunnel complex is areally the largest tunnel complex on the NTS. Locations where geophysical surveys were made in this complex are shown on plate 3. The results of the early refraction surveys listed in the table on the figure (A, B, F, G, H, and I) have been summarized in a report by Hazlewood (1961) and are not included here. The early geologic studies in E-tunnel (1958-1963) have been covered in formal geologic reports by the USGS. Geologic reports have not yet been issued for the work done since that time except for those investigations in U12e.18 and U12e.20 (U.S. Geological Survey, 1978; 1982).

The extensive electrical resistivity surveys near the portal of the E-tunnel complex were run to define the locations of clay beds in connection with experimental mining using a boring machine. The "mole" encountered difficulty in a clay bed at 5+55 in the ventilation drift.

The seismic refraction data obtained since 1967 are itemized below.

U12e.10 (Dorsal Fin)

Dorsal Fin was detonated on February 29, 1968. It was the first event detonated in E-tunnel since the 2.6 kt Antler event in U12e.03 in September 1961. This was the first drift in which serious attempts were made to record shear waves. The results of the seismic refraction survey are shown on figure 14.

U12e.11 (Diesel Train)

Diesel Train was detonated on December 5, 1969. The results of the seismic refraction survey are shown on figure 15.

U12e.12 (Hudson Moon)

Hudson Moon was detonated on May 26, 1970. The results of the seismic refraction survey in this drift are shown on figure 16. The front-end velocities in this drift are extremely low compared with most sites in the Rainier Mesa area. The low velocities have been found to be due to a relatively high air-filled porosity (5-11 percent). This is not the general case for the tuff at tunnel level in Rainier Mesa where gas voids are generally less than 2 percent. The Hudson Moon event was reentered and the postshot seismic refraction survey obtained in the reentry drift is shown on figure 17. To obtain the equivalent survey station in the preshot tunnel, 2+41 should be added to the survey stations shown on figure 17. The effects of the explosion on lowering the seismic velocity of the rock are obviously pronounced in the front end of the drift.

U12e.14 (Dido Queen)

Dido Queen was detonated on June 5, 1973. The results of the seismic refraction survey in the main drift and the HFR drift are shown on figures 18 and 19.

U12e.15-17 (pre-Mine Dust)

These tunnels were the site of high-explosive tests. Seismic refraction data were recorded in U12e.16 (fig. 20) and U12e.17 (fig. 21).

U12e.18 (Dining Car)

Dining Car was detonated on April 5, 1975. The results of the seismic refraction survey in this tunnel are shown on figure 22. Three months following this original survey a repeat survey was run (fig. 23). The data do not indicate any significant deterioration in velocity with time. (Compare U12g.10 (Camphor) in this regard.) These data and extensive additional geophysical measurements connected with this event have been reported in detail (U.S. Geological Survey, 1978).

U12e.20 (Hybla Gold)

The Hybla Gold event was detonated on November 1, 1977. The complex was unique in that the main drift was tangential to the Dining Car chimney, passing within 3 m (10 ft) of the chimney boundary. The refraction data obtained in this drift (fig. 24) and in the auxiliary drift (fig. 25) indicate pronounced effects on rock velocity due to the Dining Car explosion. These data and extensive additional geophysical measurements connected with this event have been reported (U.S. Geological Survey, 1982).

G-Tunnel Complex--Rainier Mesa

The G-tunnel complex has not been utilized for nuclear testing since the detonation of the Camphor event in the U12g.10 drift in 1971. The map of the tunnel-level locations where geophysical surveys were made until that date is shown on plate 4. The extensive tunnelling accomplished in the G-tunnel complex since 1971 for purposes other than nuclear testing are not included on the figure as essentially no geophysical data have been taken by the USGS in G-tunnel since that time. The seismic refraction data obtained for individual tunnel complexes are itemized below.

U12g.05 (Deep Well)

The Deep Well chamber was a large hemispherical cavity which was never utilized for a nuclear test. Seismic velocity data were obtained by Scott and Cunningham (1966) along the major and minor diameters of the flat face of the chamber. The results of their work are summarized in table 1. The seismic spreads used were of the order of 30 m (100 ft) in length along the horizontal and vertical diameters of the cavity. The instrument drift was about 46 m (150 ft) from the spreads. The recognition of shear-wave arrivals in this study was described as uncertain.

U12g.06 (Red Hot)

The Red Hot event was detonated on March 5, 1966, in a cavity similar in dimension to Deep Well. The velocity data for this event were also reported by Scott and Cunningham (1966). For completeness the results are listed in this report in table 1. Comments with respect to this table listed under Deep Well apply also to Red Hot.

U12g.07 (Door Mist)

The Door Mist event was detonated on August 31, 1967. The refraction velocity data obtained in the drift are shown on figure 26. Only compressional velocities were recorded. Those near the WP are excessively low for experience in Rainier Mesa. In addition, the velocity irregularities on figure 31 near 16+00 are seldom seen in tunnel refraction surveys. The anomalous results are attributed to the presence of thin siliceous beds dipping toward the WP in this interval.

U12g.09 (Cypress)

Cypress was detonated on February 12, 1969. Initial refraction surveys in the U12g.09 drift were made with 30-m (100 ft) offsets to look for the presence of deeper refractors. These were followed by additional mining which resulted in several overlapping surveys near the WP. Statistical comparisons of the overlapping segments obtained from shotpoints at the same ends of the individual spreads indicate no significant differences in velocity in the overlapping segments, and thus to avoid an unnecessary complex traveltime plot, arrival times to common geophones have been combined to obtain the data shown on figure 27. The Cypress tunnel was reentered after the event and additional seismic measurements were obtained (fig. 28). The data shown on figure 28 are unlike other results presented in this report in that they were obtained from acceleration records. Arrival times picked from records obtained in the normal manner were subsequently rejected because of the severe rounding of waveforms arising from electrical filtering. The shear waveforms on the accelerometer records were poorly developed. The lower velocities of both shear and compressional events in the postshot survey are a result of explosion effects. The tunnel stations on figure 28 are equivalent to subtracting 0+40 from those on figure 27.

U12g.10 (Camphor)

The Camphor event was detonated on June 29, 1971. The results of seismic shooting in 1968 are shown on figure 29. Shear-wave data were obtained at this time. Two additional preshot seismic refraction surveys were run. One was run in 1970 to investigate the effects on seismic velocity due to a nearby event (Diesel Train, U12e.11) which collapsed a portion of the tunnel (fig. 30). An additional survey was run on March 31-April 1, 1971, to investigate if any deterioration in velocity occurred in a shear zone associated with a fault near CS 15+00 (fig. 31). Changes in velocity can be seen in the data. Unlike other tunnel events the Camphor drift was open several years between completion of mining and event detonation.

Postevent seismic-velocity data were obtained in the Camphor reentry and, like Cypress, show severe explosion effects on both shear and compressional

Table 1.--Velocities and elastic constants of rock behind low-velocity layer, Flat face, Red Hot and Deep Well cavities
(To convert feet to meters multiply by 0.3048)

Cavity	Detector spread	Location of shotpoints	Compressional-wave velocity (ft/sec)	Shear-wave velocity (ft/sec)	Poisson's ratio	Young's modulus ^{1/} (psi)
Red Hot	Horizontal diameter	Ends of spread	7,000	3,860	0.28	1.00 x 10 ⁶
		Instrument drift	7,610	3,930	.32	1.06 x 10 ⁶
	Vertical diameter	Ends of spread	7,700	3,850	.33	1.03 x 10 ⁶
		Instrument drift	7,790	4,090	.31	1.15 x 10 ⁶
		Average.....		7,530	3,890	.31
Deep Well	Horizontal diameter	Ends of spread	6,600	3,180	0.35	0.71 x 10 ⁶
		Instrument drift	6,950	3,820	.28	0.98 x 10 ⁶
	Vertical diameter	Ends of spread	6,250	3,730	.22	0.89 x 10 ⁶
		Instrument drift	6,530	3,680	.27	0.90 x 10 ⁶
		Average.....		6,580	3,600	.28

^{1/} Young's modulus computed using density = 1.94 g/cc determined by averaging laboratory measurements of 31 natural-state core samples from Red Hot and Deep Well. Density measurements were made by the University of Illinois. Department of Civil Engineering (D. U. Deere, written commun.).

velocity near the front end of the reentry drift (fig. 32). The strike of the aforementioned shear zone near the Camphor WP was such that it was not intersected by the reentry drift. The tunnel stations on figures 29-31 are equivalent to subtracting 18+85 from those on figure 32.

Extensive additional seismic data consisting of cross-block shooting and repeated acceleration measurements were obtained in the Camphor drift. Seismic measurements were also made across a large crack near the Camphor chimney in 1978. These data were not diagnostic in sensing the presence of the crack. None of the above data are reported here.

N-Tunnel Complex--Rainier Mesa

The locations where geophysical surveys have been run in the N-tunnel area are shown on plate 5. The first nuclear event in this complex was Midi Mist which was detonated in June 1967. The most extensive geophysical surveys run in any tunnel complex have been run in the N-tunnel region. Because of the intensity of geophysical data coverage in the Mighty Epic/Diablo Hawk region (U12n.10 and U12n.10A), the locations where geophysical surveys were made in connection with the Diablo Hawk event are shown on a separate illustration (fig. 33) and table 2. Attempts at recording shear waves in this complex were first made in the U12n.04 drift.

U12n.02 (Midi Mist)

The Midi Mist event was detonated on June 26, 1967. The seismic refraction results obtained in this drift and in the hook drift are shown on figures 34 and 35. Geologic data for this location have been published (Ege and others, 1980b).

U12n.03

The U12n.03 drift was never utilized for nuclear testing. This drift is one of the two that penetrated clay-rich tuff resulting in unstable ground conditions. (The other such drift was U12n.05.) The particulars of the geology and geophysics obtained in connection with this drift have been published (Ege and others, 1980a). The results of the seismic refraction survey are shown on figure 36.

U12n.04 (Hudson Seal)

The Hudson Seal event was detonated on September 24, 1968. The results of the seismic refraction surveys are shown on figure 37. Shear waves were recorded in this drift. On the seismic spread near the tunnel front end, however, shear waves could not be recognized on the records. The reason for the inability to generate recognizable shear waves at this location is unknown.

U12n.05 (Misty North)

The Misty North event was detonated on May 2, 1972. The results of the seismic refraction survey in this drift are shown on figure 38. This drift, like the U12n.03 drift, encountered clay-rich, mechanically unstable tuff. Unfortunately, at the time of the seismic survey the presence of construction

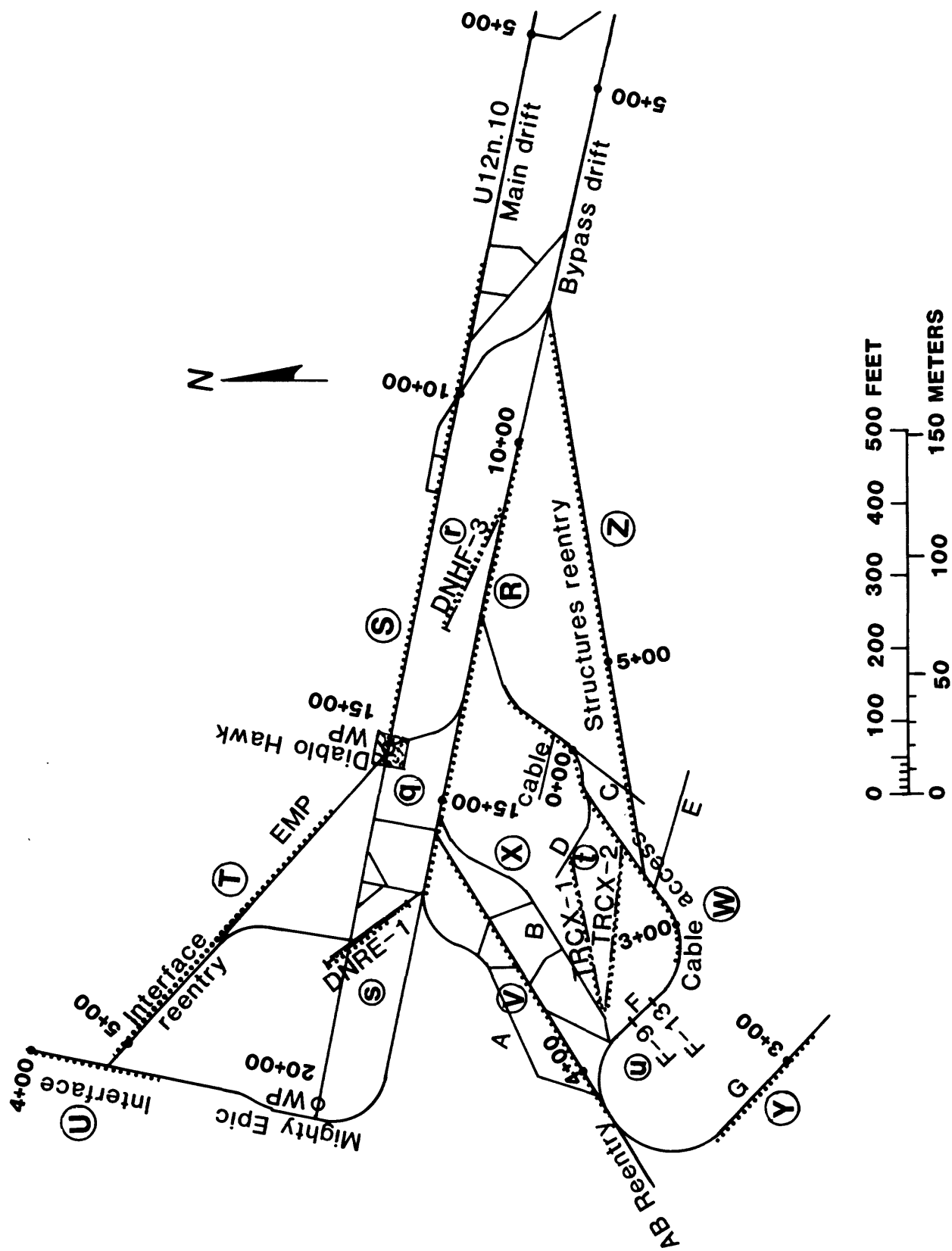


Figure 33.--Locations where geophysical surveys were made in connection with the U12n.10A (Diablo Hawk) event, U12n-tunnel complex (letters refer to table 2).

Table 2.--Geophysical surveys made in the U12n.10A complex.

[Key letters refer to tunnel seismic surveys (upper case) and drill-hole surveys (lower case) shown on figure 22.]

Key	Date	Hole	Interval	TD	Description
R	7/76	U12n.10A Bypass	9+95-16+35	---	P seismic S seismic
	10/76	U12n.10A Bypass (repeat)	9+95-16+35	---	P seismic S seismic
S	10/76	U12n.10A Main	15+20-8+20	14+90	P seismic S seismic
T	9/77	U12n.10A, Inter- face Reentry and Emp	1+07(EMP) +5+27(IR)	---	P seismic S seismic
U	9/77	U12n.10, Inter- face	2+19-3+98	---	P seismic S seismic
V	10/76	U12n.10A, AB reentry	0+55-4+75	---	P seismic S seismic
	6/80	(Boeing) and Boeing reentry	0+50-2+75		
W	10/76	U12n.10A, Cable access and C and F	1+25(C drift) --- 3+60(Cable Acc)		P seismic S seismic
X	10/76	U12n.10A, fan from main (15+00) to AB reentry and F and cable access and C and G	---	---	P seismic S seismic
	6/80	fan from D drift to F- and G-drifts			
Y	7/77	U12n.10A, "G" structures	1+51-3+51	---	P seismic S seismic
	6/80	"G" structures reentry	1+51-3+51		
Z	6/80	U12n.10A structures reentry	0+45-7+35	---	P seismic S seismic
q	7/77	U12n.10A,DNUG-5	8-88		resistivity
			10-90		sonic
	10/76	U12n.10A,GSGH-1	6-92	100	resistivity
	11/76		12-90		sonic
		U12n.10A,GSCH-2	8-92	101	resistivity
		U12n.10A,GSCH-3	8-116	125	resistivity
			12-118		sonic
	10/76	U12n.10A,GSHF-Y	10-42	50	resistivity
	11/76		11-41		sonic
	10/76	U12n.10A,LLCI-1	6-49	55	resistivity
	11/76		9-49		sonic
r	12/76	U12n.10A,DNHF-3	8-188 9-187	195	resistivity sonic
s	10/76	U12n.10A,DNRE-1	34-137	138	resistivity
t	11/77	U12n.10A,TRCX-1	9-208		resistivity
			7-212		sonic
		U12n.10A,TRCX-2	18-220		resistivity
			7-222		sonic
	2/78	U12n.10A,TRCX-1 and TRCX-2			sonic (shear wave and cross hole)
u	11/79	U12n.10A,F-9,F-13			sonic (shear)

features prevented obtaining seismic data in other than the zone near the WP which did not include any clay-rich tuff.

U12n.06 (Diana Mist)

The Diana Mist event was detonated on February 11, 1970. The seismic refraction results obtained in this drift are shown on figure 39.

U12n.07 (Husky Ace)

The Husky Ace event was detonated on October 12, 1973. The results of the seismic refraction survey are shown on figure 40. Additional measurements, not reported here, which were made in connection with Husky Ace consisted of recording seismic velocity from tunnel level to the surface of Rainier Mesa.

U12n.08 (Ming Blade)

The Ming Blade event was detonated on June 19, 1974. The results of the seismic refraction survey are shown on figure 41. The low velocity and extensive fractures near the WP resulted in additional surveys to attempt to separate the effect of these fractures from the effect of the drift on the observed velocity (fig. 42).

U12n.09 (Hybla Fair--SPLAT)

Hybla Fair was detonated on October 28, 1974. The length of seismic line used in the survey was restricted and consisted of only four geophones between shotpoints which were 39 m (127 ft) apart in the WP region. The average velocity obtained was $2,313 \pm 30$ m/s ($7,590 \pm 100$ f/s). The traveltime data are not presented in this report. The SPLAT experiment was a high-explosive test situated in two crosscuts off the Hybla Fair (U12n.09) drift. A restricted refraction line of only 18 m (58 ft) consisting of four geophones along the main crosscut invert yielded a velocity of 2,210 m/s (7,250 f/s). The traveltime data are not presented in this report.

U12n.10 (Mighty Epic)

The Mighty Epic event was detonated on May 12, 1976. The tunnel complex associated with this event was the most extensive of those discussed in this report and numerous geophysical measurements, including repeat seismic measurements, were made throughout the entire complex. The details of these measurements in both tunnel and drill holes have been published (U.S. Geological Survey, 1979) and only the seismic refraction data in the main and bypass drifts are reported here (figs. 43 and 44).

U12n.10A (Diablo Hawk)

The Diablo Hawk event was detonated on September 13, 1978, at a WP 183 m (600 ft) from the Mighty Epic WP and located in the same drift. Extensive tunnel excavations were added to the Mighty Epic complex for the Diablo Hawk event. For clarity, the locations where geophysical surveys were made in connection with Diablo Hawk are shown on a separate figure (fig. 33) and table 2. As in the case of Mighty Epic, extensive geophysical surveys were run in

the Diablo Hawk complex. The refraction surveys are all included in this report. Many of these surveys may also be considered as postshot Mighty Epic data. Standard refraction surveys were run in the main drift (fig. 45) and in the bypass drift (fig. 46). A repeat survey was run in the bypass drift 3 months after the original survey (fig. 47). Additional seismic refraction surveys run in connection with this event were in the structures (cable access) reentry drift (fig. 48), the interface reentry drift (fig. 49), the G-structures drift (fig. 50), and the AB reentry (Boeing) drift (fig. 51). A postshot (Mighty Epic) survey was run in the interface drift (fig. 52) and fan shooting was done from the Diablo Hawk WP to the structures drifts. The fan shooting is not included in this report. Following the Diablo Hawk event seismic surveys were done in the reentry drift to the Diablo Hawk structure drifts (figs. 53-54) and in the cable access (Boeing) drift reentry (figs. 55-56). Additional reentry seismic surveys run in the G-structures drift and fan shooting from D-drift to F- and G-drifts are not reported here.

U12n.11 (Miners Iron)

The Miners Iron event was detonated on October 31, 1980. This was the last event for which data have been included in this report. The results of the seismic refraction surveys in the main and bypass drifts are shown on figures 57 and 58.

SUMMARY OF REFRACTION DATA

The seismic refraction data presented in this report have been synthesized in table 3. The data in the table are averages of the velocities obtained from the two-way traveltime plots for the survey lines nearest the WP of each event. Exceptions to this are locations where long offset shear velocities are not included in the average because they suggest refraction, e.g., Husky Pup (fig. 4). The data are restricted to those drifts in which a geophone spread extended at least 60 m (200 ft) from the WP. Thus, esoteric geometries such as Red Hot (U12g.06), short drifts such as Hybla Fair (U12g.09), and postshot surveys representative of changes in velocity arising from ground shock loading of the tuff such as Hybla Gold (U12e.20) are not included.

Looking at extremes in the data indicates that the highest compressional velocities were recorded in the Husky Ace (U12n.07) and Diesel Train (U12e.11) drifts. The lowest compressional velocities were recorded in the Door Mist (U12g.07), Hudson Moon (U12e.12), Diablo Hawk (U12n.10A), and Double Play (U16a.03) drifts. The highest shear velocities are found near the Dido Queen (U12e.14) WP and all three WP's in T-tunnel. The lowest shear velocities were recorded for Diablo Hawk (U12n.10A), Camphor (U12g.10), and Hudson Moon (U12e.12).

The low shear velocity recorded for Diablo Hawk is intriguing in that this event was located in the same drift as, and at a distance of 183 m (600 ft) from, the Mighty Epic WP. The possibility that this velocity may be partially a result of some dislocation of preexisting fractures by ground shock arising from the Mighty Epic detonation cannot be entirely ruled out.

There may be some question as to whether the velocities recorded in the Camphor drift constitute relevant preshot velocity experience. The collapse of the tunnel, the deteriorating velocity in the shear zone near the WP with

time, and the long period between mining completion and event detonation render inclusion of the data subjective. The data listed in table 3 for this event are a straight average of the individual velocity segments shown on figure 36.

The averages listed at the bottom of the table for the moduli may be more rigorously calculated using the propagation of error equations previously listed in this report.

The data in table 3 have been further arranged into the histograms on figures 59 through 61. Experience suggests that the range in the data shown is less a function of the composition of the volcanic tuff and overburden stress than of rock saturation and the extent of fracturing present. The range in the compressional velocity data about the mean is about twice that of the shear velocity. This is to be expected however, since the two variables are not independent but are related through Poisson's ratio. This relationship requires the compressional velocity to be at least the square-root-of-two times the shear velocity, and for a perfectly elastic condition to be the root-of-three times the shear velocity. The mean Poisson's ratio of 0.31 obtained for the data reported here suggests a mean compressional velocity of about 1.9 times the shear velocity. Thus for data approximating a normal distribution the mean, range, and standard deviation of the shear velocity can be expected to result in the distribution shown for the compressional velocity.

Table 3.--Average velocity and dynamic moduli data obtained near the WP of Tunnel events. Density of 1.9 g/cm³ (119 lb/ft³ assumed in calculations
[To convert meters/second to feet/second multiply m/s by 3.28.]

Tunnel	Compressional velocity m/s	Shear velocity m/s	Poisson's ratio	Young's modulus k/bar	Bulk modulus k/bar	Shear modulus k/bar
U12n.02	2,384	---	---	---	---	---
U12n.03	2,460	---	---	---	---	---
U12n.04	2,687	---	---	---	---	---
U12n.05	2,565	1,302	0.33	85	82	32
U12n.06	2,658	1,172	.38	72	99	26
U12n.07	2,711	1,273	.36	84	99	31
U12n.08	2,385	1,206	.33	73	71	28
U12n.10	2,062	1,245	.21	71	42	29
U12n.10A	2,161	1,140	.31	65	56	25
U12n.11	2,692	1,325	.34	89	93	33
U16a.03	2,099	---	---	---	---	---
U16a.04	2,472	---	---	---	---	---
U12e.10	2,380	1,277	.30	80	66	31
U12e.11	2,753	1,301	.36	87	101	32
U12e.12	1,980	1,159	.24	63	40	26
U12e.14	2,498	1,384	.28	93	70	36
U12e.18	2,588	1,260	.34	81	87	30
U12g.07	1,846	---	---	---	---	---
U12g.09	2,512	1,347	.30	90	74	34
U12g.10	2,330	1,151	.34	67	70	25
U12t.01	2,450	1,375	.27	91	66	36
U12t.02	2,587	1,392	.30	95	78	37
U12t.03	2,652	1,381	.31	95	85	36
Mean	2,430	1,276	.31	81	75	31
Stand. dev.	249.9	86.4	.044	10.7	18.3	4.0

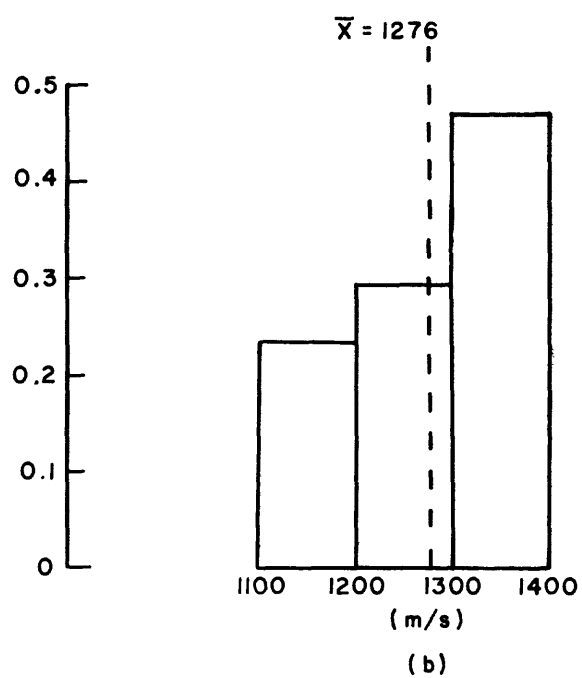
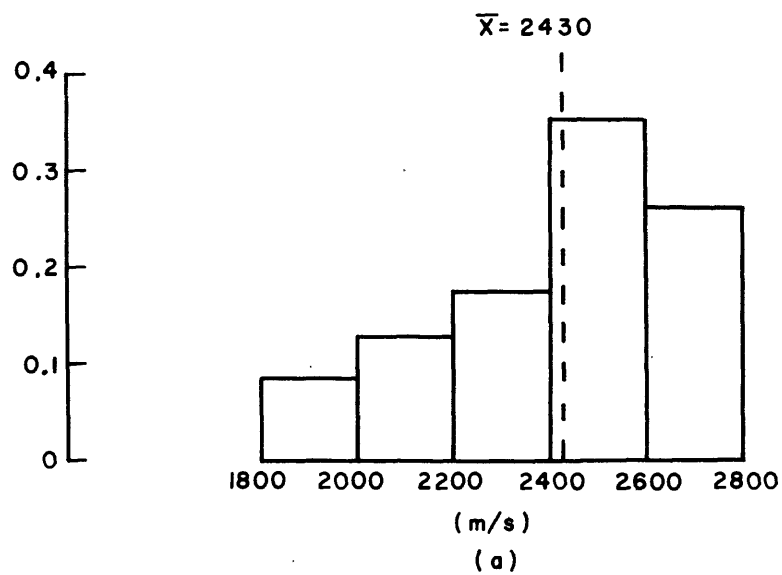


Figure 59.--Relative frequency histogram of (a) 23 compressional and (b) 17 shear velocities obtained near the WP of tunnel events.

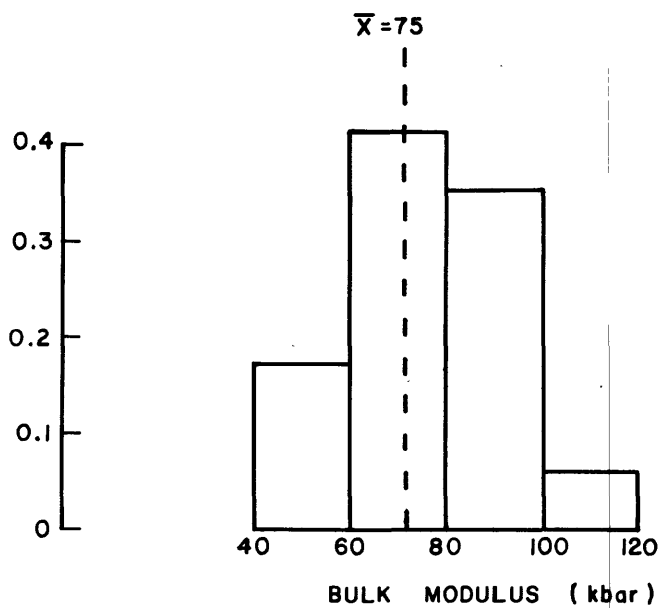
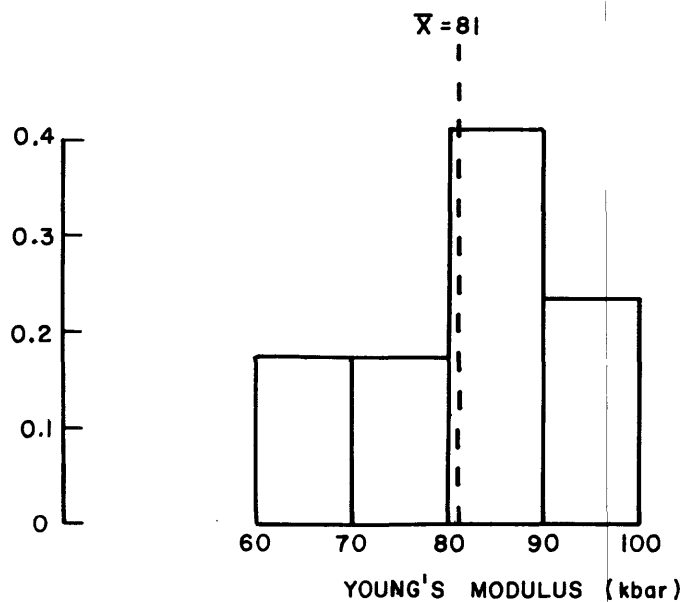


Figure 60.--Relative frequency histograms of Young's and bulk moduli calculated from shear and compressional velocities for 17 tunnel events.

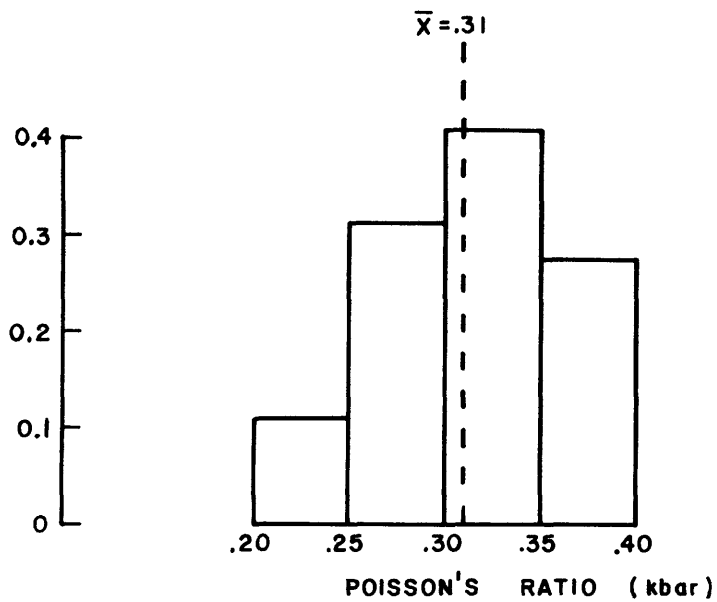
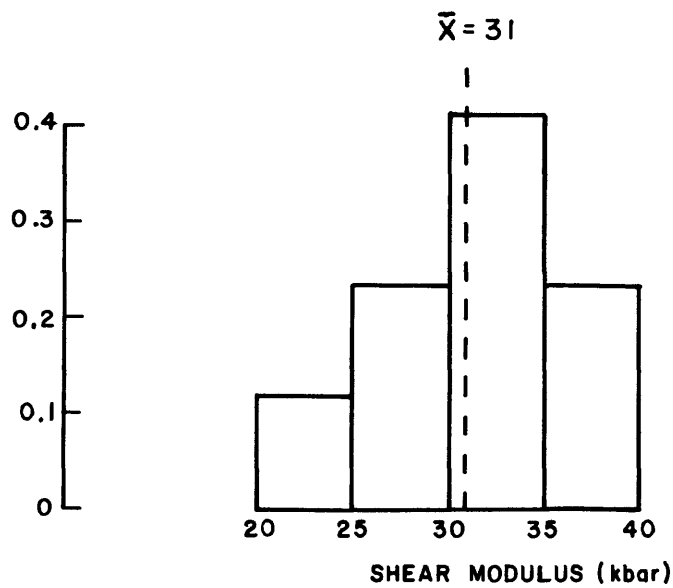


Figure 61.--Relative frequency histograms of shear modulus and Poisson's ratio calculated from shear and compressional velocities for 17 tunnel events.

Figures 7-32 and 34-58 follow.

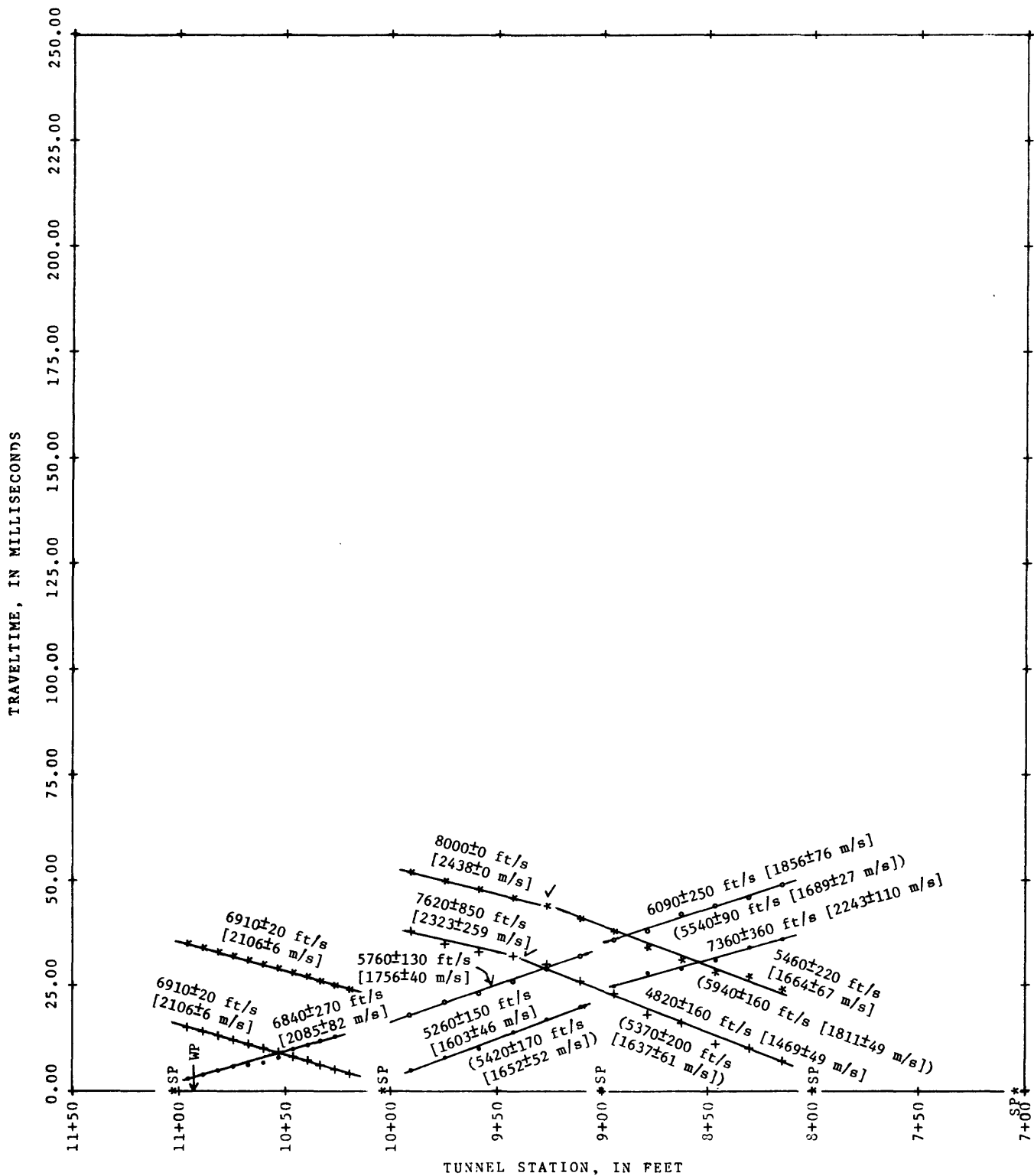


Figure 7.--Results of seismic shooting in the U16a.03 drift (February 17, 1966).
*, °, ' , + indicate individual geophone lines; SP, shotpoint.

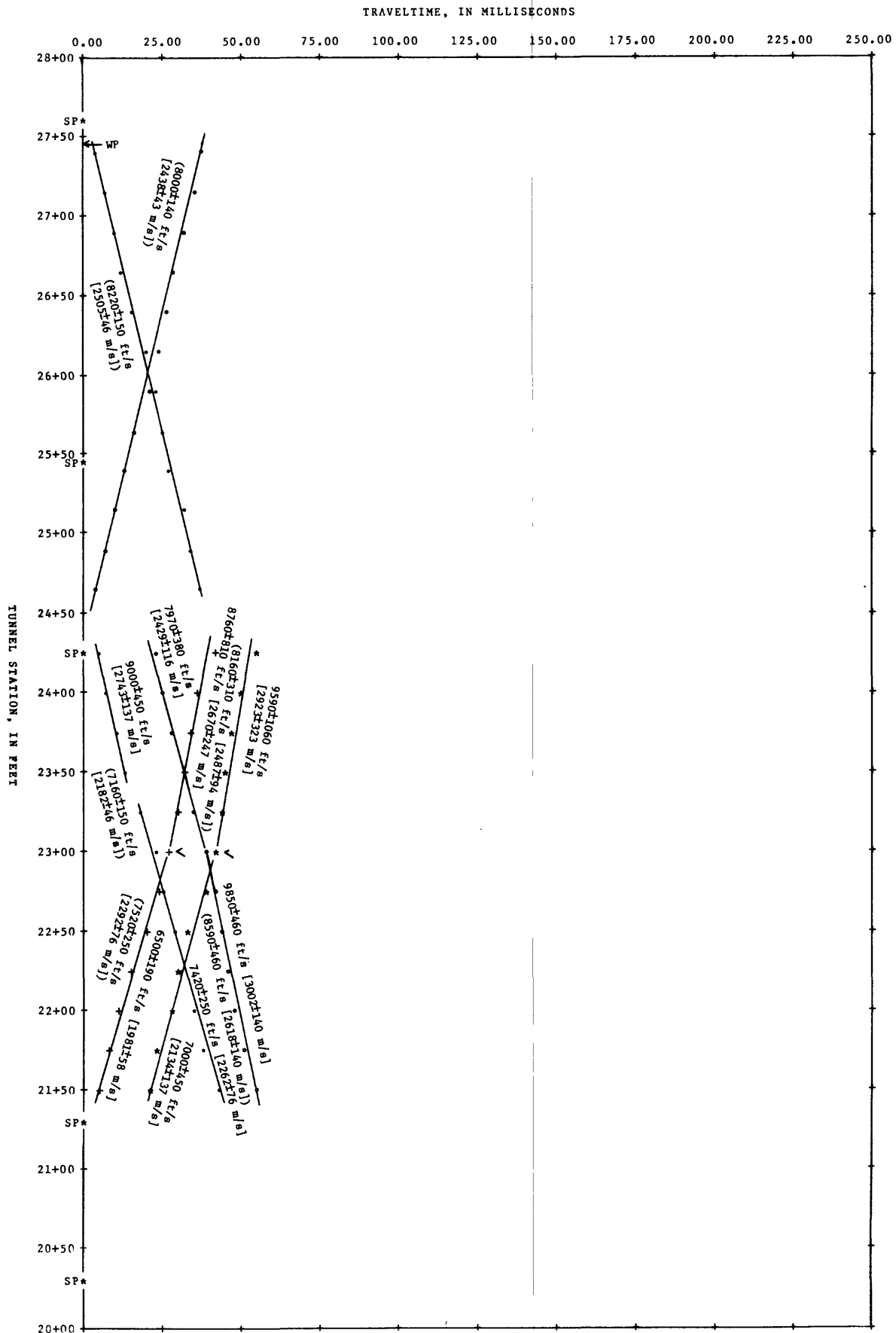


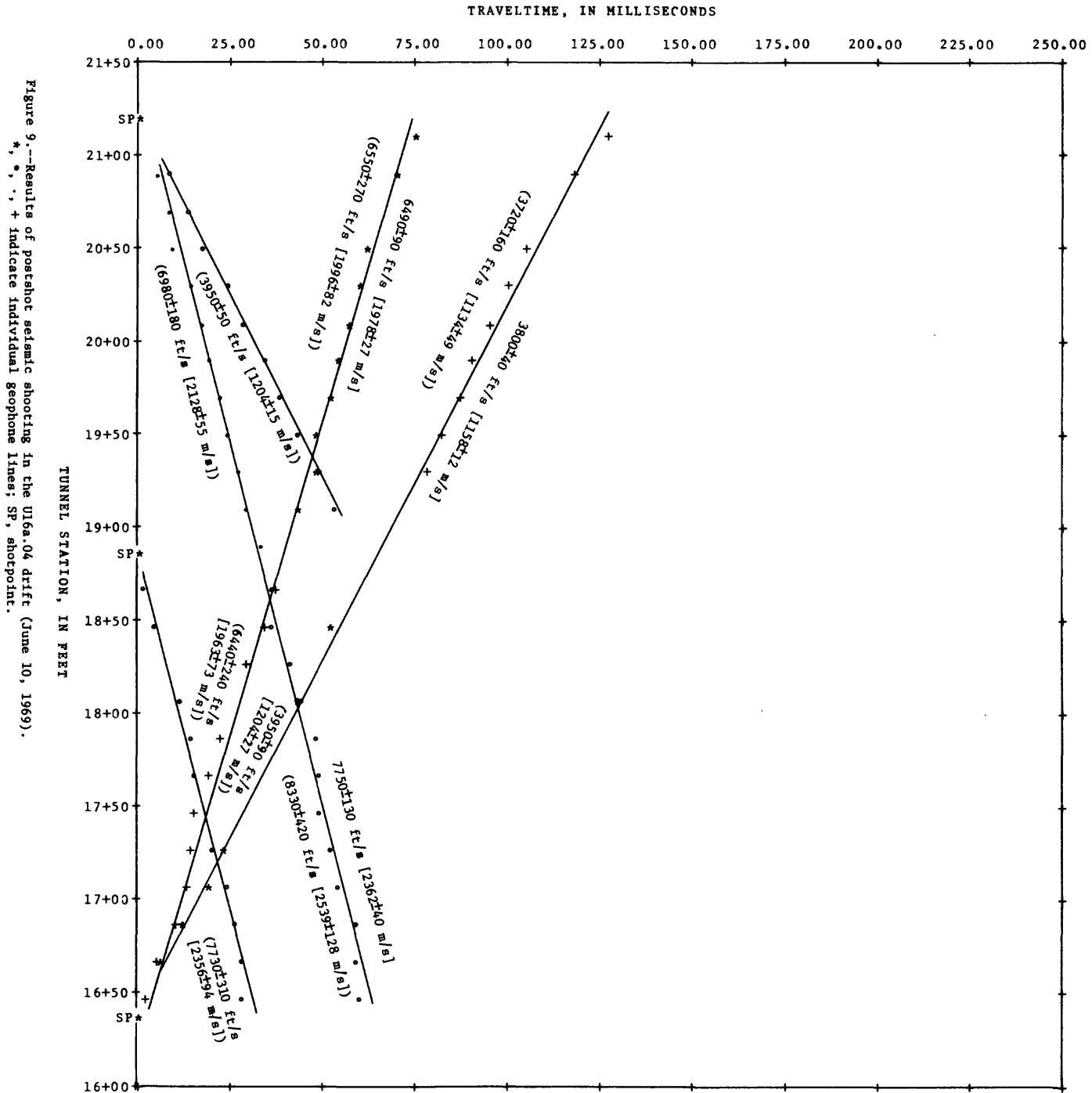
Figure 8.—Results of seismic shooting in the Ula.06 drift (June 1967).
 *, o, , + indicate individual geophone lines; SP, shotpoint.

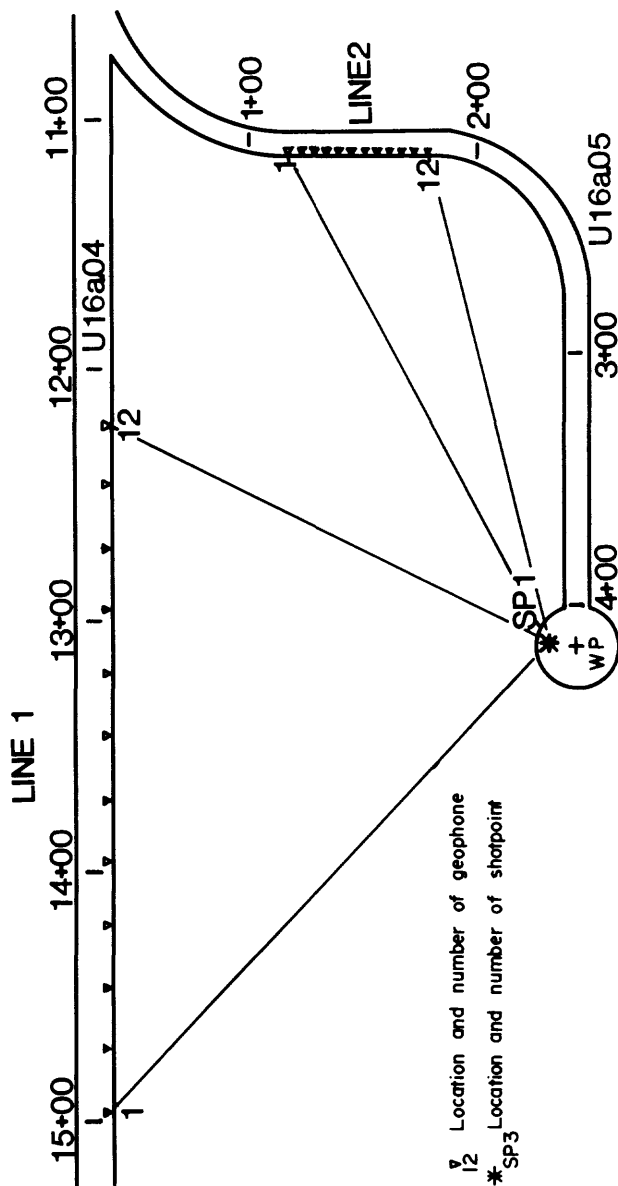
ACOUSTIC PARAMETERS

(Based on an assumed rock specific gravity of 1.90 ± 0.05)

INTERVAL (feet) ^{1/}	COMPRESSIONAL VELOCITY (m/s)	SHEAR VELOCITY (m/s)	CHARACTERISTIC COMPRESSIONAL IMPEDANCE (10 ⁶ mks Rayls)	CHARACTERISTIC SHEAR IMPEDANCE (10 ⁶ mks Rayls)	POISSON'S RATIO	YOUNG'S MODULUS (kbar)	BULK MODULUS (kbar)	SHEAR MODULUS (kbar)
21+10 - 18+90	2128 \pm 55	1203 \pm 15	4.04 \pm 0.15	2.29 \pm 0.07	0.26 \pm 0.02	69.6 \pm 5.0	49.3 \pm 5.5	27.5 \pm 1.0
16+47 - 21+10	1978 \pm 27	1158 \pm 12	3.76 \pm 0.11	2.20 \pm 0.06	0.24 \pm 0.01	63.2 \pm 2.8	40.4 \pm 2.8	25.5 \pm 0.9

^{1/} meters = 0.3048 x feet





12 Location and number of geophone
 * SP3 Location and number of shotpoint

ACOUSTIC PARAMETERS FROM ALL RADIAL VELOCITIES

(Based on an assumed rock specific gravity of 1.90±0.05)

COMPRESSIONAL VELOCITY (m/s)	SHEAR VELOCITY (m/s)	CHARACTERISTIC COMPRESSIONAL IMPEDANCE (10 ⁶ mks Rayls)	CHARACTERISTIC SHEAR IMPEDANCE (10 ⁶ mks Rayls)	POISSON'S RATIO	YOUNG'S MODULUS (kbar)	BULK MODULUS (kbar)	SHEAR MODULUS (kbar)
1896± 52	1137± 27	3.60±0.14	2.16±0.08	0.21±0.03	59.9±4.6	35.5±4.9	24.6±1.3

Figure 10.--Results of seismic shooting in the U16a.05 drift.

ACOUSTIC PARAMETERS
(Based on an assumed rock specific gravity of 1.90±0.05)

DRILL HOLE	COMPRESSIONAL VELOCITY (m/s)	SHEAR VELOCITY (m/s)	CHARACTERISTIC COMPRESSIONAL IMPEDANCE (10 ⁶ mks Rayls)	CHARACTERISTIC SHEAR IMPEDANCE (10 ⁶ mks Rayls)	POISSON'S RATIO	YOUNG'S MODULUS (kbar)	BULK MODULUS (kbar)	SHEAR MODULUS (kbar)
GGA#1	2362±79	1210±12	4.49±0.19	2.30±0.06	0.32±0.02	73.6±6.8	68.9±9.1	27.3±0.9
GGA#3	2597±116	1509±21	4.93±0.26	2.87±0.09	0.25±0.04	107.7±12.2	70.5±12.8	43.3±1.7
PI#3	2493±70	1292±24	4.74±0.18	2.46±0.08	0.32±0.02	83.5±6.9	75.8±9.4	31.7±1.5
Average	2484±52	1338±12	4.72±0.16	2.54±0.07	0.30±0.01	88.2±5.4	71.9±6.4	34.0±1.1

1/ meters = 0.3048 x feet

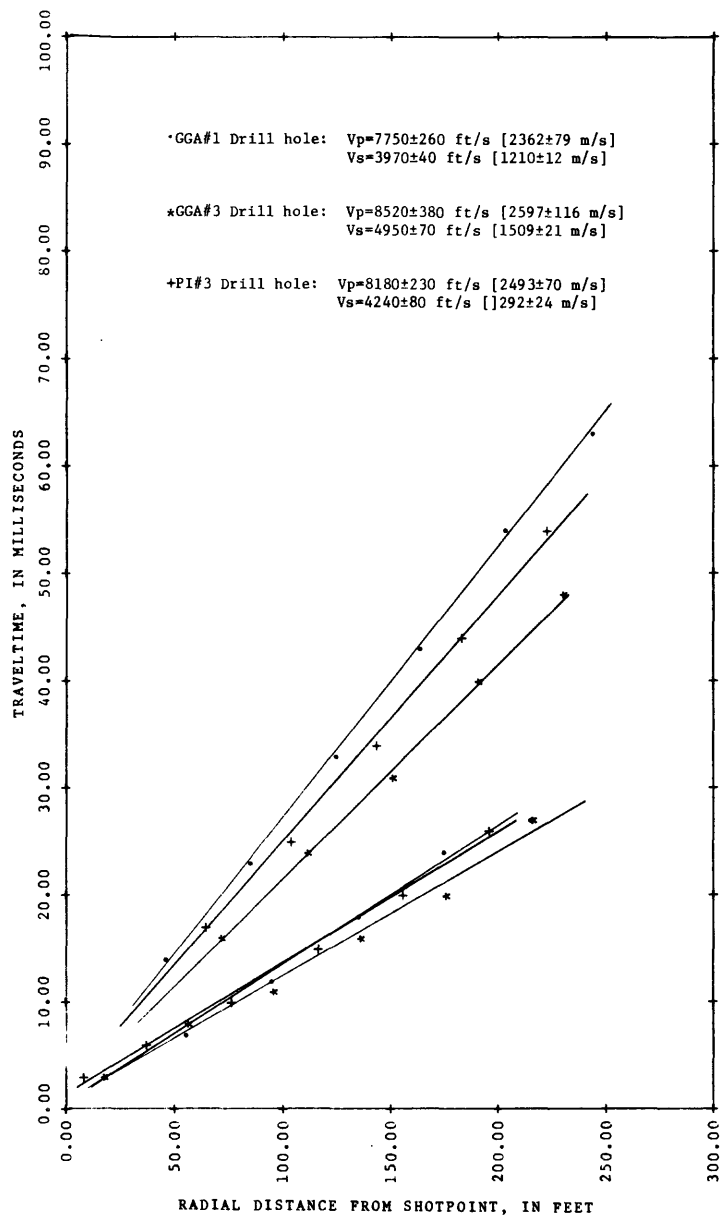
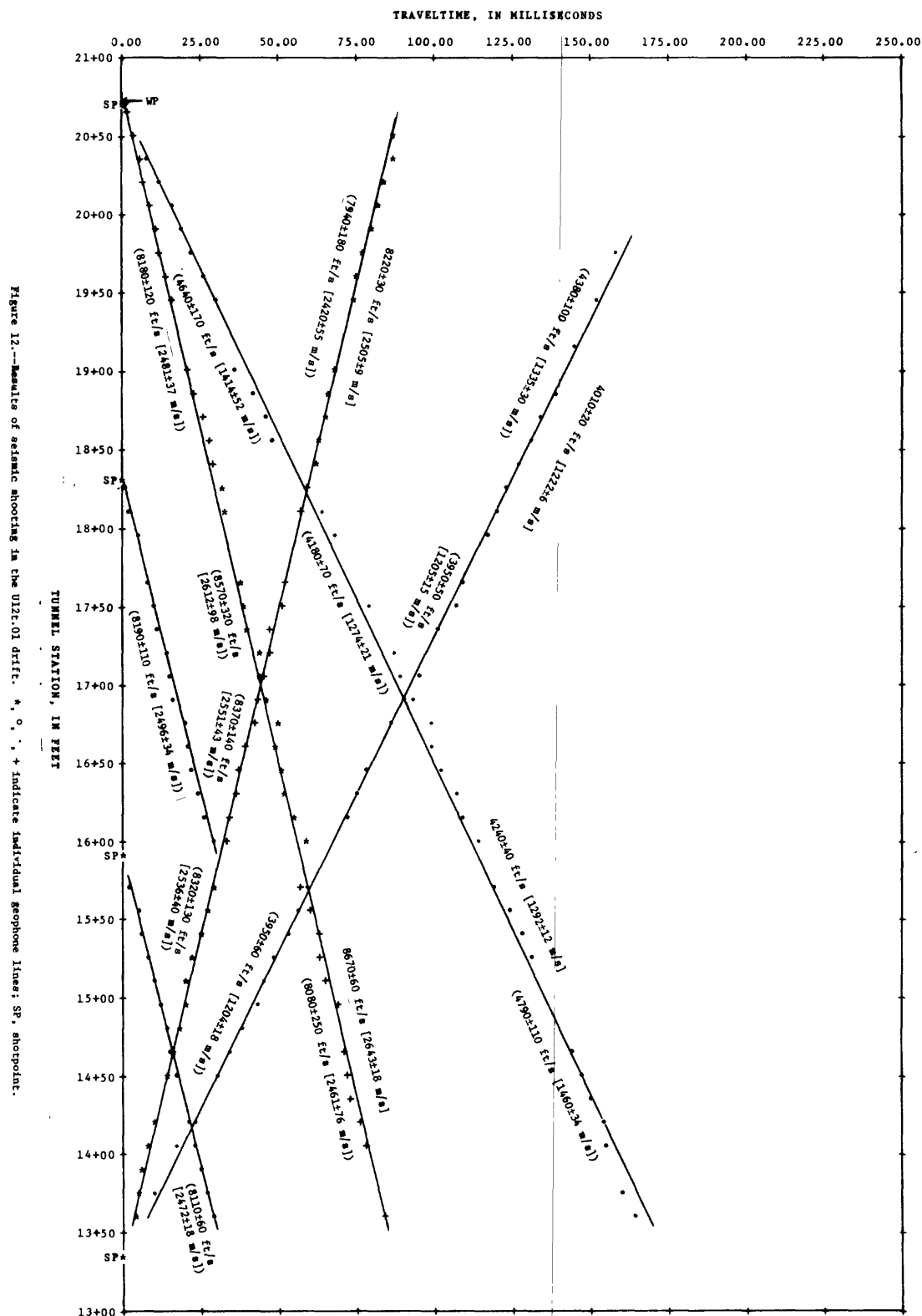


Figure 11.--Results of seismic shooting in drill holes radial from the cavity in U16a.06 drift

(Based on an assumed rock specific gravity of 1.90+0.05)

INTERVAL (feet) ^{1/}	COMPRESSIONAL VELOCITY (m/s)	SHEAR VELOCITY (m/s)	CHARACTERISTIC COMPRESSIONAL IMPEDANCE (10 ⁶ mks Rayls)	CHARACTERISTIC SHEAR IMPEDANCE (10 ⁶ mks Rayls)	POISSON'S RATIO	YOUNG'S MODULUS (kbar)	BULK MODULUS (kbar)	SHEAR MODULUS (kbar)
20+65 - 13+61	2643± 18	1292± 12	5.02±0.14	2.46±0.07	0.34±0.00	85.2±3.0	90.4±4.2	31.7±1.0
13+61 - 20+65	2505± 9	1222± 6	4.76±0.13	2.32±0.06	0.34±0.00	76.3±2.2	81.4±2.7	28.4±0.8

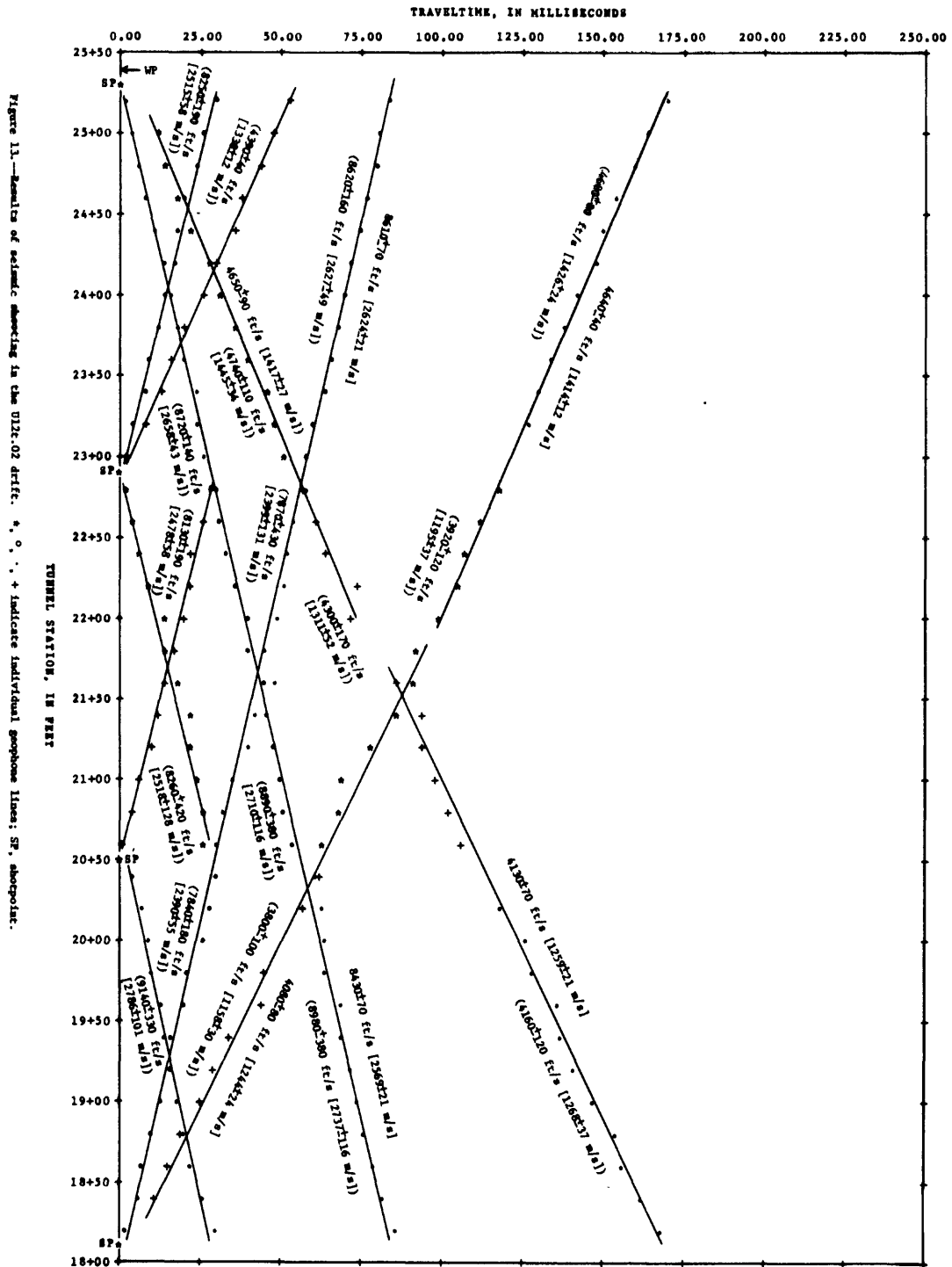
1/ meters = 0.3048 x feet



ACOUSTIC PARAMETERS
(Based on an assumed rock specific gravity of 1.90±0.03)

INTERVAL (feet) $\frac{1}{2}$	COMPRESSIONAL VELOCITY (m/s)	SHEAR VELOCITY (m/s)	CHARACTERISTIC COMPRESSIONAL IMPEDANCE (10 ⁶ mks Rayls)	CHARACTERISTIC SHEAR IMPEDANCE (10 ⁶ mks Rayls)	POISSON'S RATIO	YOUNG'S MODULUS (kbar)	BULK MODULUS (kbar)	SNEAR MODULUS (kbar)
25+20 - 22+00	2369± 21	1417± 27	4.88±0.13	2.69±0.09	0.28±0.01	97.6±4.4	74.6±5.6	38.2±1.8
21+60 - 18+20	2369± 21	1239± 21	4.88±0.13	2.39±0.07	0.34±0.01	80.8±3.6	85.3±5.7	30.1±1.3
18+20 - 21+80	2624± 21	1244± 24	4.99±0.14	2.36±0.08	0.36±0.01	79.6±3.8	91.7±6.7	29.4±1.4
22+00 - 23+20	2624± 21	1414± 12	4.99±0.14	2.69±0.07	0.30±0.01	98.3±3.5	80.2±3.9	38.0±1.2

$\frac{1}{2}$ meters = 0.3048 x feet

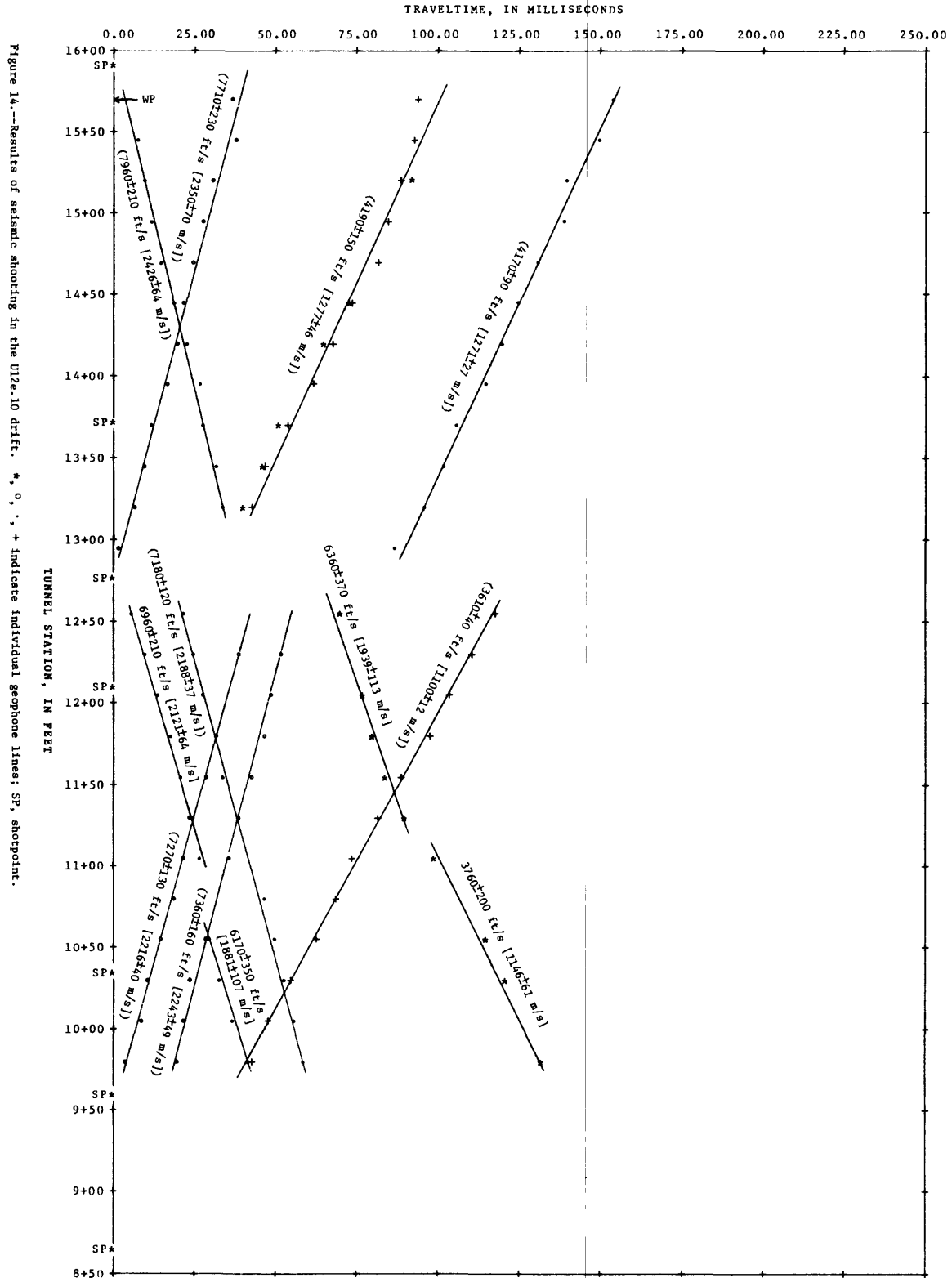


ACOUSTIC PARAMETERS

(Based on an assumed rock specific gravity of 1.90±0.05)

INTERVAL (feet)±1/	COMPRESSIONAL VELOCITY (m/s)	SHEAR VELOCITY (m/s)	CHARACTERISTIC COMPRESSIONAL IMPEDANCE (10 ⁶ mks Rayls)	CHARACTERISTIC SHEAR IMPEDANCE (10 ⁶ mks Rayls)	POISSON'S RATIO	YOUNG'S MODULUS (kbar)	BULK MODULUS (kbar)	SHEAR MODULUS (kbar)
15+70 - 12+95	2390± 67	1274± 37	4.54±0.17	2.42±0.09	0.30±0.02	80.3±7.1	67.4±9.6	30.8±1.9
12+55 - 9+80	2216± 43	1100± 12	4.21±0.14	2.09±0.06	0.34±0.01	61.5±3.7	62.6±5.3	23.0±0.8

1/ meters = 0.3048 x feet

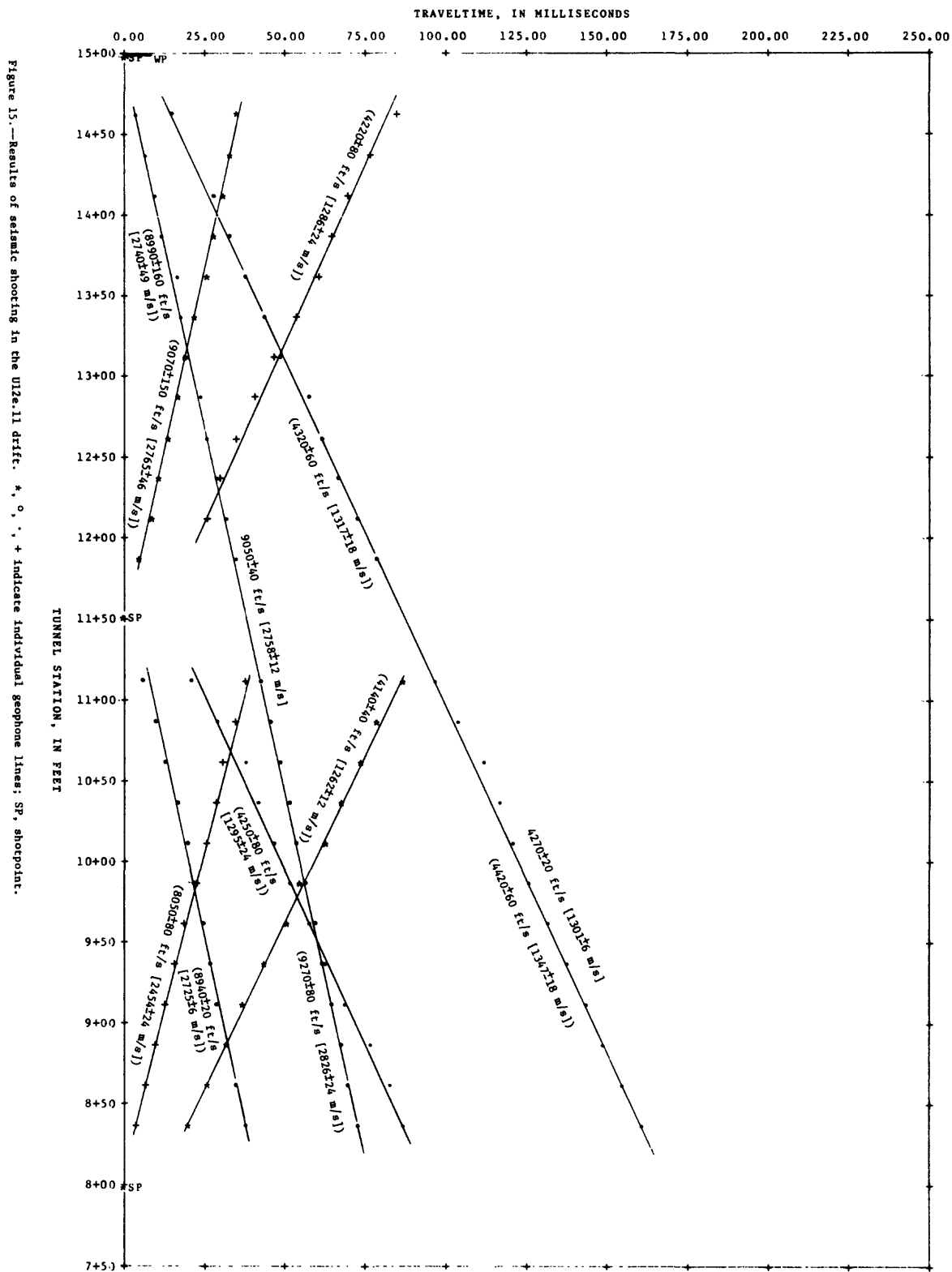


ACOUSTIC PARAMETERS

(based on an assumed rock specific gravity of 1.90±0.05)

INTERVAL (feet) ^{1/}	COMPRESSIONAL VELOCITY (m/s)	SHEAR VELOCITY (m/s)	CHARACTERISTIC COMPRESSIONAL IMPEDANCE (10 ⁶ mks Ravls)	CHARACTERISTIC SHEAR IMPEDANCE (10 ⁶ mks Ravls)	POISSON'S RATIO	YOUNG'S MODULUS (kbar)	BULK MODULUS (kbar)	SHEAR MODULUS (kbar)
14+62 - 8+37	2758± 12	1301± 6	5.24±0.14	2.47±0.07	0.36±0.00	87.3±2.6	101.7±3.5	32.2±0.9

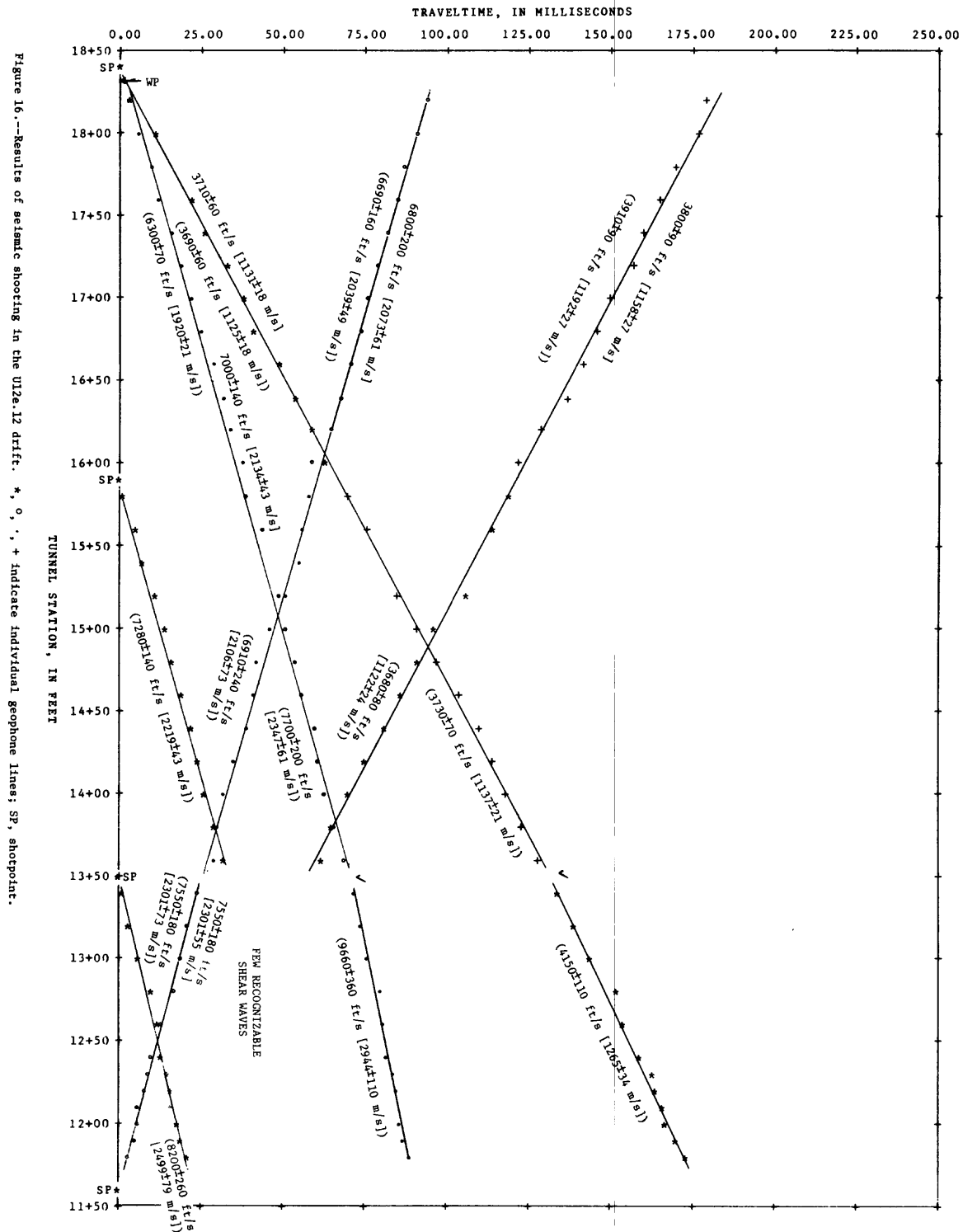
^{1/} meters = 0.3048 x feet



(Based on an assumed rock specific gravity of 1.90±0.05)

INTERVAL (feet) ^{1/}	COMPRESSIONAL VELOCITY (m/s)	SHEAR VELOCITY (m/s)	CHARACTERISTIC COMPRESSIONAL IMPEDANCE (10 ⁶ mks Rayls)	CHARACTERISTIC SHEAR IMPEDANCE (10 ⁶ mks Rayls)	POISSON'S RATIO	YOUNG'S MODULUS (kbar)	BULK MODULUS (kbar)	SHEAR MODULUS (kbar)
18+20 - 13+60	2134± 43	1131± 18	4.05±0.13	2.15±0.07	0.30±0.01	63.4±4.0	54.1±5.2	24.3±1.0
13+40 - 11+80	2944±110	1265± 34	5.59±0.26	2.40±0.09	0.39±0.01	84.3±9.6	124.2±19.9	30.4±1.8
11+80 - 13+40	2301± 55	---	4.37±0.16	---	---	---	---	---
13+60 - 18+20	2073± 61	1158± 27	3.94±0.16	2.20±0.08	0.27±0.02	64.9±5.5	47.6±6.6	25.5±1.4

1/ meters = 0.3048 x feet
Leaders (---) indicate no data.

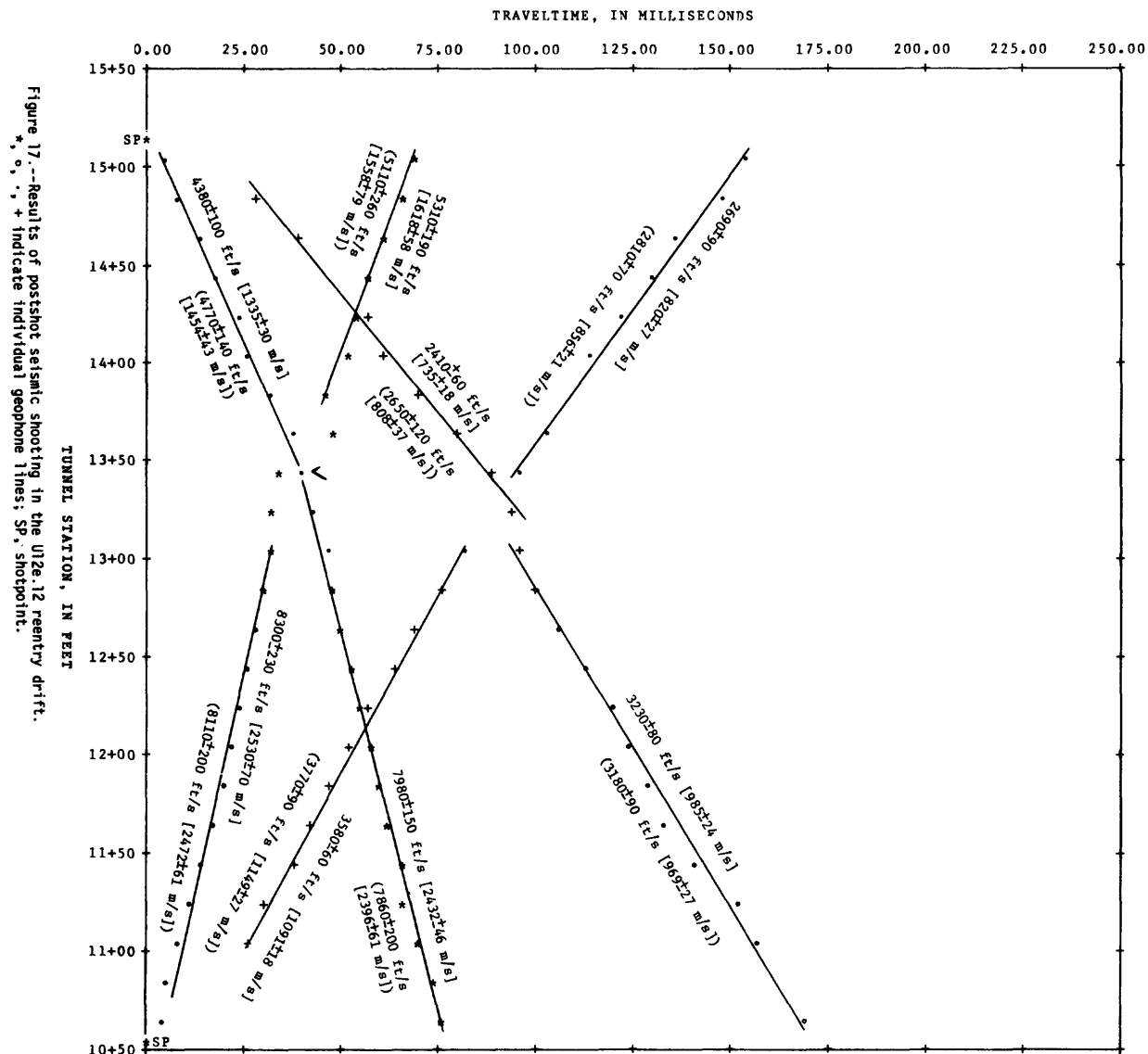


ACOUSTIC PARAMETERS

(Based on an assumed rock specific gravity of 1.90 ± 0.05)

INTERVAL (feet) $\frac{1}{2}$	COMPRESSIONAL VELOCITY (m/s)	SHEAR VELOCITY (m/s)	CHARACTERISTIC COMPRESSIONAL IMPEDANCE (10^6 mks Rayls)	CHARACTERISTIC SHEAR IMPEDANCE (10^6 mks Rayls)	POISSON'S RATIO	YOUNG'S MODULUS (kbar)	BULK MODULUS (kbar)	SHEAR MODULUS (kbar)
15+04 - 13+44	1335 ± 30	735 ± 18	2.54 ± 0.09	1.40 ± 0.05	0.28 ± 0.02	26.3 ± 1.9	20.2 ± 2.5	10.3 ± 0.6
13+24 - 10+64	2432 ± 46	985 ± 24	4.62 ± 0.15	1.87 ± 0.07	0.40 ± 0.01	51.6 ± 3.8	87.9 ± 9.2	18.4 ± 1.0
10+64 - 13+44	2530 ± 70	1091 ± 18	4.81 ± 0.18	2.07 ± 0.06	0.39 ± 0.01	62.7 ± 5.3	91.4 ± 10.5	22.6 ± 1.0
13+64 - 15+04	1618 ± 58	820 ± 27	3.08 ± 0.14	1.56 ± 0.07	0.33 ± 0.02	33.9 ± 3.8	32.7 ± 5.6	12.8 ± 0.9

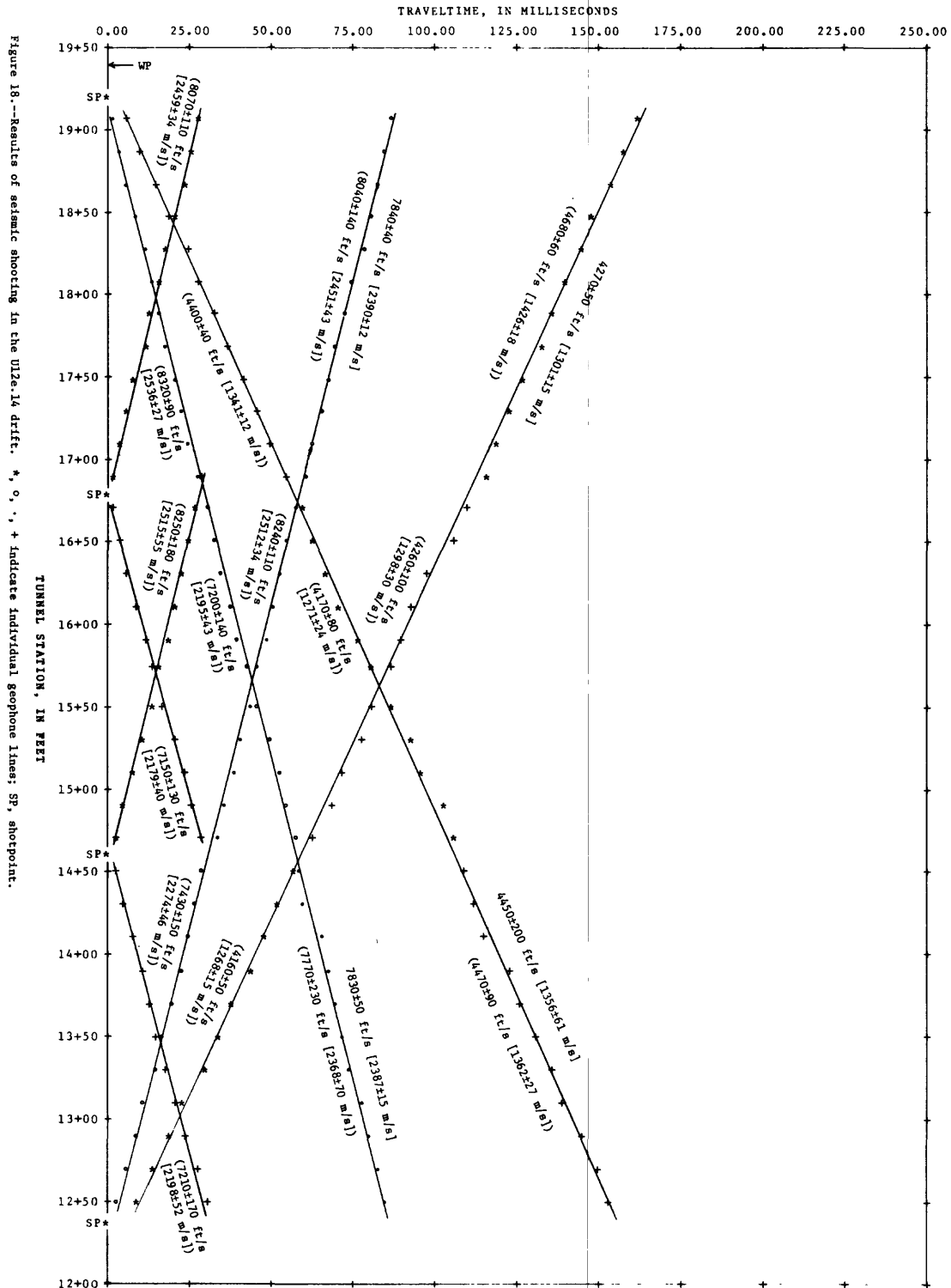
$\frac{1}{2}$ meters = $0.3048 \times$ feet



ACOUSTIC PARAMETERS
(Based on an assumed rock specific gravity of 1.90 ± 0.05)

INTERVAL (feet) $\frac{1}{2}$	COMPRESSIONAL VELOCITY (m/s)	SHEAR VELOCITY (m/s)	CHARACTERISTIC COMPRESSIONAL IMPEDANCE (10^6 mks Rayls)	CHARACTERISTIC SHEAR IMPEDANCE (10^6 mks Rayls)	POISSON'S RATIO	YOUNG'S MODULUS (kbar)	BULK MODULUS (kbar)	SHEAR MODULUS (kbar)
12+50 - 19+07	2390 ± 12	1301 ± 15	4.54 ± 0.12	2.48 ± 0.07	0.29 ± 0.01	83.3 ± 2.9	65.4 ± 3.3	32.3 ± 1.1
19+07 - 12+50	2387 ± 15	1356 ± 61	4.53 ± 0.12	2.58 ± 0.13	0.26 ± 0.03	38.2 ± 6.3	61.6 ± 9.4	35.0 ± 3.3

$\frac{1}{2}$ meters = $0.3048 \times$ feet



ACOUSTIC PARAMETERS

(Based on an assumed rock specific gravity of 1.90 ± 0.05)

INTERVAL (feet) $\frac{1}{2}$	COMPRESSIONAL VELOCITY (m/s)	SHEAR VELOCITY (m/s)	CHARACTERISTIC COMPRESSIONAL IMPEDANCE (10^6 mks Rayls)	CHARACTERISTIC SHEAR IMPEDANCE (10^6 mks Rayls)	POISSON'S RATIO	YOUNG'S MODULUS (kbar)	BULK MODULUS (kbar)	SHEAR MODULUS (kbar)
0+71 - 2+47	2438 ± 0	1292 ± 15	4.63 ± 0.12	2.46 ± 0.07	0.30 ± 0.01	82.8 ± 2.7	70.7 ± 3.3	31.7 ± 1.1
2+47 - 0+71	2457 ± 27	1301 ± 18	4.67 ± 0.13	2.47 ± 0.07	0.30 ± 0.01	84.0 ± 3.8	71.8 ± 4.8	32.2 ± 1.2

$\frac{1}{2}$ meters = 0.3048 x feet

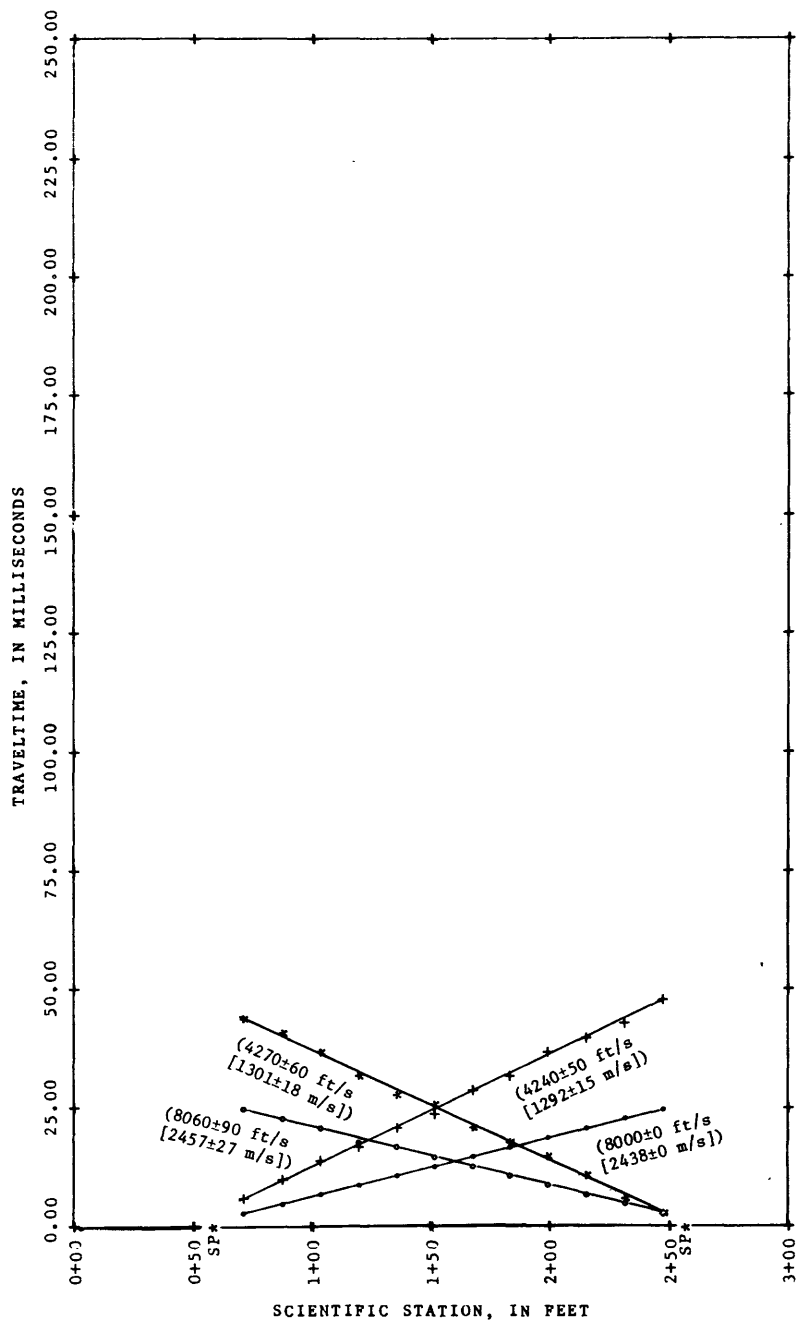


Figure 19.--Results of seismic shooting in the U12e.14 HFR drift.
*, o, ., + indicate individual geophone lines; SP, shotpoint.

ACOUSTIC PARAMETERS

(Based on an assumed rock specific gravity of 1.90 ± 0.05)

INTERVAL (feet) $\frac{1}{2}$	COMPRESSIONAL VELOCITY (m/s)	SHEAR VELOCITY (m/s)	CHARACTERISTIC COMPRESSIONAL IMPEDANCE (10^6 mks Rayls)	CHARACTERISTIC SHEAR IMPEDANCE (10^6 mks Rayls)	POISSON'S RATIO	YOUNG'S MODULUS (kbar)	BULK MODULUS (kbar)	SHEAR MODULUS (kbar)
0+14 - 0+64	2121 ± 119	978 ± 37	4.03 ± 0.25	1.86 ± 0.08	0.36 ± 0.02	49.7 ± 8.2	61.3 ± 14.5	18.2 ± 1.4

$\frac{1}{2}$ meters = 0.3048 x feet

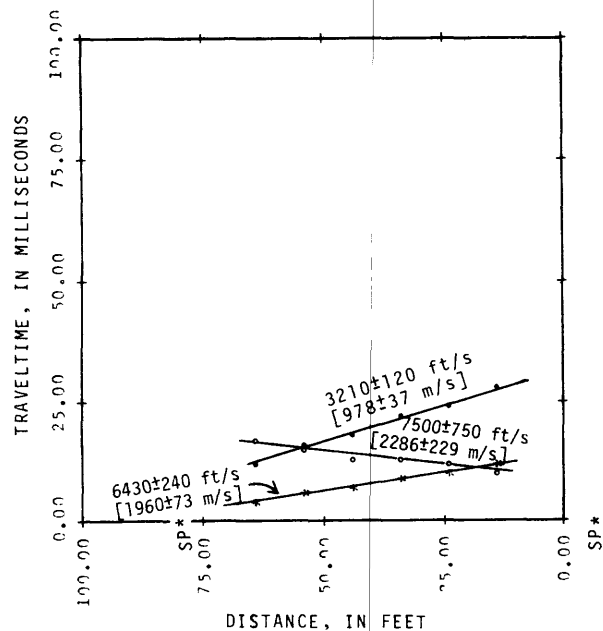


Figure 20.--Results of seismic shooting in the U12e.16 drift. Distance measured from the center line in the U12e.06 drift. *, o, ., + indicate individual geophone lines; SP, shotpoint.

ACOUSTIC PARAMETERS

(Based on an assumed rock specific gravity of 1.90 ± 0.05)

INTERVAL (feet) $\frac{1}{2}$	COMPRESSIONAL VELOCITY (m/s)	SHEAR VELOCITY (m/s)	CHARACTERISTIC COMPRESSIONAL IMPEDANCE (10^6 mks Rayls)	CHARACTERISTIC SHEAR IMPEDANCE (10^6 mks Rayls)	POISSON'S RATIO	YOUNG'S MODULUS (kbar)	BULK MODULUS (kbar)	SHEAR MODULUS (kbar)
0+09 - 0+69	1765 ± 94	844 ± 58	3.35 ± 0.20	1.60 ± 0.12	0.35 ± 0.03	36.6 ± 6.8	41.1 ± 12.0	13.5 ± 1.9

$\frac{1}{2}$ meters = 0.3048 x feet

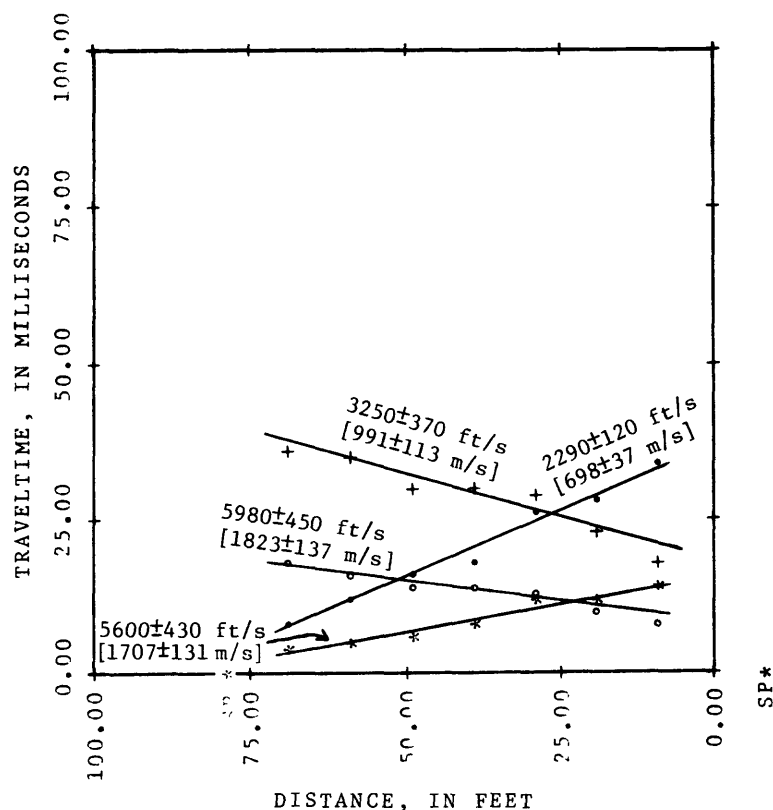
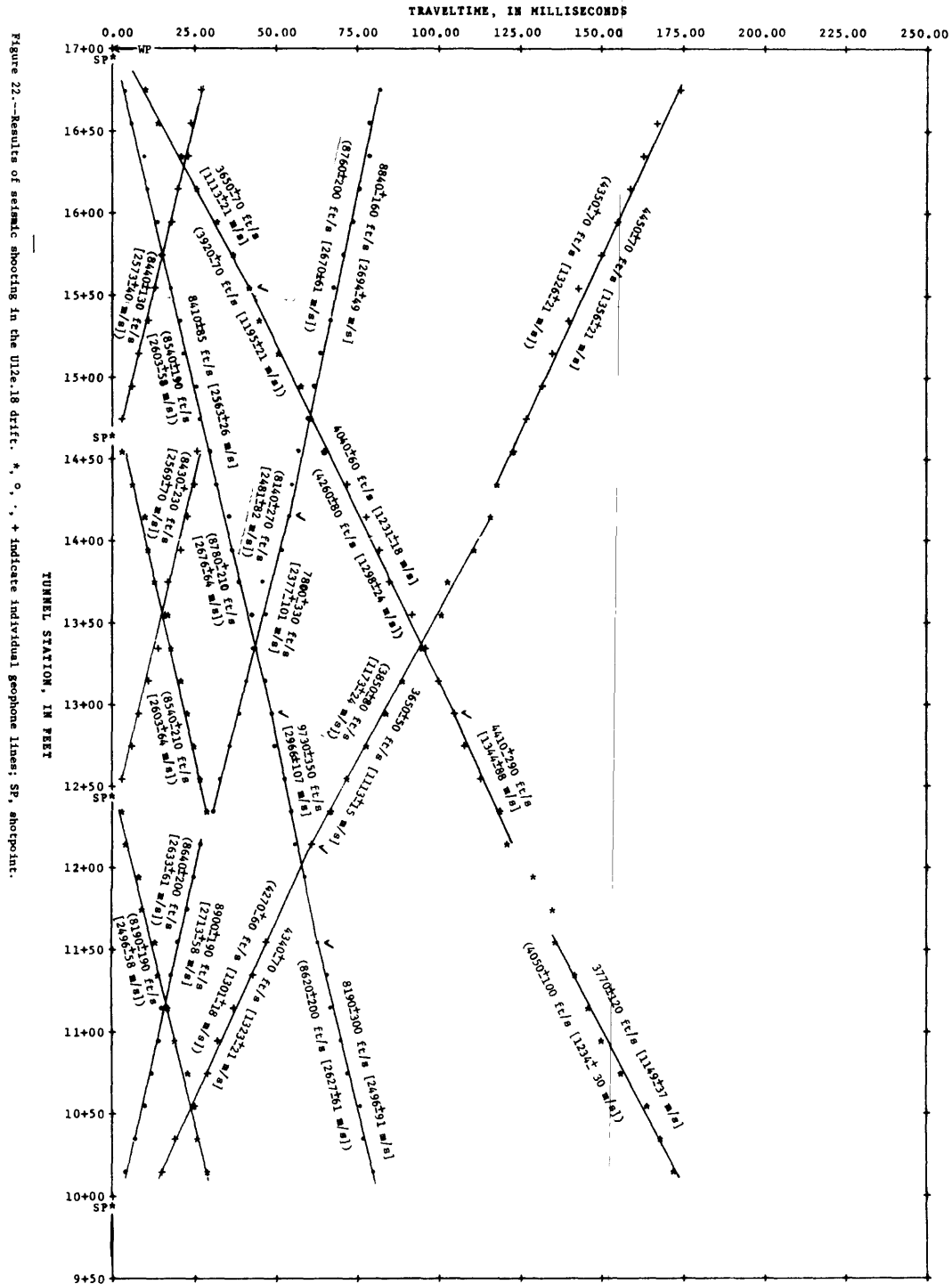


Figure 21.-- Results of seismic shooting in the U12e.17 drift. Distance measured from the center line in the U12e.06 drift. *, °, ·, + indicate individual geophone lines; SP, shotpoint.

(Based on an assumed rock specific gravity of 1.90 ± 0.05)

INTERVAL (feet) ^{1/}	COMPRESSIONAL VELOCITY (m/s)	SHEAR VELOCITY (m/s)	CHARACTERISTIC COMPRESSIONAL IMPEDANCE (10 ⁶ mks Rayls)	CHARACTERISTIC SHEAR IMPEDANCE (10 ⁶ mks Rayls)	POISSON'S RATIO	YOUNG'S MODULUS (kber)	BULK MODULUS (kbar)	SHEAR MODULUS (kbar)
16+75 - 15+55	2563 _± 26	1113 _± 21	4.87 _± 0.14	2.11 _± 0.07	0.38 _± 0.01	65.1 _± 3.3	93.5 _± 6.9	23.5 _± 1.1
15+55 - 12+95	2563 _± 26	1231 _± 18	4.87 _± 0.14	2.34 _± 0.07	0.35 _± 0.01	77.8 _± 3.5	86.4 _± 5.6	28.8 _± 1.1
12+95 - 12+15	2966 _± 107	1344 _± 88	5.63 _± 0.25	2.55 _± 0.18	0.37 _± 0.02	94.1 _± 14.4	121.3 _± 29.5	34.3 _± 4.6
11+55 - 10+15	2496 _± 91	1149 _± 37	4.74 _± 0.21	2.18 _± 0.09	0.37 _± 0.02	68.5 _± 7.9	84.9 _± 14.3	25.1 _± 1.7
10+15 - 12+15	2713 _± 58	1323 _± 21	5.15 _± 0.17	2.51 _± 0.08	0.34 _± 0.01	89.4 _± 6.0	95.5 _± 9.3	33.2 _± 1.4
12+35 - 14+15	2377 _± 101	1113 _± 15	4.52 _± 0.23	2.11 _± 0.06	0.36 _± 0.02	64.0 _± 7.5	76.0 _± 12.4	23.5 _± 0.9
14+35 - 16+75	2694 _± 49	1356 _± 21	5.12 _± 0.16	2.58 _± 0.08	0.33 _± 0.01	93.0 _± 5.6	91.3 _± 8.0	35.0 _± 1.4

1/ meters = 0.3048 x feet



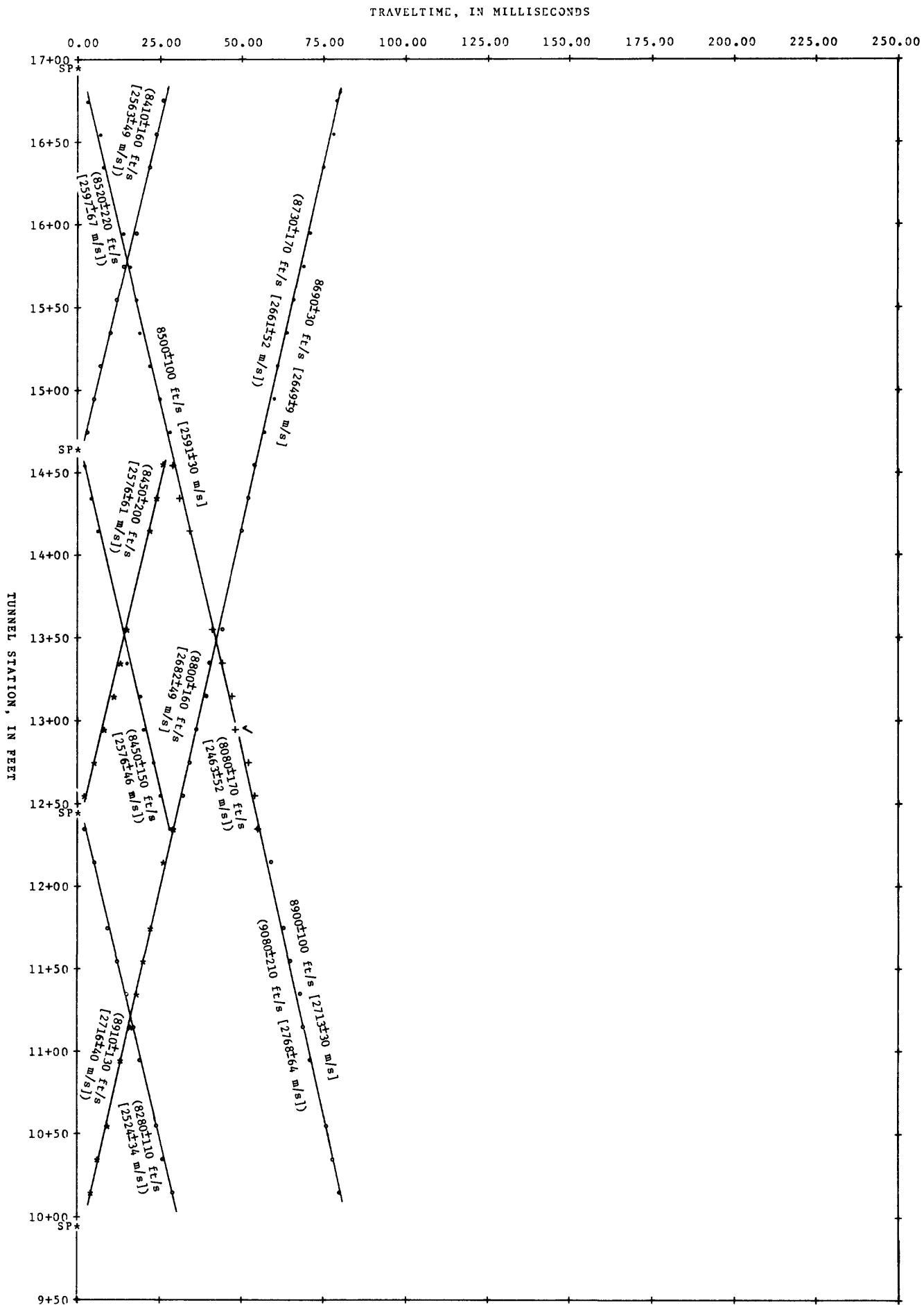


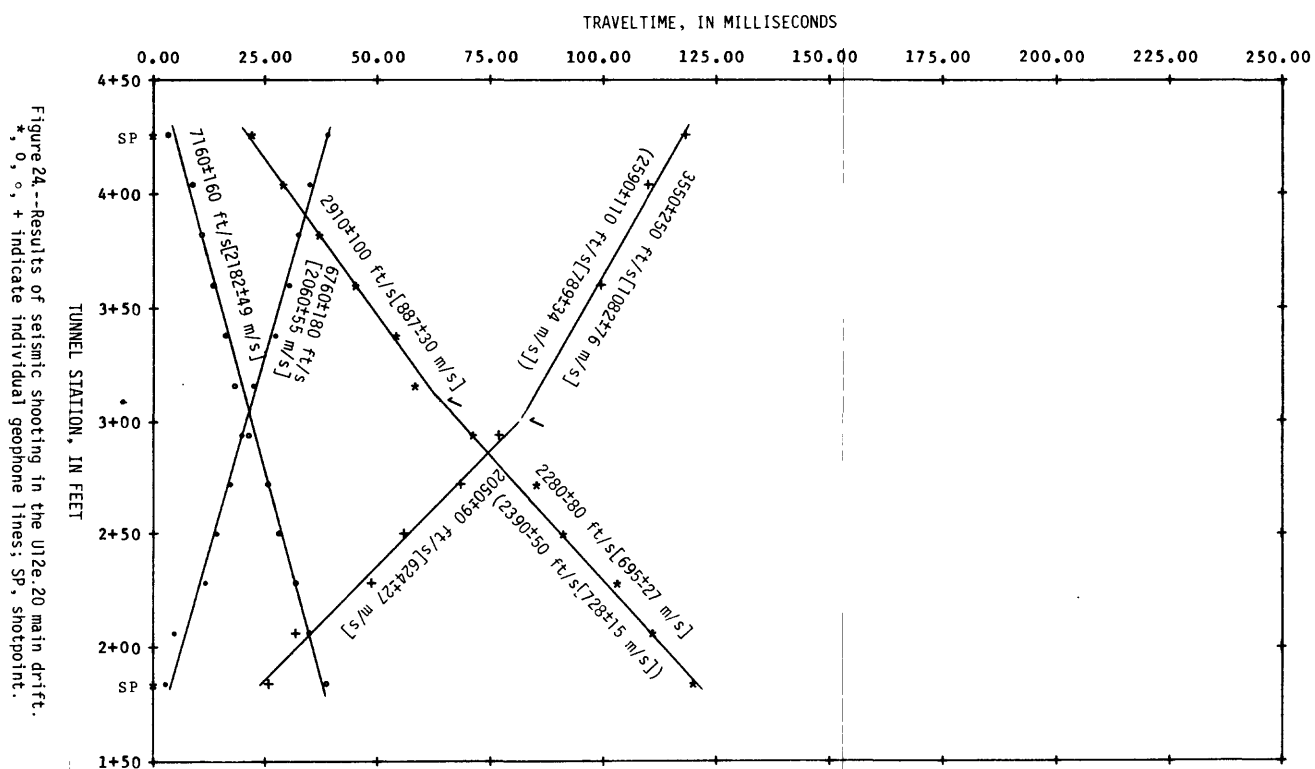
Figure 23.—Results of repeat seismic shooting in the U12e.18 drift.
 *, o, + indicate individual geophone lines; SP, shotpoint.

ACOUSTIC PARAMETERS

(Based on an assumed rock specific gravity of 1.90±0.05)

INTERVAL (feet) ^{1/}	COMPRESSIONAL VELOCITY (m/s)	SHEAR VELOCITY (m/s)	CHARACTERISTIC COMPRESSIONAL IMPEDANCE (10 ⁶ mks Rayls)	CHARACTERISTIC SHEAR IMPEDANCE (10 ⁶ mks Rayls)	POISSON'S RATIO	YOUNG'S MODULUS (kbar)	BULK MODULUS (kbar)	SHEAR MODULUS (kbar)
1+84 - 2+94	2060± 55	624± 27	3.91±0.15	1.19±0.06	0.44±0.01	21.5±2.5	70.8±11.4	7.4±0.7
3+16 - 4+26	2060± 55	1082± 76	3.91±0.15	2.06±0.15	0.31±0.04	58.3±7.8	51.0±12.6	22.2±3.2
4+26 - 3+16	2182± 49	887± 30	4.15±0.14	1.69±0.07	0.40±0.01	41.9±3.8	70.6±9.5	14.9±1.1
2+94 - 1+84	2182± 49	695± 27	4.15±0.14	1.32±0.06	0.44±0.01	26.5±2.7	78.3±11.2	9.2±0.8

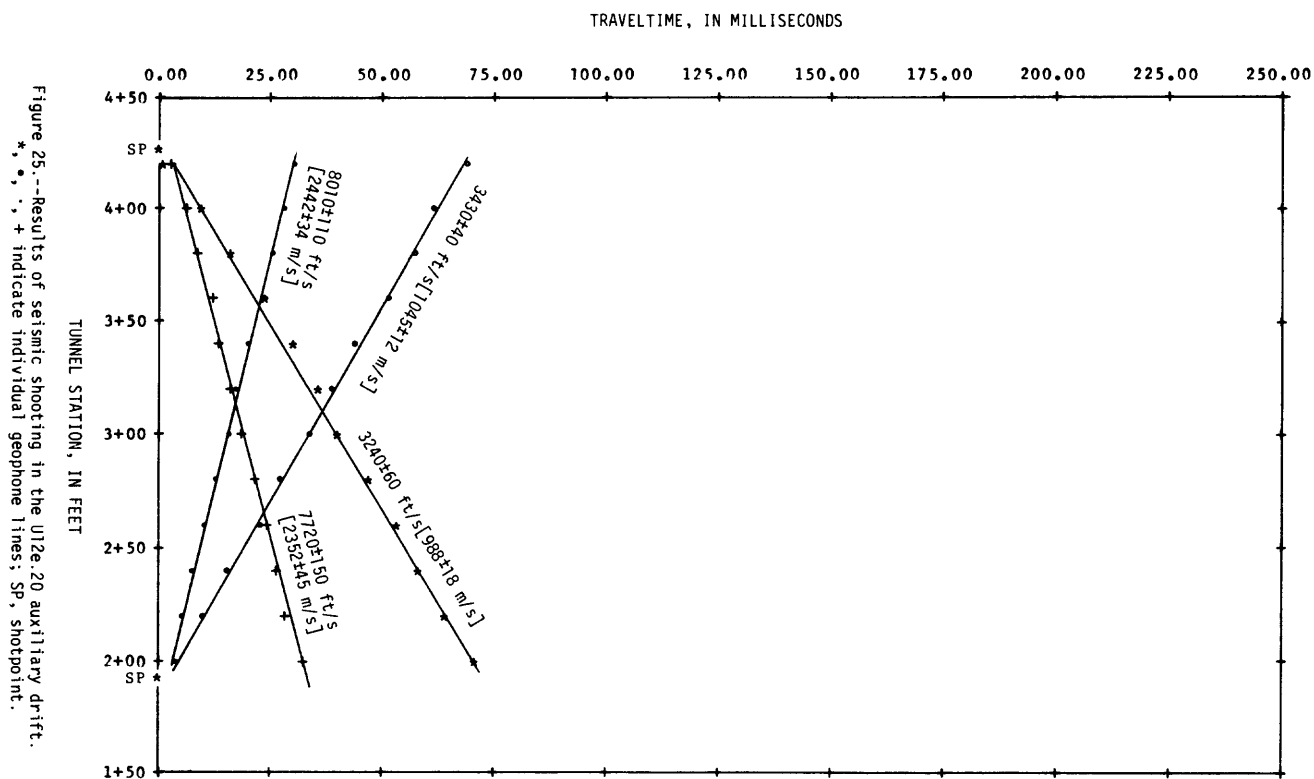
^{1/} meters = 0.3048 x feet

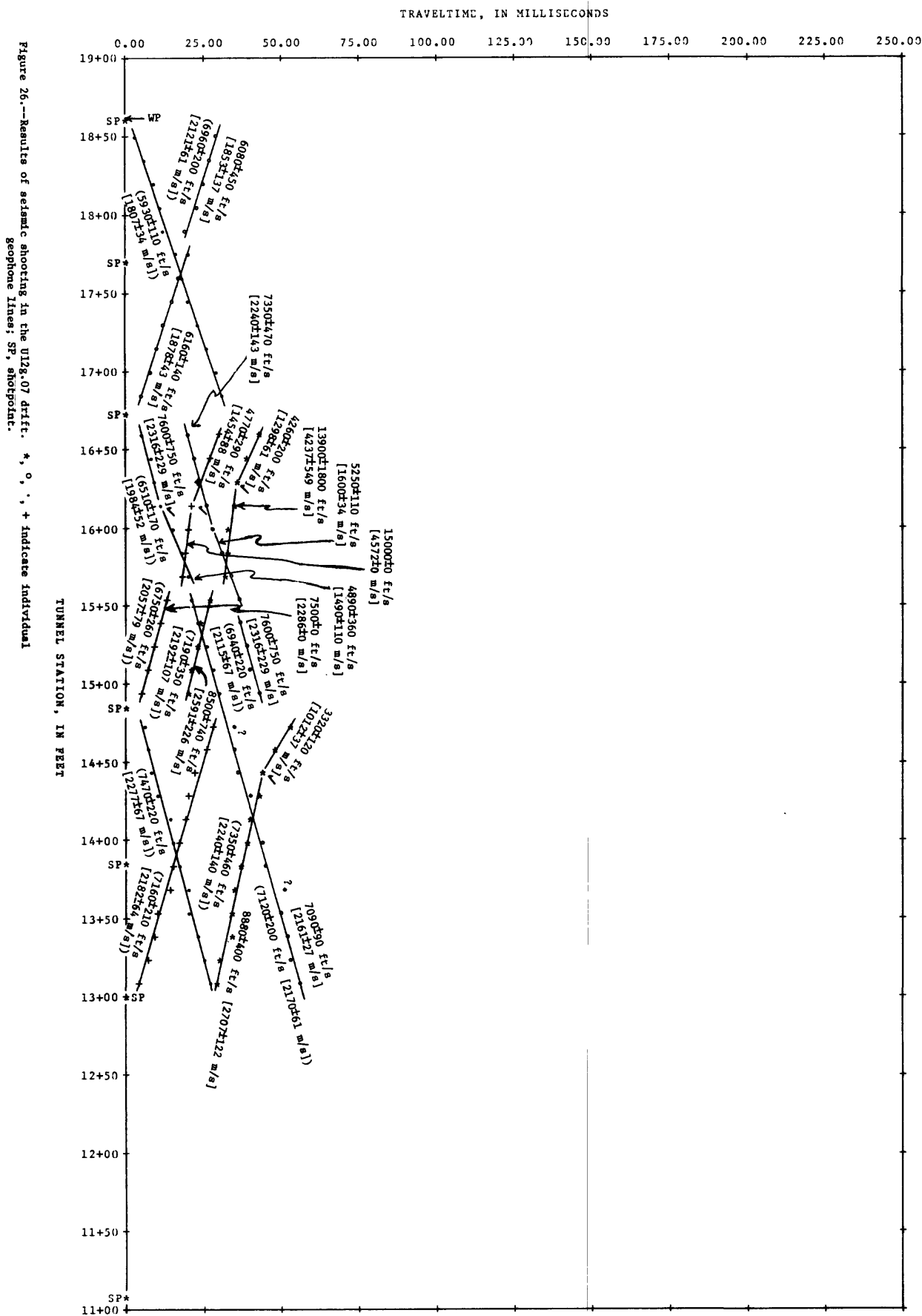


ACOUSTIC PARAMETERS
(Based on an assumed rock specific gravity of 1.90 ± 0.05)

INTERVAL (feet) $\frac{1}{2}$	COMPRESSIONAL VELOCITY (m/s)	SHEAR VELOCITY (m/s)	CHARACTERISTIC COMPRESSIONAL IMPEDANCE (10^6 mks Rayls)	CHARACTERISTIC SHEAR IMPEDANCE (10^6 mks Rayls)	POISSON'S RATIO	YOUNG'S MODULUS (kbar)	BULK MODULUS (kbar)	SHEAR MODULUS (kbar)
2+00 - 4+20	2442 ± 34	1045 ± 12	4.64 ± 0.14	1.99 ± 0.06	0.39 ± 0.00	57.6 ± 2.9	85.6 ± 5.7	20.8 ± 0.7
4+20 - 2+00	2353 ± 46	988 ± 18	4.47 ± 0.15	1.88 ± 0.06	0.39 ± 0.01	51.6 ± 3.5	80.5 ± 7.6	18.5 ± 0.8

$\frac{1}{2}$ meters = 0.3048 x feet



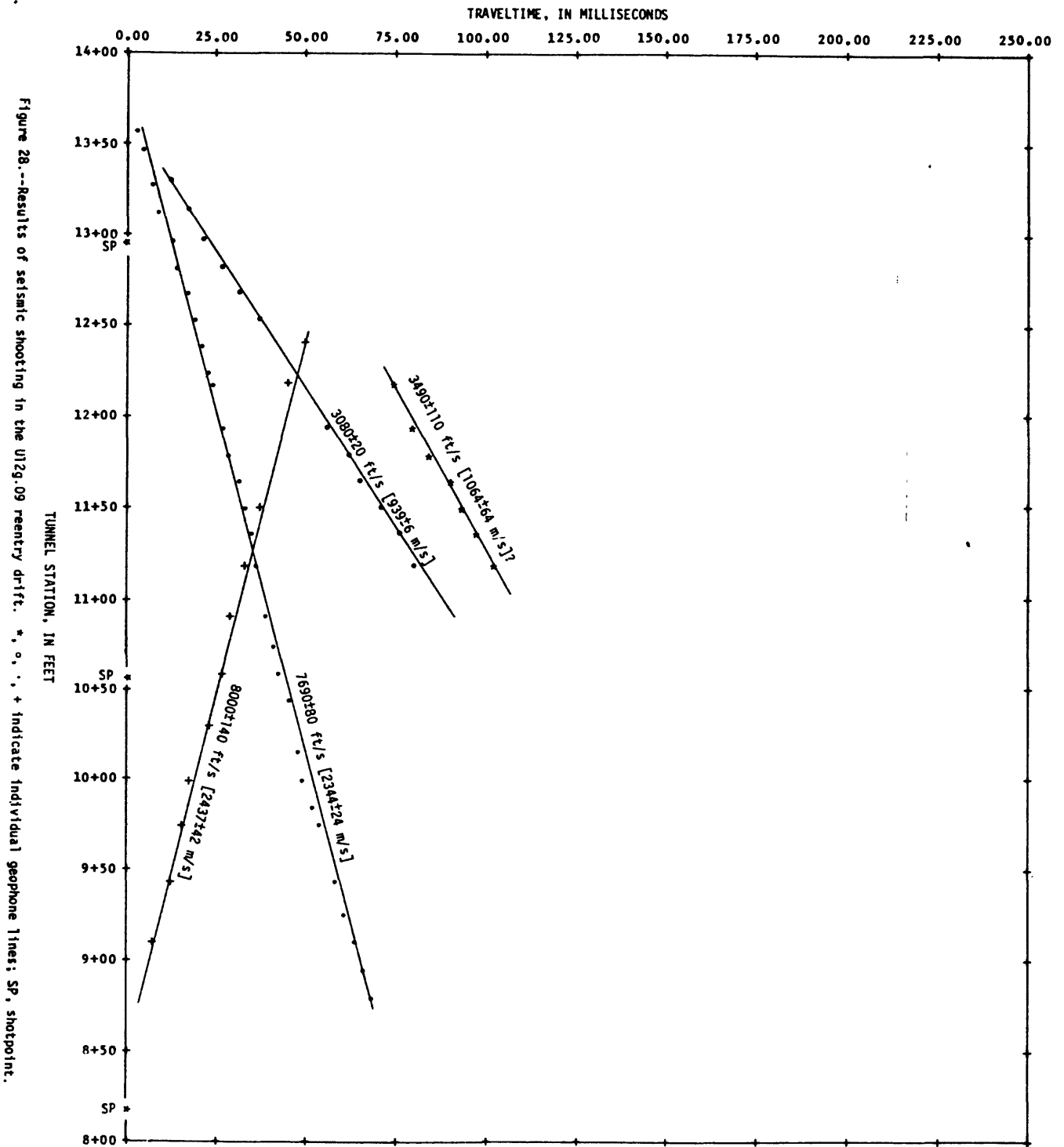


ACOUSTIC PARAMETERS

(Based on an assumed rock specific gravity of 1.90 ± 0.05)

INTERVAL (feet) $\frac{1}{2}$	COMPRESSIONAL VELOCITY (m/s)	SHEAR VELOCITY (m/s)	CHARACTERISTIC COMPRESSIONAL IMPEDANCE (10^6 mks Rayls)	CHARACTERISTIC SHEAR IMPEDANCE (10^6 mks Rayls)	POISSON'S RATIO	YOUNG'S MODULUS (kbar)	BULK MODULUS (kbar)	SHEAR MODULUS (kbar)
10+91 - 13+59	2344 ± 24	939 ± 6	4.45 ± 0.13	1.78 ± 0.48	0.40 ± 0.03	47.0 ± 1.9	82.1 ± 4.1	16.7 ± 0.5

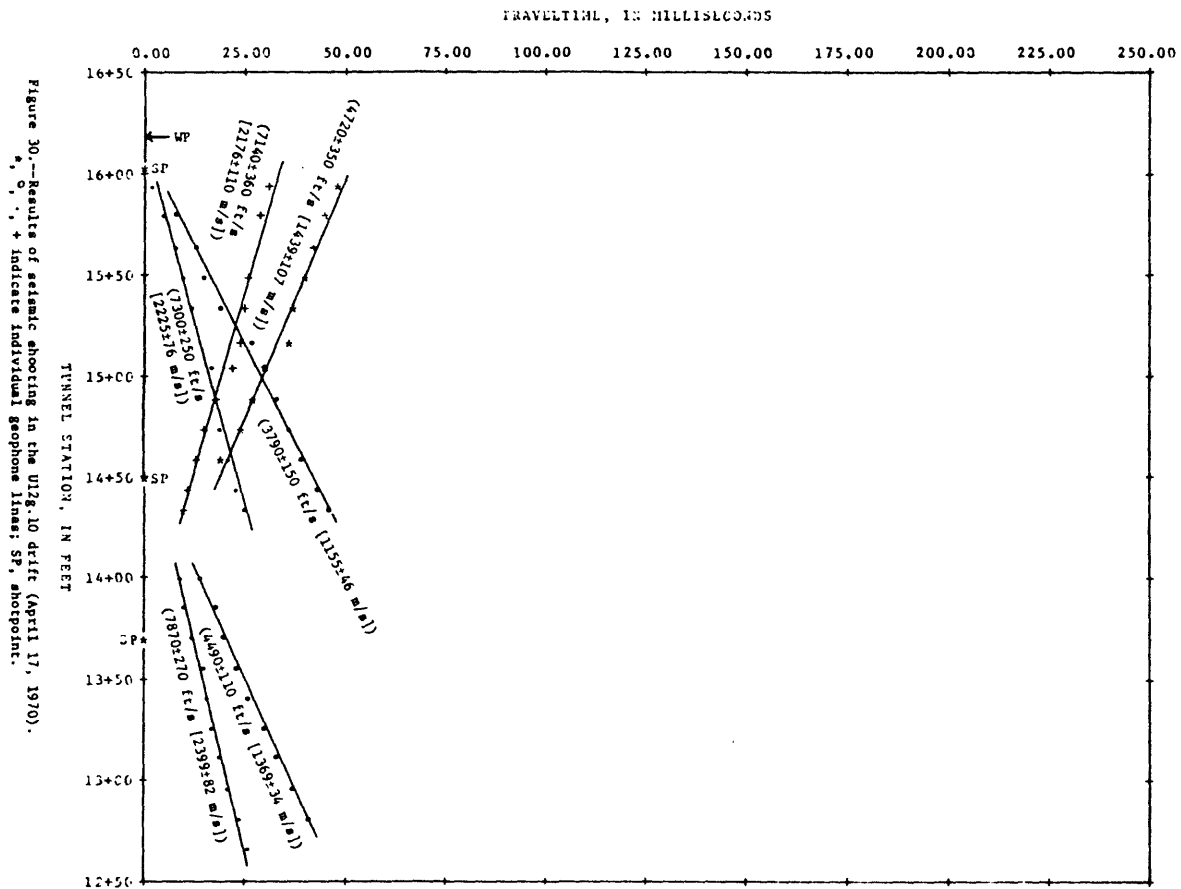
$\frac{1}{2}$ meters = 0.3048 x feet



ACOUSTIC PARAMETERS
(Based on an assumed rock specific gravity of 1.90 ± 0.05)

INTERVAL (feet) ^{1/}	COMPRESSIONAL VELOCITY (m/s)	SHEAR VELOCITY (m/s)	CHARACTERISTIC COMPRESSIONAL IMPEDANCE (10^6 nks Ravls)	CHARACTERISTIC SHEAR IMPEDANCE (10^6 nks Ravls)	POISSON'S RATIO	YOUNG'S MODULUS (kbar)	BULK MODULUS (kbar)	SHEAR MODULUS (kbar)
15+94 - 14+34	2225 ± 76	1155 ± 46	4.23 ± 0.18	2.19 ± 0.10	0.31 ± 0.03	66.7 ± 7.5	60.3 ± 11.0	25.4 ± 2.1
14+34 - 15+94	2176 ± 110	1439 ± 107	4.13 ± 0.24	2.73 ± 0.22	0.11 ± 0.12	87.4 ± 10.9	37.6 ± 12.8	39.3 ± 5.9

^{1/} meters = $0.3048 \times$ feet



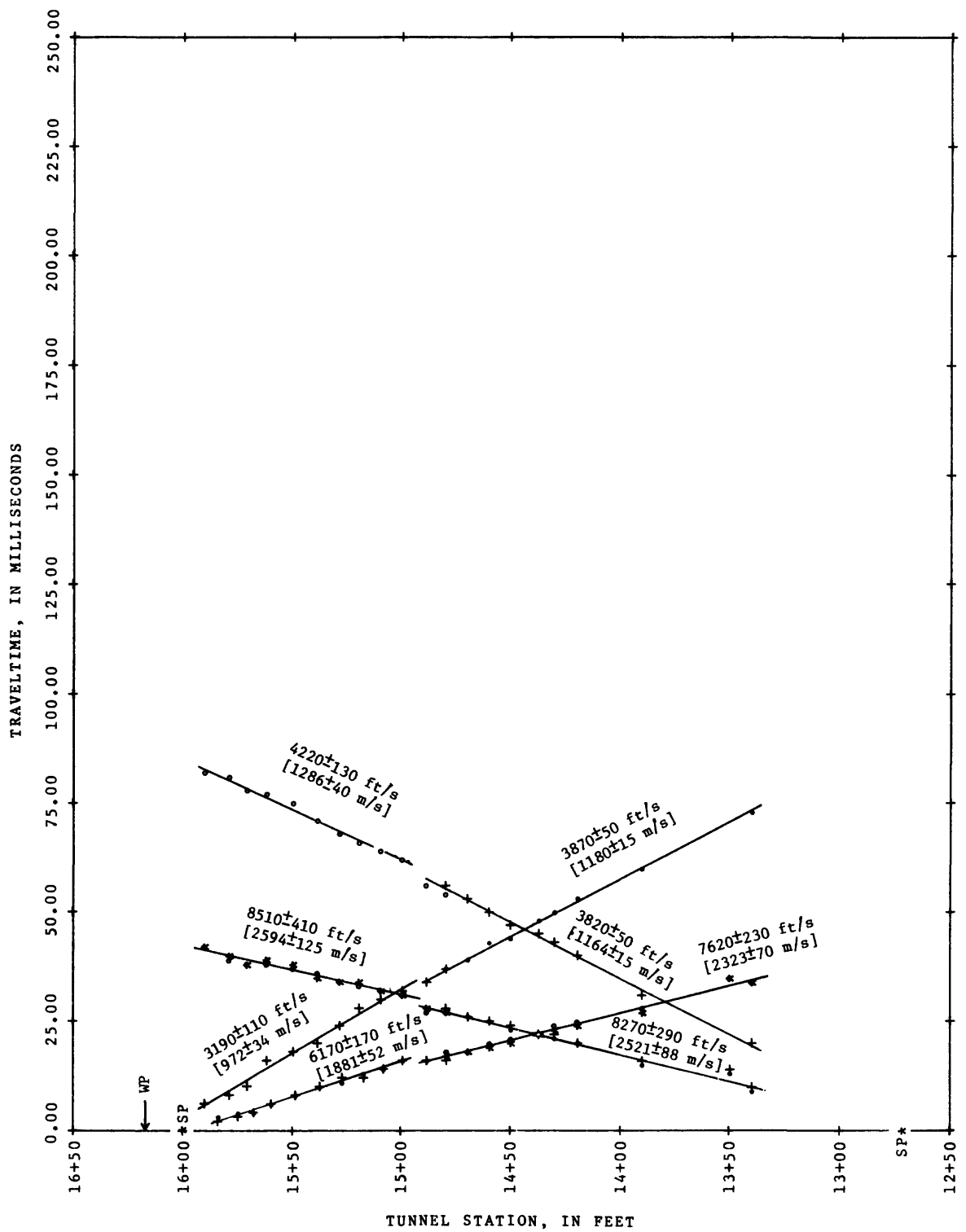
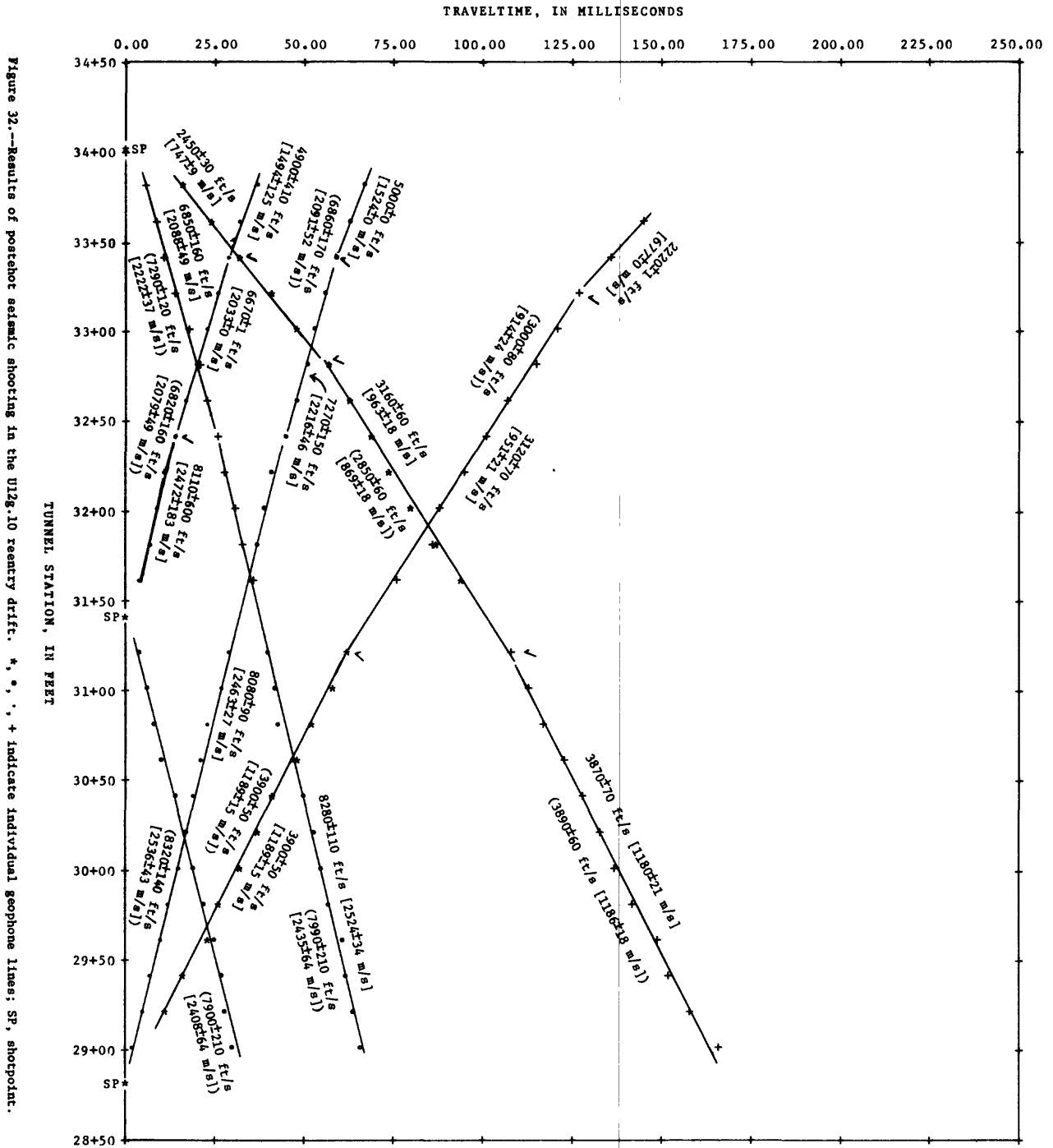


Figure 31.--Results of seismic shooting in the U12g.10 experiment drift (March 1971).
*, °, ·, + indicate individual geophone lines; SP, shotpoint.

ACOUSTIC PARAMETERS
(Based on an assumed rock specific gravity of 1.90±0.05)

INTERVAL (feet) 1/	COMPRESSIONAL VELOCITY (m/s)	SHEAR VELOCITY (m/s)	CHARACTERISTIC COMPRESSIONAL IMPEDANCE (10 ⁶ mks Rayls)	CHARACTERISTIC SHEAR IMPEDANCE (10 ⁶ mks Rayls)	POISSON'S RATIO	YOUNG'S MODULUS (kbar)	BULK MODULUS (kbar)	SHEAR MODULUS (kbar)
33+83 - 32+63	2088± 49	747± 9	3.97±0.14	1.42±0.04	0.43±0.00	30.2±2.2	68.7±6.5	10.6±0.4
32+63 - 31+11	2524± 34	963± 18	4.80±0.14	1.83±0.06	0.41±0.00	49.9±2.8	97.5±7.7	17.6±0.8
31+11 - 29+02	2524± 34	1180± 21	4.80±0.14	2.24±0.07	0.36±0.01	71.9±3.9	85.8±6.8	26.4±1.2
29+02 - 31+23	2463± 27	1189± 15	4.68±0.13	2.26±0.07	0.35±0.01	72.4±3.3	79.4±5.0	26.8±1.0
31+23 - 33+23	2216± 46	951± 21	4.21±0.14	1.81±0.06	0.39±0.01	47.7±3.5	70.4±7.4	17.2±0.9
33+23 - 33+83	1524± 0	677± 0	2.90±0.08	1.29±0.03	0.38±0.00	24.0±0.0	32.5±0.9	8.7±0.2

1/ meters = 0.3048 x feet



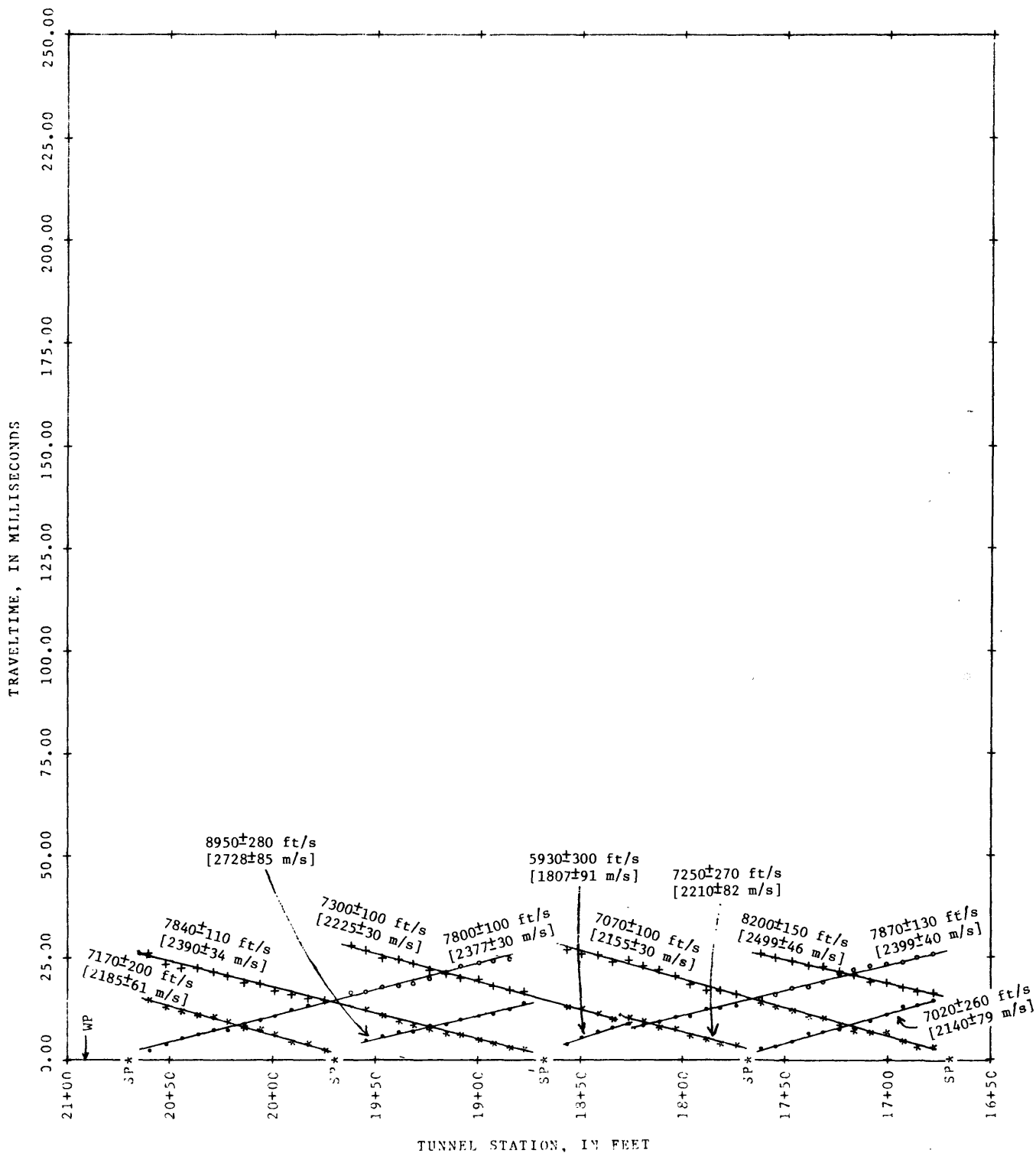


Figure 34.--Results of seismic shooting in the U12n.02 drift. *, °, ·, + indicate individual geophone lines; SP, shotpoint.

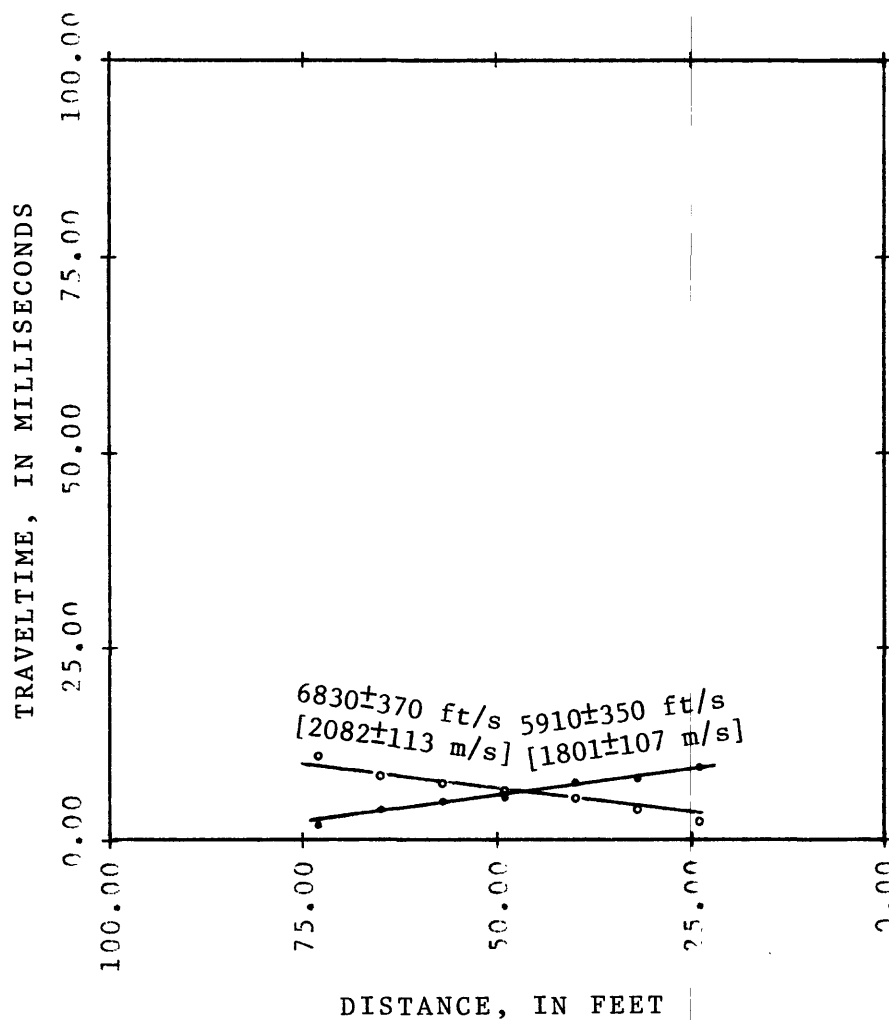


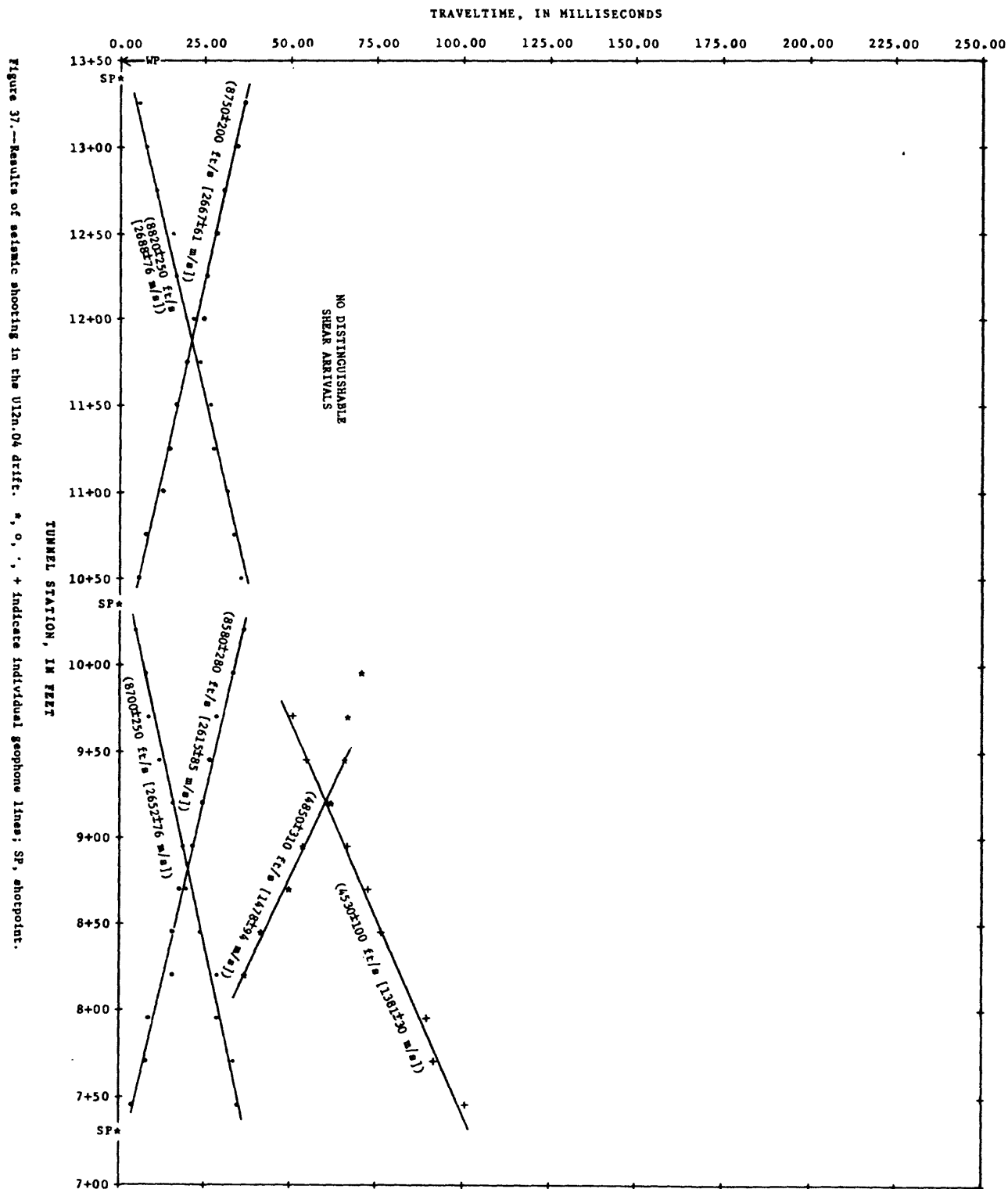
Figure 35.--Results of seismic shooting in the U12n.02 hook drift.
Distance measured from working point in U12n.02 main drift.
°, ·, indicate individual geophone lines.

ACOUSTIC PARAMETERS

(Based on an assumed rock specific gravity of 1.90±0.05)

INTERVAL (feet) ^{1/}	COMPRESSIONAL VELOCITY (m/s)	SHEAR VELOCITY (m/s)	CHARACTERISTIC COMPRESSIONAL IMPEDANCE (10 ⁶ mks Rayls)	CHARACTERISTIC SHEAR IMPEDANCE (10 ⁶ mks Rayls)	POISSON'S RATIO	YOUNG'S MODULUS (kbar)	BULK MODULUS (kbar)	SHEAR MODULUS (kbar)
10+21 - 7+46	2652± 76	1381± 30	5.04±0.20	2.62±0.09	0.31±0.02	95.2±8.2	85.3±11.2	36.2±1.9
7+46 - 10+21	2615± 85	1478± 94	4.97±0.21	2.81±0.19	0.27±0.05	105.1±13.2	74.6±18.3	41.5±5.4

^{1/} meters = 0.3048 x feet



ACOUSTIC PARAMETERS

(Based on an assumed rock specific gravity of 1.90±0.05)

INTERVAL (feet) $\frac{1}{2}$	COMPRESSIONAL VELOCITY (m/s)	SHEAR VELOCITY (m/s)	CHARACTERISTIC COMPRESSIONAL IMPEDANCE (10 ⁶ mks Rayls)	CHARACTERISTIC SHEAR IMPEDANCE (10 ⁶ mks Rayls)	POISSON'S RATIO	YOUNG'S MODULUS (kbar)	BULK MODULUS (kbar)	SHEAR MODULUS (kbar)
25+74 - 22+67	2542±37	1259±15	4.83±0.14	2.39±0.07	0.34±0.01	80.5±4.0	82.6±5.8	30.1±1.1
22+67 - 25+74	2538±43	1344±18	4.92±0.15	2.55±0.08	0.32±0.01	90.3±4.9	81.5±6.5	34.3±1.3

$\frac{1}{2}$ meters = 0.3048 x feet

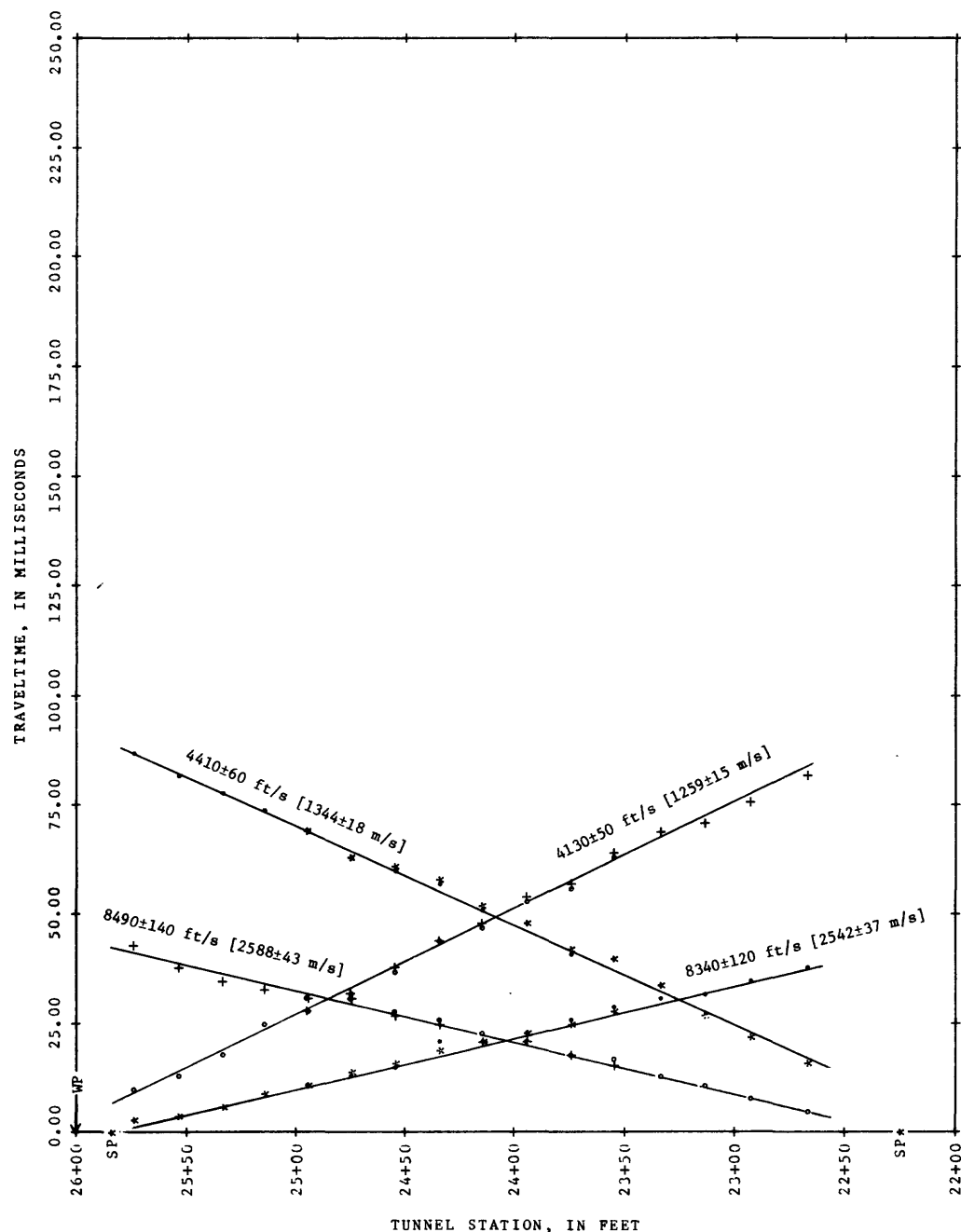


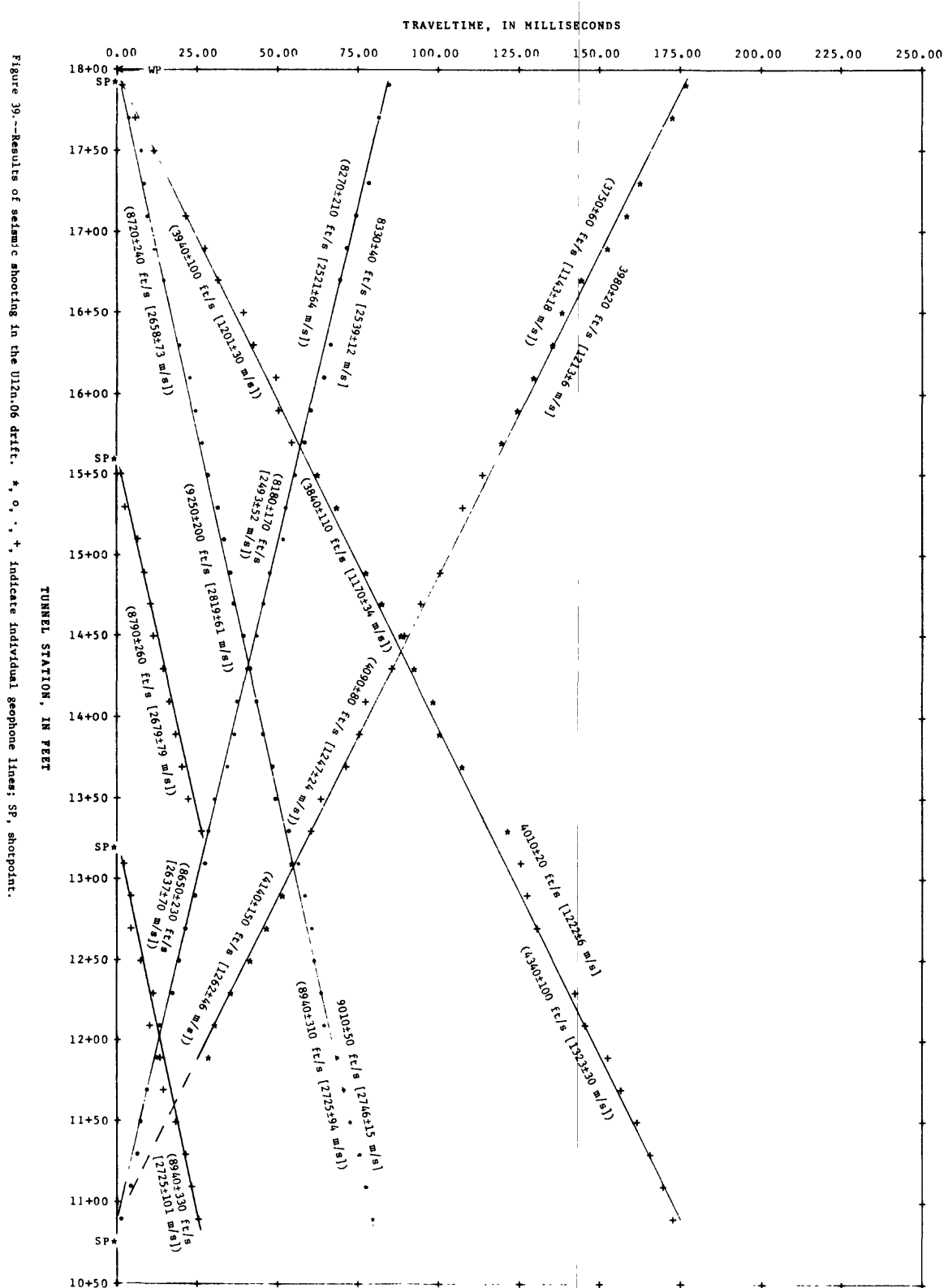
Figure 38.--Results of seismic shooting in the U12n.05 drift. *, °, ·, + indicate individual geophone lines; SP, shotpoint.

ACOUSTIC PARAMETERS

(Based on an assumed rock specific gravity of 1.90±0.05)

INTERVAL (feet) $\frac{1}{2}$	COMPRESSIONAL VELOCITY (m/s)	SHEAR VELOCITY (m/s)	CHARACTERISTIC COMPRESSIONAL IMPEDANCE (10 ⁶ mks Ravls)	CHARACTERISTIC SHEAR IMPEDANCE (10 ⁶ mks Ravls)	POISSON'S RATIO	YOUNG'S MODULUS (kbar)	BULK MODULUS (kbar)	SHEAR MODULUS (kbar)
17+90 - 10+90	2746±15	1222±6	5.22±0.14	2.32±0.06	0.38±0.00	78.1±2.5	105.5±3.9	28.4±0.8
10+90 - 17+90	2539±12	1213±6	4.82±0.13	2.30±0.06	0.35±0.00	75.6±2.3	85.2±3.0	28.0±0.8

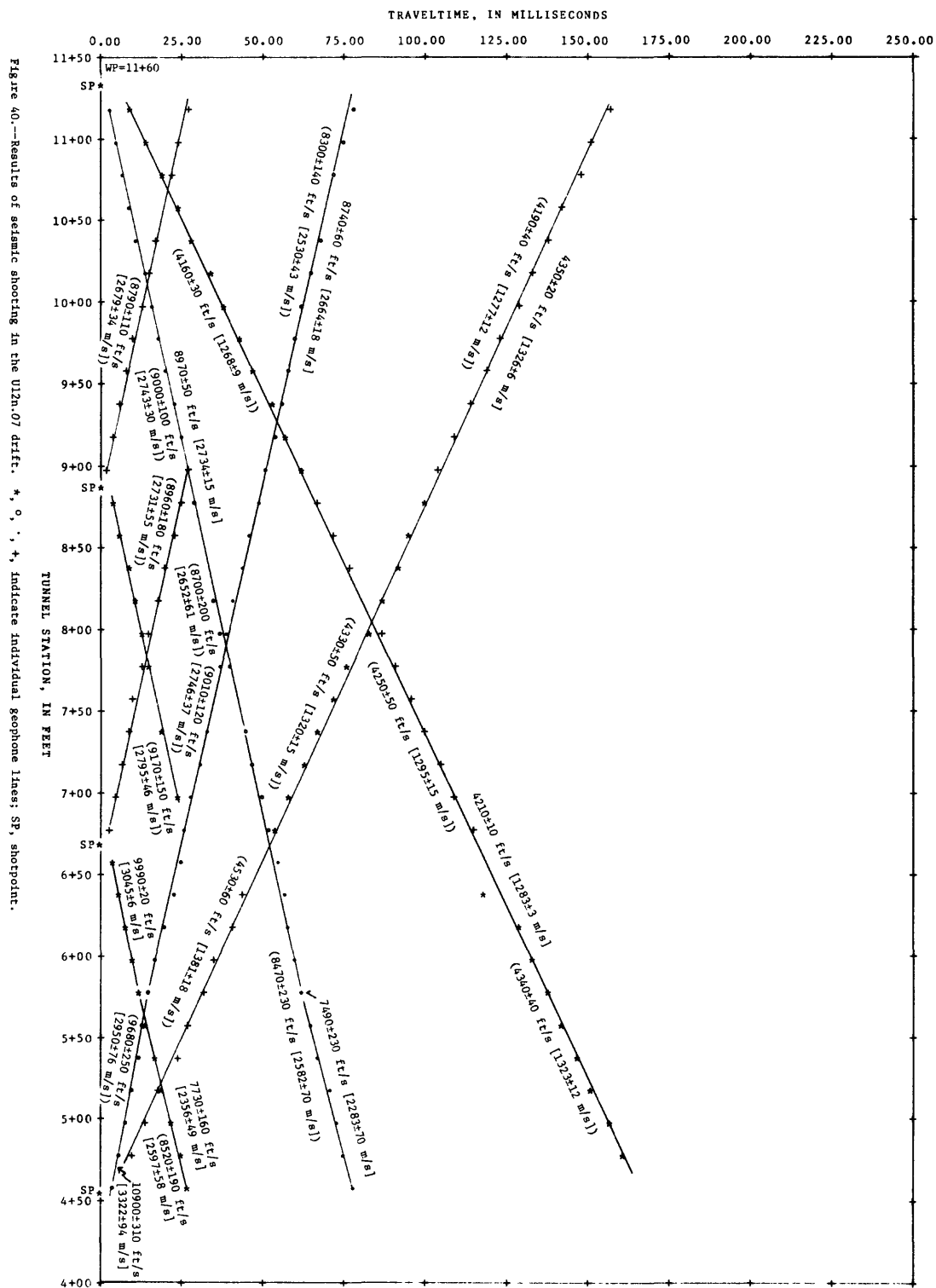
$\frac{1}{2}$ meters = 0.3048 x feet



(Based on an assumed rock specific gravity of 2.90±0.05)

INTERVAL (feet) ^{1/2}	COMPRESSIONAL	CHARACTERISTIC		COMPRESSIONAL	CHARACTERISTIC	POISSON'S	YOUNG'S	BULK	SHEAR
	VELOCITY	SHEAR	IMPEDANCE	SHEAR	IMPEDANCE	RATIO	MODULUS	MODULUS	MODULUS
	(m/s)	VELOCITY	(10 ⁶ mks Rayls)	(10 ⁶ mks Rayls)			(kbar)	(kbar)	(kbar)
4+58 - 5+73	3316± 94	1326± 6	6.30±0.24	2.52±0.07	0.40±0.01	93.8±7.7	164.4±17.6	33.4±0.9	
5+78 - 11+13	2664± 18	1326± 6	5.06±0.14	2.52±0.07	0.34±0.00	89.2±2.9	90.3±3.6	33.4±0.9	
11+18 - 5+73	2734± 15	1283± 3	5.19±0.14	2.44±0.06	0.36±0.00	85.0±2.6	100.3±3.4	31.3±0.8	
5+78 - 4+53	2283± 70	1283± 3	4.34±0.18	2.44±0.06	0.27±0.02	79.4±6.4	57.3±6.9	31.3±0.8	

1/ meters = 0.3048 x feet



(Based on an assumed rock specific gravity of 1.90±0.05)

INTERVAL (feet) ^{1/}	COMPRESSIONAL VELOCITY (m/s)	SHEAR VELOCITY (m/s)	CHARACTERISTIC COMPRESSIONAL IMPEDANCE (10 ⁶ mks Ravis)	CHARACTERISTIC SHEAR IMPEDANCE (10 ⁶ mks Rayls)	POISSON'S RATIO	YOUNG'S MODULUS (kbar)	BULK MODULUS (kbar)	SHEAR MODULUS (kbar)
17+34 - 14+14	2399± 34	1222± 12	4.56±0.14	2.32±0.07	0.32±0.01	75.2±3.6	71.5±4.8	28.4±0.9
14+14 - 10+31	2679± 52	1378± 15	5.09±0.17	2.62±0.07	0.32±0.01	95.2±5.6	88.3±7.5	36.1±1.2
10+31 - 14+34	2682± 21	1356± 9	5.10±0.14	2.58±0.07	0.33±0.00	92.9±3.3	90.1±4.1	35.0±1.0
14+34 - 17+34	2405± 43	1213± 15	4.57±0.15	2.30±0.07	0.33±0.01	74.3±4.2	72.6±5.9	28.0±0.9

1/ meters = 0.3048 x feet

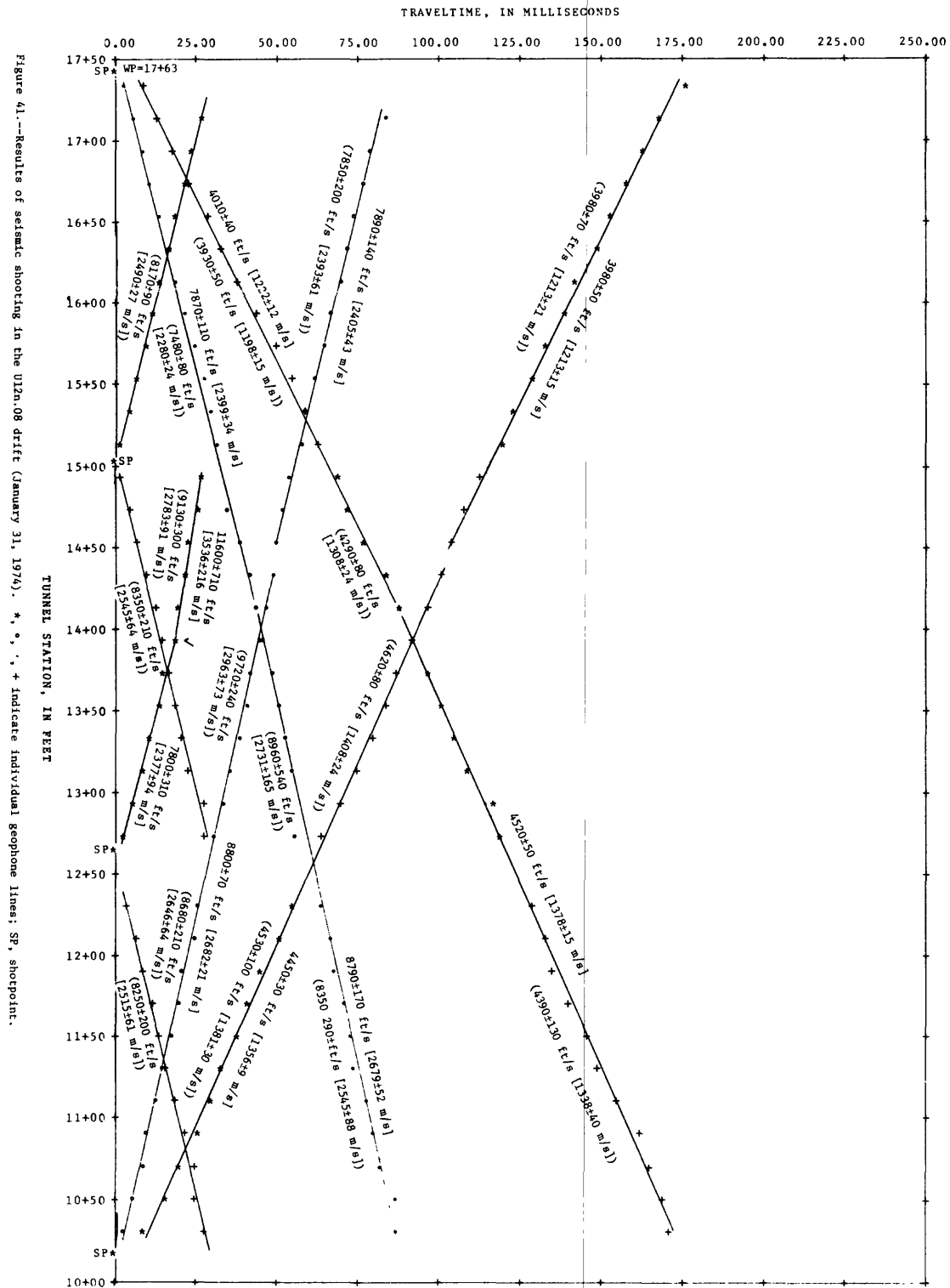
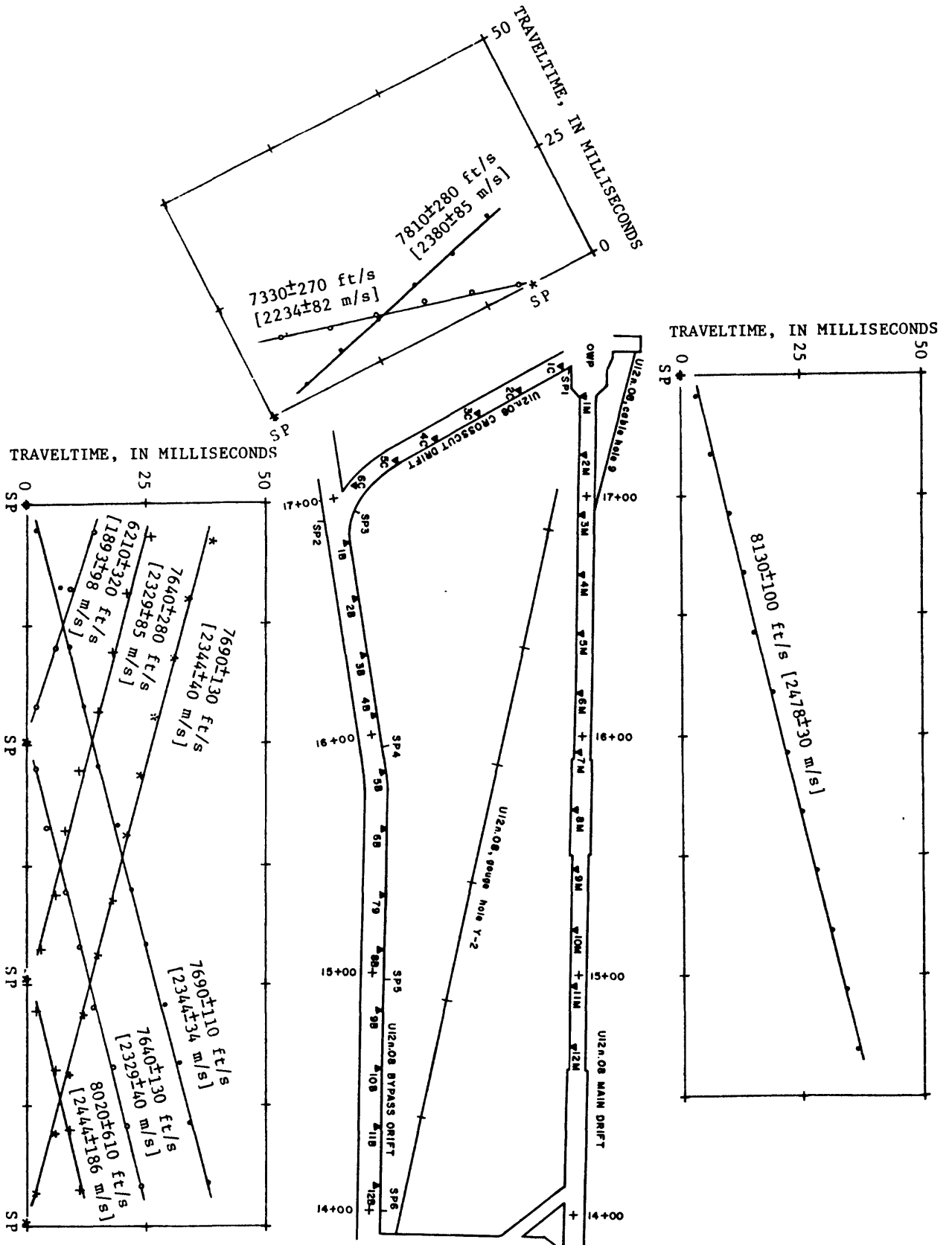


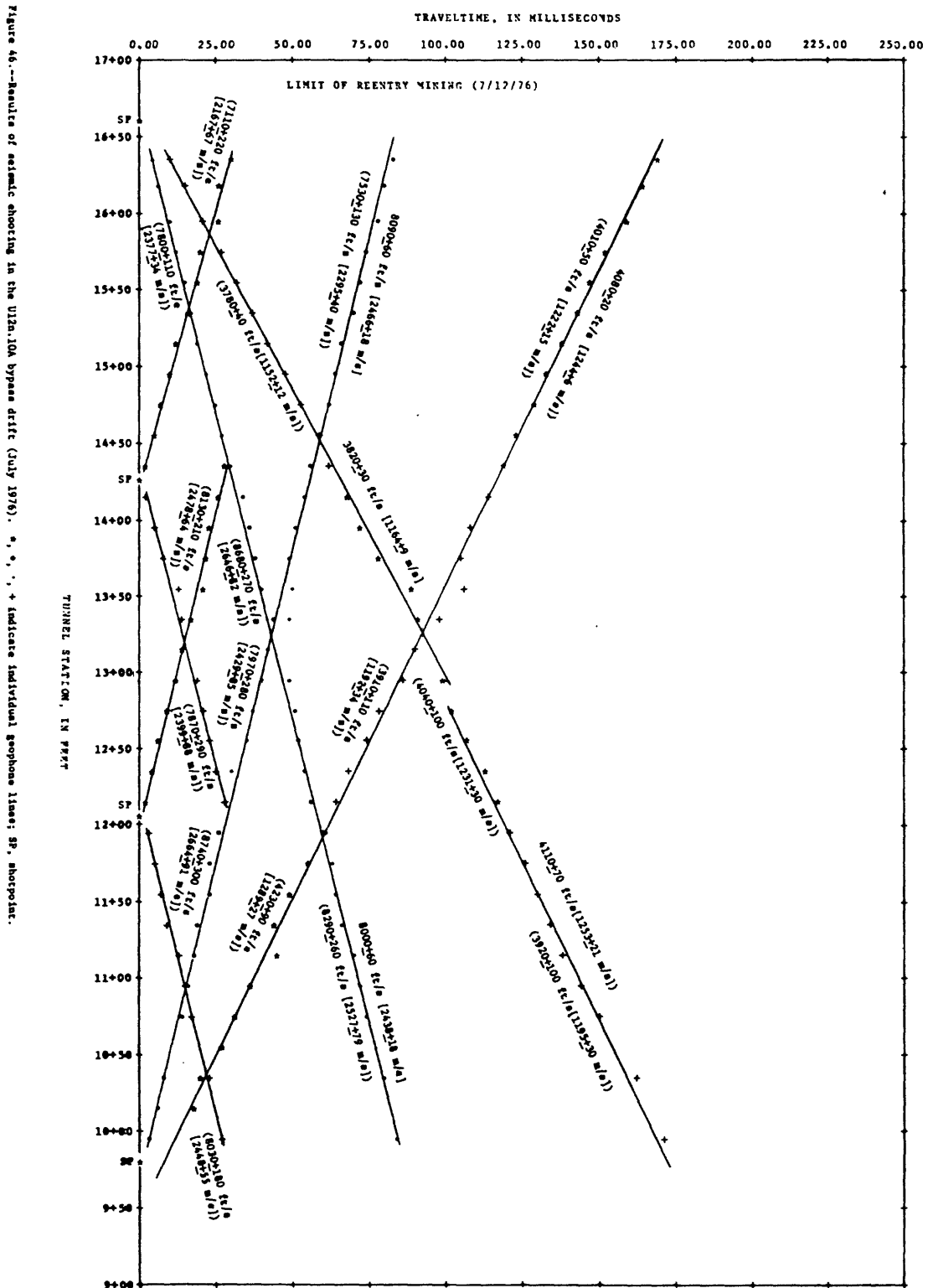
Figure 42.--Results of additional seismic shooting in the U12n.08 drift (February 16, 1974).
 *, o, +, indicate individual geophone lines; SP, shotpoint; A3B, location and
 number of geophone.



(based on an assumed rock specific gravity of 1.90 ± 0.05)

INTERVAL (feet) $\frac{1}{2}$	COMPRESSIONAL VELOCITY (u/s)	SOLAR VELOCITY (u/s)	CHARACTERISTIC COMPRESSIONAL IMPEDANCE (10^6 nks Rayls)	CHARACTERISTIC SOLAR IMPEDANCE (10^6 nks Rayls)	POISSON'S RATIO	VOLUME'S MODULUS (kbar)	SOLAR MODULUS (kbar)	SOLAR MODULUS (kbar)
16+35 - 12+95	2438 \pm 10	1164 \pm 9	4.63 \pm 0.13	2.21 \pm 0.06	0.35 \pm 0.00	69.7 \pm 2.5	72.6 \pm 3.6	25.3 \pm 7.8
12+95 - 9+95	2438 \pm 10	1253 \pm 21	4.63 \pm 0.13	2.38 \pm 0.07	0.32 \pm 0.01	78.8 \pm 3.4	73.2 \pm 4.9	29.3 \pm 1.3
9+95 - 16+33	2466 \pm 13	1244 \pm 6	4.69 \pm 0.13	2.36 \pm 0.06	0.33 \pm 0.00	70.1 \pm 2.6	76.3 \pm 3.1	29.4 \pm 0.8

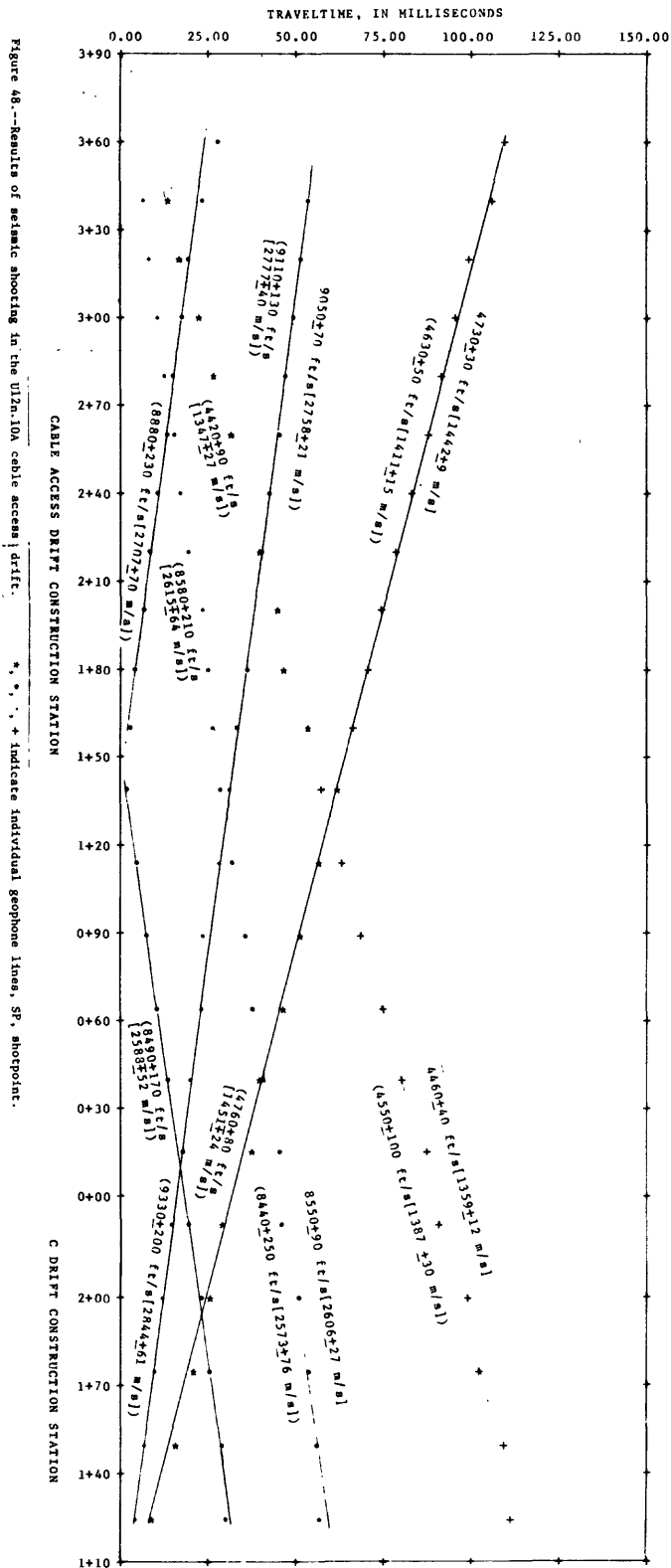
1/ meters = 0.3048 x feet



ACOUSTIC PARAMETERS
(Based on an assumed rock specific gravity of 1.90±0.05)

INTERVAL (feet) $\frac{1}{2}$	COMPRESSIONAL VELOCITY (m/s)	SHEAR VELOCITY (m/s)	CHARACTERISTIC COMPRESSIOIAL IMPEDANCE (10^6 mks Ravis)	CHARACTERISTIC SHEAR IMPEDANCE (10^6 mks Ravis)	POISSON'S RATIO	YOUNG'S MODULUS (kbar)	BULK MODULUS (kbar)	SIFAR MODULUS (kbar)
1+25 - 3+60	2758± 21	1442± 9	5.24±0.14	2.74±0.07	0.31±0.01	103.7±3.6	91.8±4.0	39.5±1.2
3+60 - 1+25	2606± 27	1359± 12	4.95±0.14	2.58±0.07	0.31±0.01	92.2±3.7	82.2±4.5	35.1±1.1

$\frac{1}{2}$ meters = 0.3048 x feet

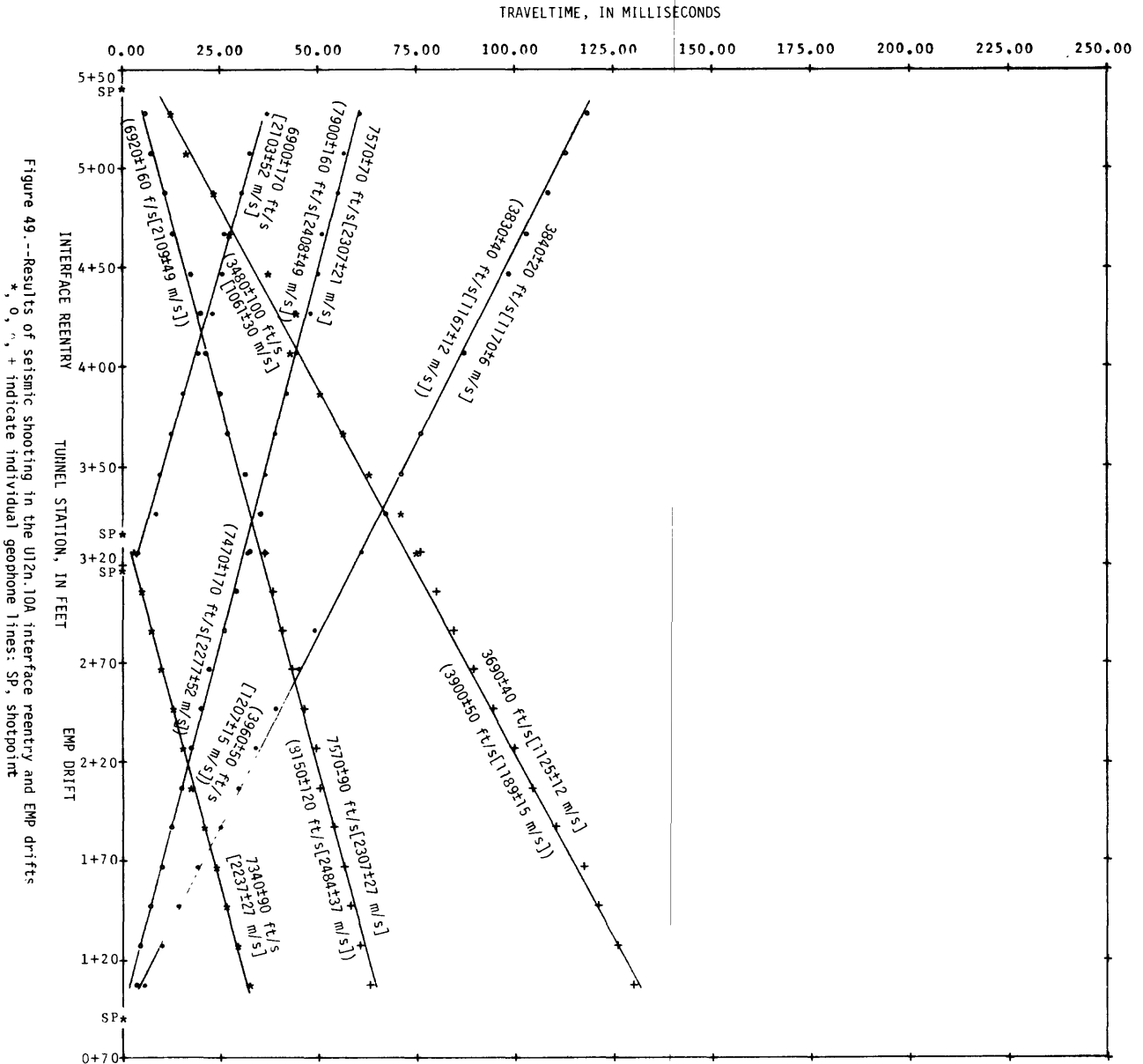


ACOUSTIC PARAMETERS

(Based on an assumed rock specific gravity of 1.90±0.05)

INTERVAL (feet) 1/	COMPRESSIONAL VELOCITY (m/s)	SHEAR VELOCITY (m/s)	CHARACTERISTIC COMPRESSIONAL IMPEDANCE (10 ⁶ nks Ravls)	CHARACTERISTIC SHEAR IMPEDANCE (10 ⁶ mks Ravls)	POISSON'S RATIO	YOUNG'S MODULUS (kbar)	BULK MODULUS (kbar)	SHEAR MODULUS (kbar)
LONG LINES								
1+07EMP-5+27IR	2307± 21	1170± 6	4.38±0.12	2.22±0.06	0.33±0.00	69.0±2.5	66.4±3.1	26.0±0.7
5+27IR -1+07EMP	2307± 27	1125± 12	4.38±0.13	2.14±0.06	0.34±0.01	64.6±2.9	69.1±4.3	24.0±0.8
SHORT LINES								
1+07EMP-3+26EMP	2277± 52	1207± 15	4.33±0.15	2.29±0.07	0.30±0.01	72.2±4.8	61.6±6.1	27.7±1.0
5+27IR -3+26EMP	2109± 49	1061± 30	4.01±0.14	2.02±0.08	0.33±0.02	56.9±4.6	56.2±7.2	21.4±1.4

1/ meters = 0.3048 x feet



ACOUSTIC PARAMETERS

(Based on an assumed rock specific gravity of 1.90 ± 0.05)

INTERVAL (feet) $\frac{1}{2}$	COMPRESSIONAL VELOCITY (m/s)	SHEAR VELOCITY (m/s)	CHARACTERISTIC COMPRESSIONAL IMPEDANCE (106 mks Rayls)	CHARACTERISTIC SHEAR IMPEDANCE (106 mks Rayls)	POISSON'S RATIO	YOUNG'S MODULUS (kbar)	BULK MODULUS (kbar)	SHEAR MODULUS (kbar)
1+51 - 3+51	2277 ± 76	1189 ± 18	4.33 ± 0.18	2.26 ± 0.07	0.31 ± 0.02	70.4 ± 6.6	62.7 ± 8.6	26.8 ± 1.1

$\frac{1}{2}$ meters = 0.3048 x feet

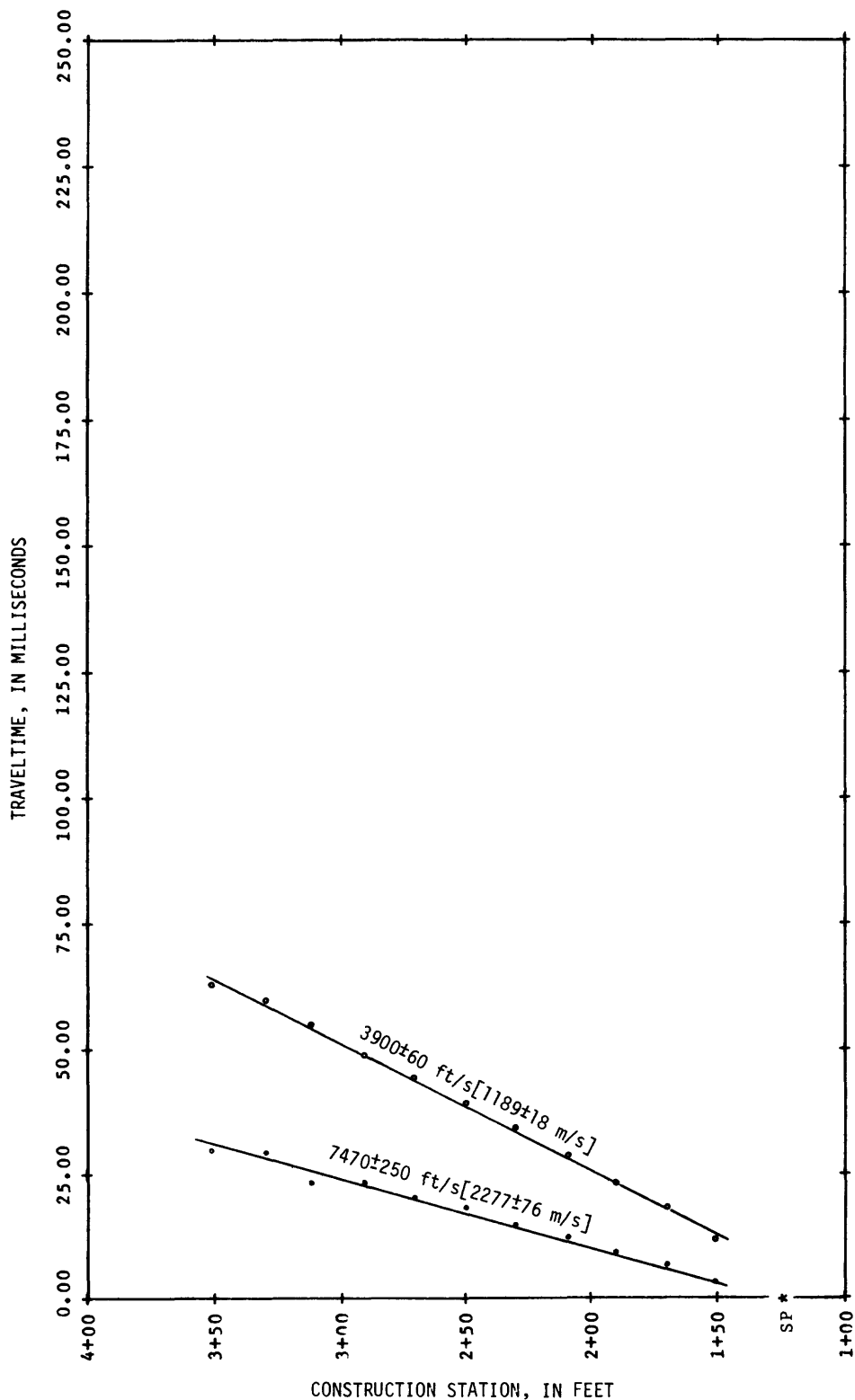


Figure 50.--Results of seismic shooting in the U12n.10A G drift.
*, o, +, ° indicate individual geophone lines; SP, shotpoint.

(Based on an assumed rock specific gravity of 1.90±0.05)

INTERVAL (feet) ^{1/}	COMPRESSIONAL VELOCITY (m/s)	SHEAR VELOCITY (m/s)	CHARACTERISTIC COMPRESSIONAL IMPEDANCE (10 ⁶ mks Rayls)	CHARACTERISTIC SHEAR IMPEDANCE (10 ⁶ mks Rayls)	POISSON'S RATIO	YOUNG'S MODULUS (kbar)	BULK MODULUS (kbar)	SOLAR MODULUS (kbar)
0+55 ~ 2+55	2603± 27	1213± 21	4.95±0.14	2.30±0.07	0.36±0.01	76.1±3.7	91.5±6.5	28.0±1.2
2+55 ~ 4+55	2603± 27	1335± 6	4.95±0.14	2.54±0.07	0.32±0.01	89.5±3.4	83.6±4.1	31.9±0.9
2+75 ~ 0+55	2508± 40	1201± 18	4.75±0.13	2.28±0.07	0.35±0.01	74.0±4.1	82.4±6.6	27.4±1.1
2+95 ~ 4+55	2707± 35	1298± 12	5.14±0.17	2.47±0.07	0.35±0.01	86.5±5.3	96.5±8.2	32.0±1.0
4+55 ~ 0+55	2585± 27	1262± 6	4.91±0.14	2.40±0.06	0.34±0.01	81.3±3.2	86.6±4.3	30.3±0.8

1/ meters = 0.3048 x feet

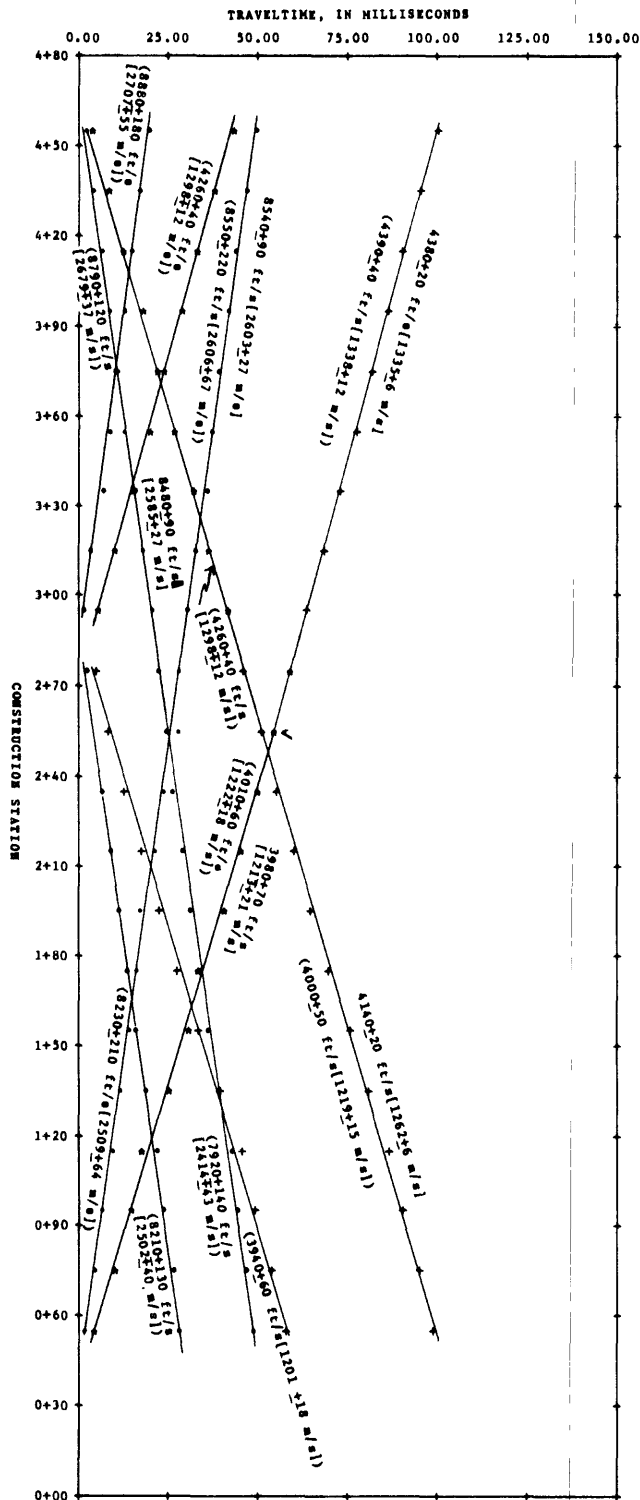


Figure 51.--Results of seismic shooting in the Ulna-10A A-B vicinity (Boeing) drift. *, °, ', + indicate individual geophone lines; SP, shotpoint.

ACOUSTIC PARAMETERS

(Based on an assumed rock specific gravity of 1.90 ± 0.05)

INTERVAL (feet) 1/	COMPRESSIONAL VELOCITY (m/s)	SHEAR VELOCITY (m/s)	CHARACTERISTIC COMPRESSIONAL IMPEDANCE (10 ⁶ mks Rayls)	CHARACTERISTIC SHEAR IMPEDANCE (10 ⁶ mks Rayls)	POISSON'S RATIO	YOUNG'S MODULUS (kbar)	BULK MODULUS (kbar)	SHEAR MODULUS (kbar)
2+19 - 3+92	1911 ± 49	1338 ± 61	3.63 ± 0.13	2.54 ± 0.13	0.02 ± 0.10	69.3 ± 4.0	24.0 ± 5.1	34.0 ± 3.2
3+92 - 3+18	2679 ± 104	1042 ± 55	5.09 ± 0.24	1.98 ± 0.12	0.41 ± 0.01	58.3 ± 8.5	109.0 ± 22.1	20.6 ± 2.2
3+18 - 2+19	1664 ± 271	1045 ± 43	2.16 ± 0.52	1.90 ± 0.10	0.17 ± 0.18	48.8 ± 19.3	94.9 ± 16.7	20.8 ± 1.9

1/ meters = 0.3048 x feet

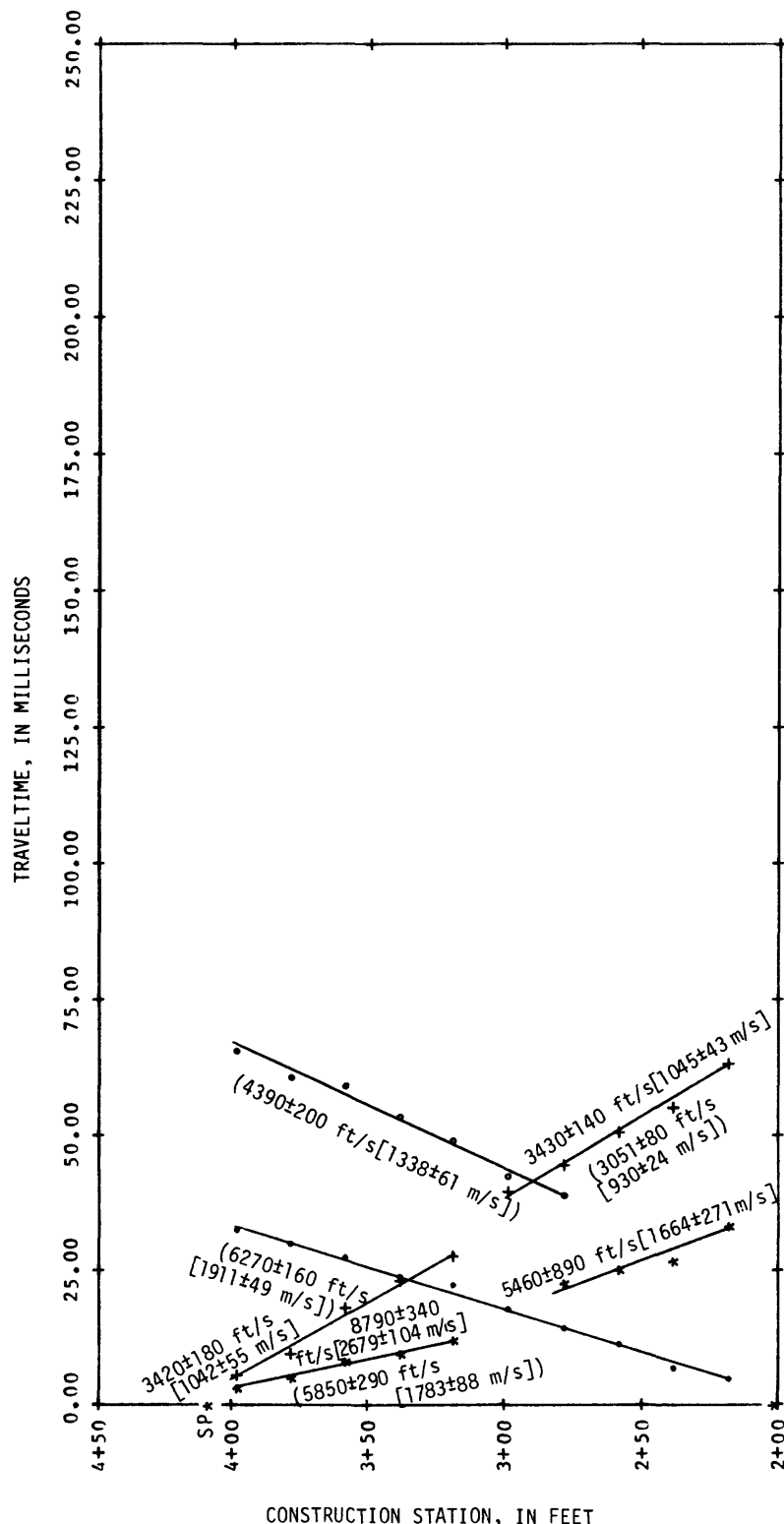


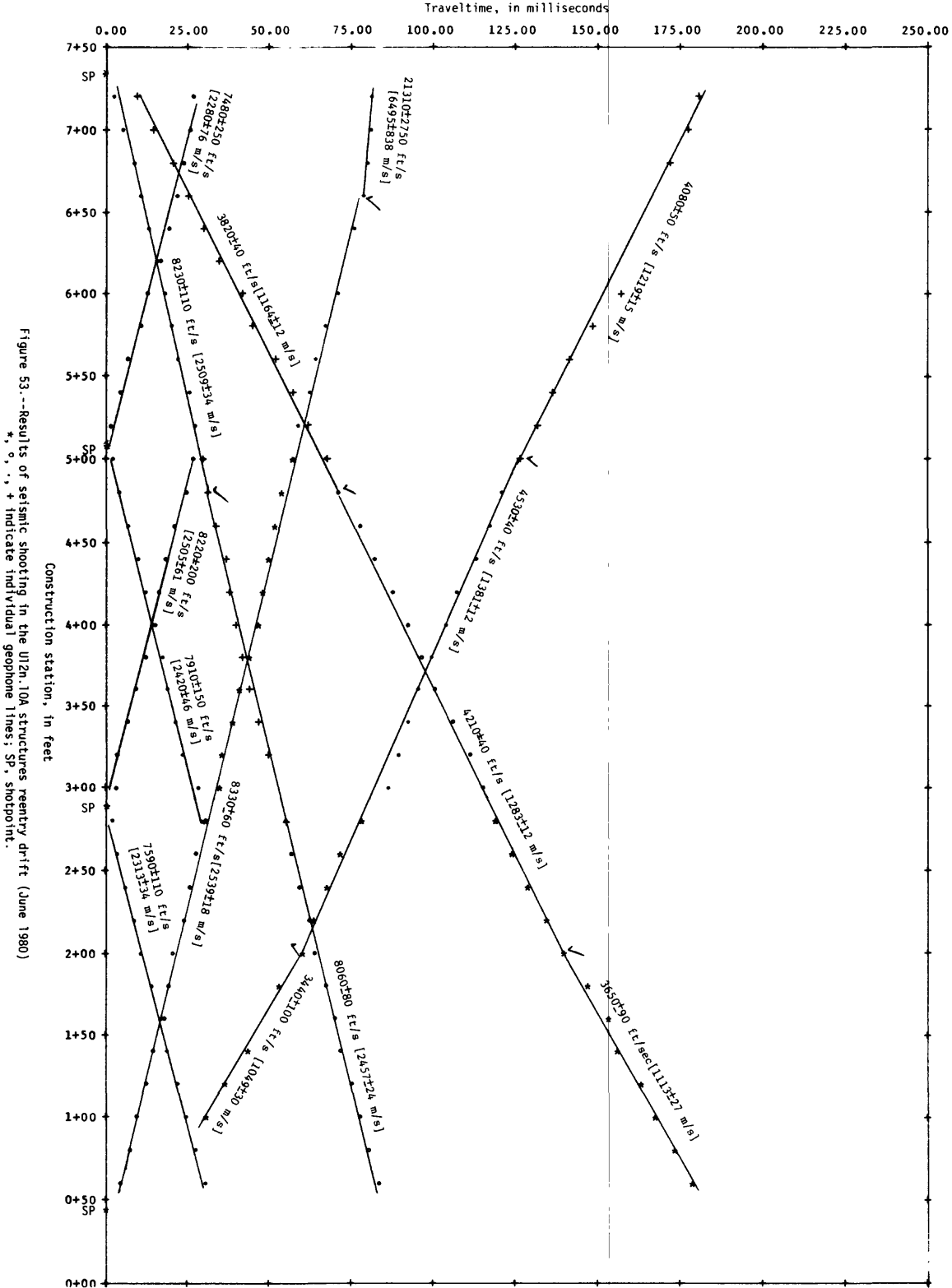
Figure 52.--Results of seismic shooting in the U12n.10A interface drift, post-Mighty Epic. *, °, ·, + indicate individual geophone lines; SP, shotpoint.

ACOUSTIC PARAMETERS

(Based on an assumed rock specific gravity of 1.90±0.05)

INTERVAL (feet) $\frac{1}{2}$	COMPRESSIONAL VELOCITY (m/s)	SHEAR VELOCITY (m/s)	CHARACTERISTIC COMPRESSIONAL IMPEDANCE (10^6 mks Ravis)	CHARACTERISTIC SHEAR IMPEDANCE (10^6 mks Ravis)	POISSON'S RATIO	YOUNG'S MODULUS (kbar)	BULK MODULUS (kbar)	SHEAR MODULUS (kbar)
0+60 - 2+00	2499	1082	4.75	2.06	0.38	61.6	89.0	22.2
2+00 - 4+80	2499	1332	4.75	2.53	.30	87.8	73.7	33.7
4+80 - 7+20	2524	1192	4.80	2.26	.36	73.2	85.0	27.0

$\frac{1}{2}$ meters = 0.3048 x feet



Traveltime, in milliseconds

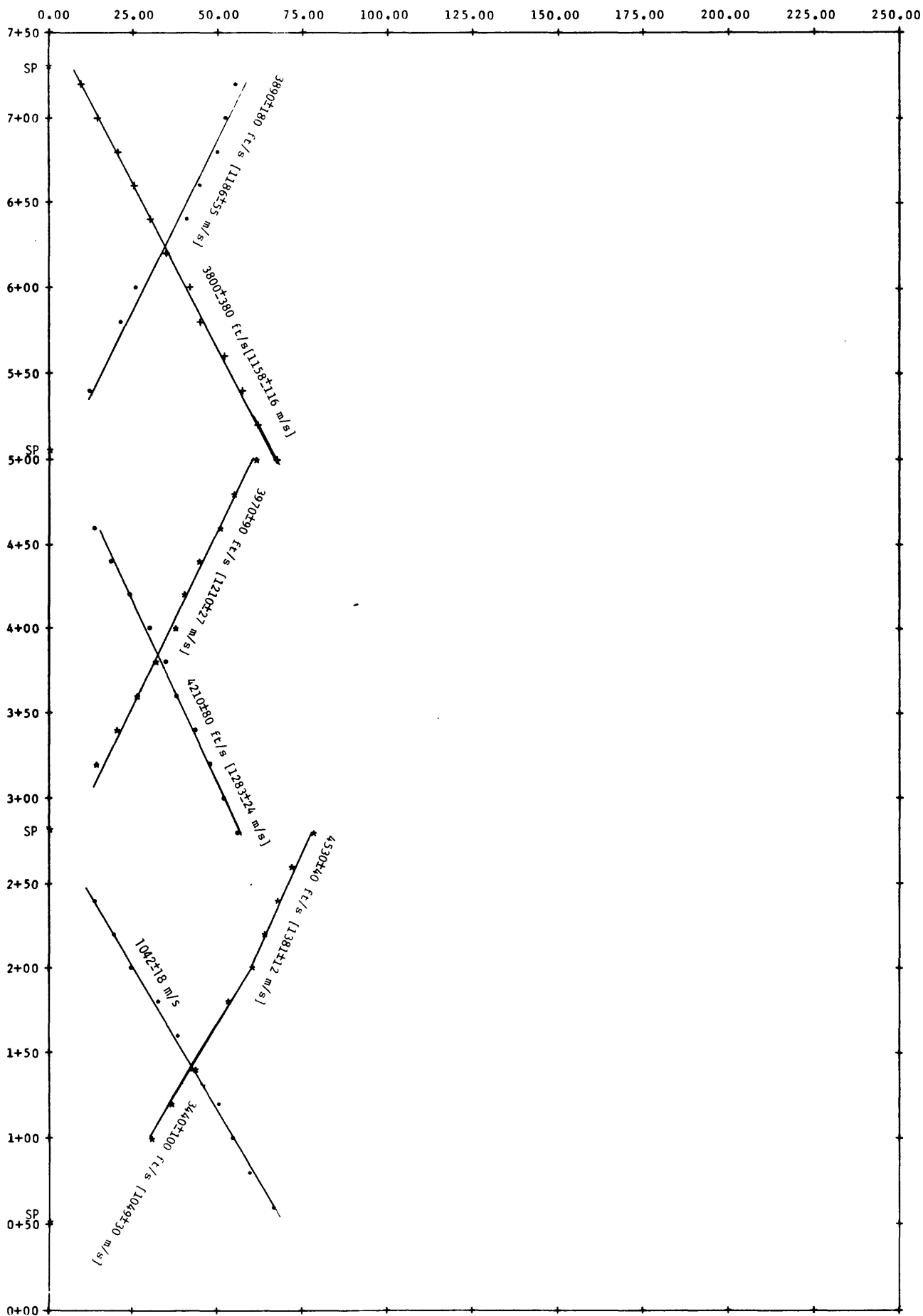


Figure 54.--Results of shear-wave recording in the U12n.10A structures reentry drift (June 1980)
*, ., + indicate individual geophone lines; SP, shotpoint.

ACOUSTIC PARAMETERS

(Based on an assumed rock specific gravity of 1.90±0.05)

INTERVAL (feet) $\frac{1}{2}$	COMPRESSIONAL VELOCITY (m/s)	SHEAR VELOCITY (m/s)	CHARACTERISTIC COMPRESSIONAL IMPEDANCE (10^6 mks Rayls)	CHARACTERISTIC SHEAR IMPEDANCE (10^6 mks Rayls)	POISSON'S RATIO	YOUNG'S MODULUS (kbar)	BULK MODULUS (kbar)	SHEAR MODULUS (kbar)
0+52 - 1+42	2283	972	4.34	1.85	0.39	49.9	75.1	18.0
1+42 - 2+72	2283	1280	4.34	2.43	.27	79.1	57.5	31.1

$\frac{1}{2}$ meters = 0.3048 x feet

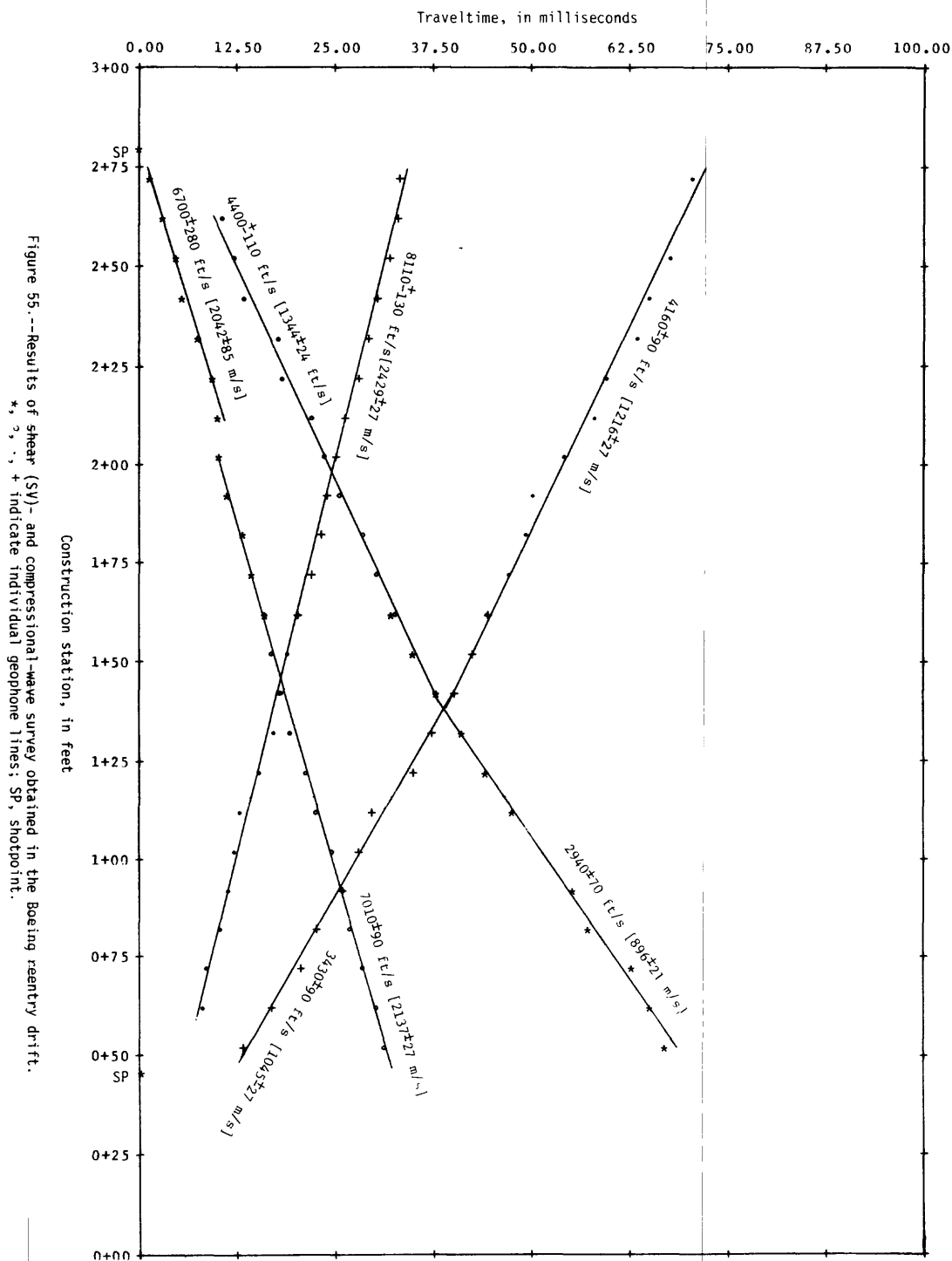
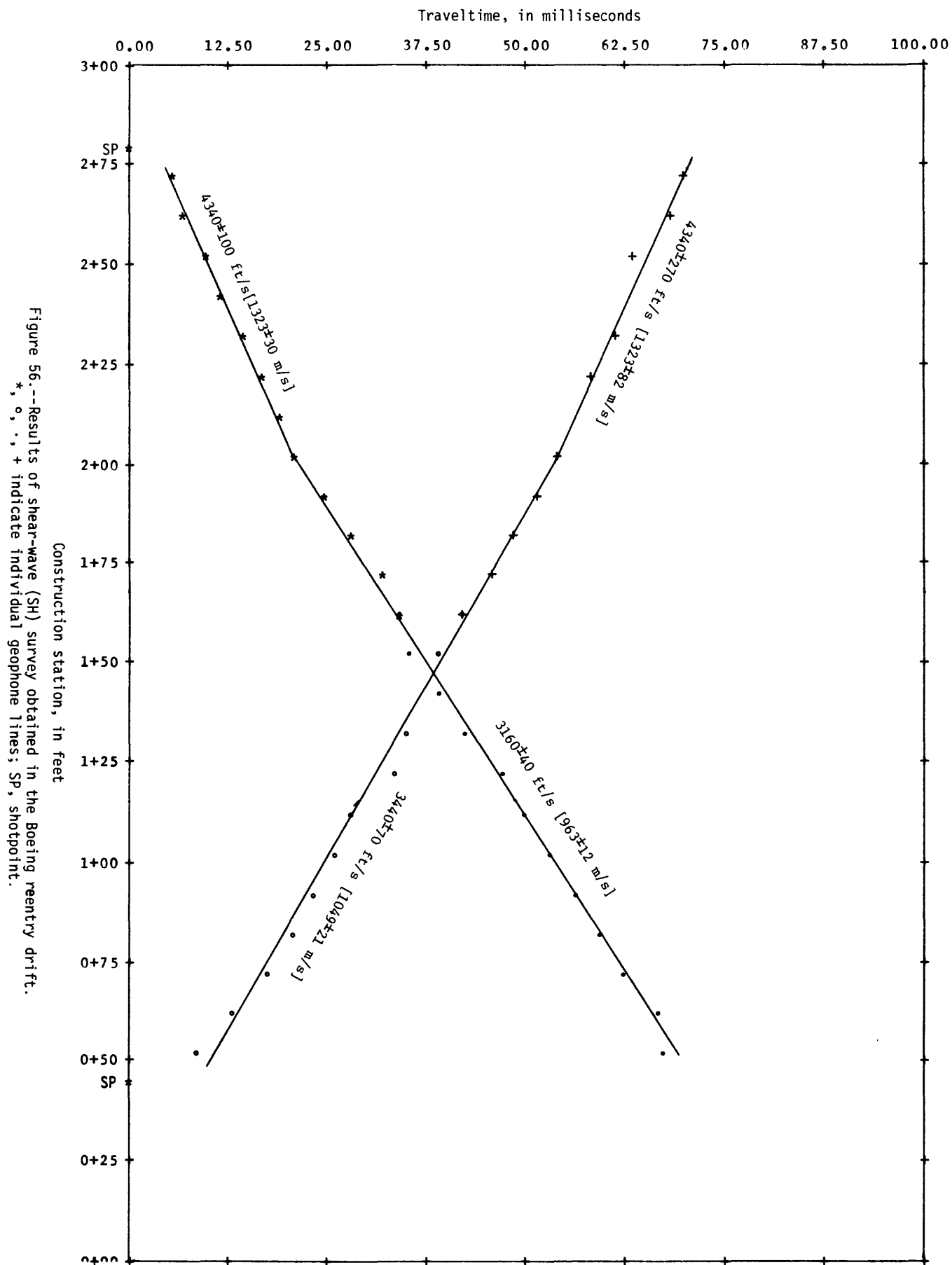


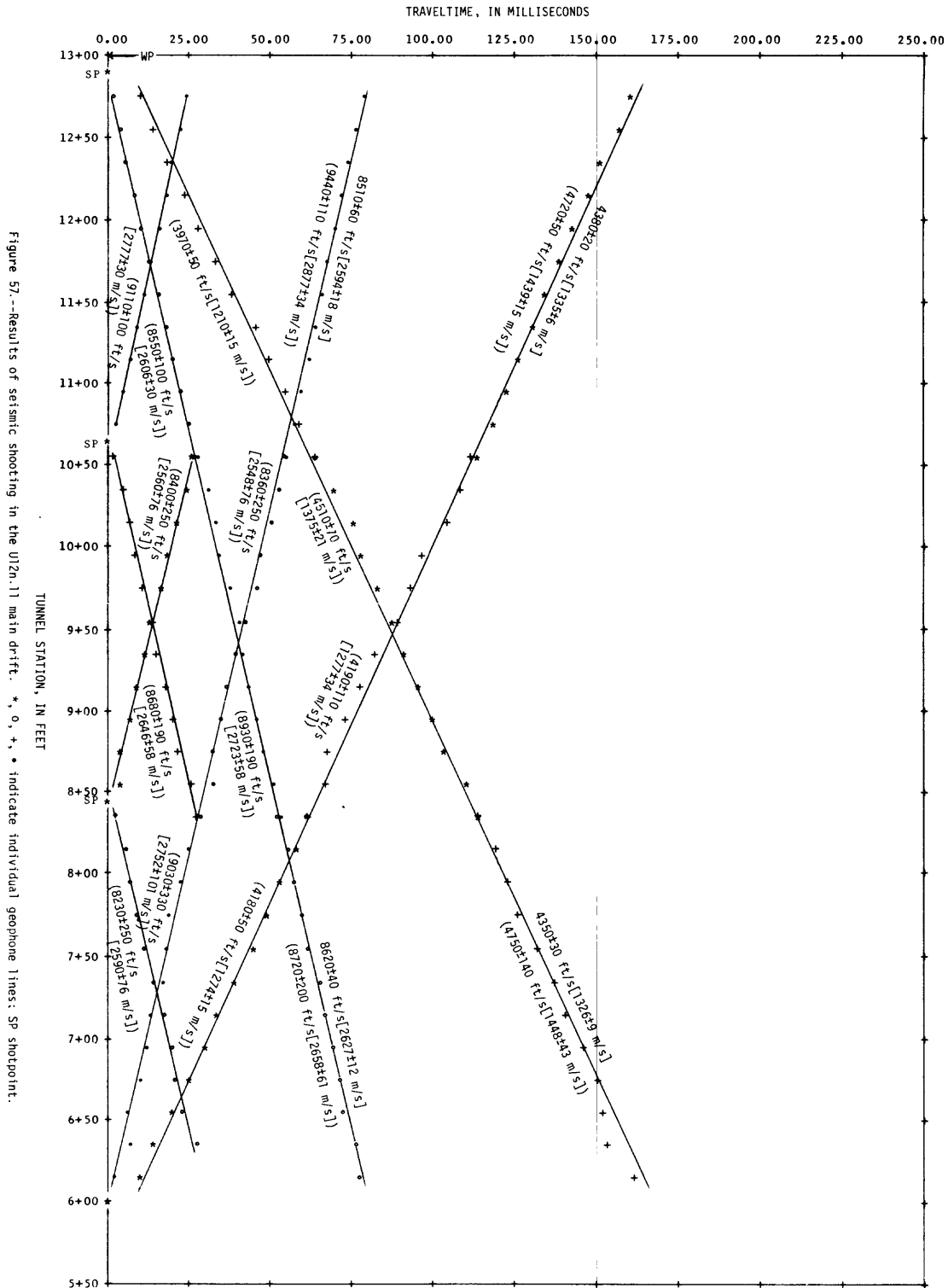
Figure 55.--Results of shear (SV) and compressional-wave survey obtained in the Boeing reentry drift.
*, 1, 2, 3 indicate individual geophone lines; SP, shotpoint.

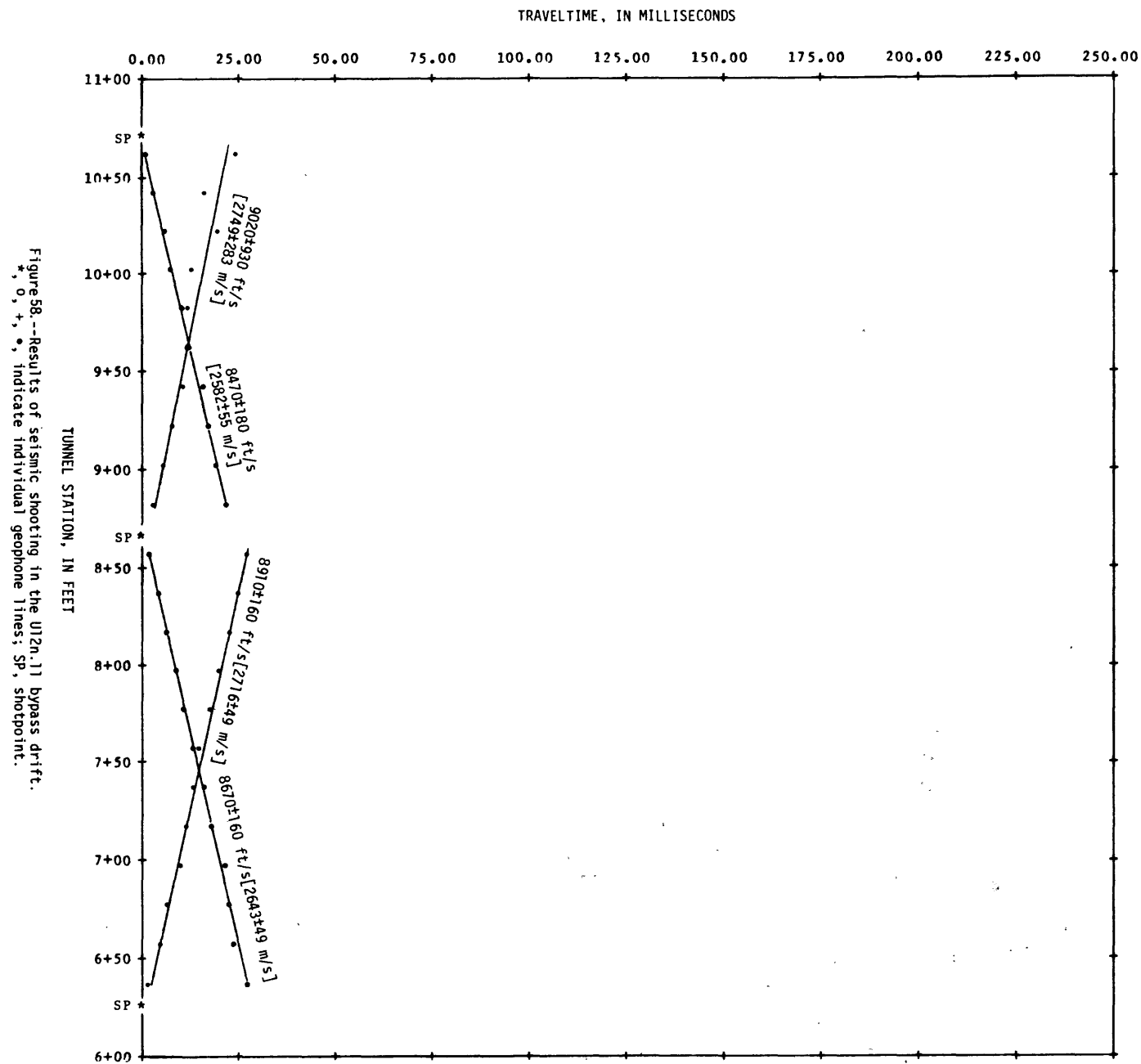


ACOUSTIC PARAMETERS
(Based on an assumed rock specific gravity of 1.90 ± 0.05)

INTERVAL (feet) $\frac{1}{2}$	COMPRESSIONAL VELOCITY (m/s)	SHEAR VELOCITY (m/s)	CHARACTERISTIC COMPRESSIONAL IMPEDANCE (10^6 mks Rayls)	CHARACTERISTIC SHEAR IMPEDANCE (10^6 mks Rayls)	POISSON'S RATIO	YOUNG'S MODULUS (kbar)	BULK MODULUS (kbar)	SHEAR MODULUS (kbar)
12+75 - 6+15	2627 \pm 12	1326 \pm 9	4.99 \pm 0.13	2.52 \pm 0.07	0.33 \pm 0.00	88.8 \pm 2.8	86.6 \pm 3.3	33.4 \pm 1.0
6+15 - 12+75	2594 \pm 18	1335 \pm 6	4.92 \pm 0.13	2.54 \pm 0.07	0.32 \pm 0.00	89.4 \pm 2.9	82.7 \pm 3.3	33.9 \pm 0.9
WP to 128m 12+75 - 8+75	2569 \pm 24	1268 \pm 12	4.88 \pm 0.14	2.41 \pm 0.07	0.34 \pm 0.01	81.8 \pm 3.2	84.7 \pm 4.5	30.5 \pm 1.0

$\frac{1}{2}$ meters = 0.3048 x feet





REFERENCES CITED

- Brethauer, G. E., Magner, J. E., and Miller, D. R., 1980, Statistical evaluation of physical properties in Area 12, Nevada Test Site, Using the USGS/DNA storage and retrieval system: U.S. Geological Survey Report USGS-474-309, 96 p.; available only from U.S. Department of Commerce, National Technical Information Service, Springfield, VA 22161.
- Carroll, R. D., and Cunningham, M. J., 1980, Geophysical investigations in deep horizontal holes drilled ahead of tunnelling: International Journal of Rock Mechanics and Mining Sciences, v. 17, no. 2, p. 89-107.
- Carroll, R. D., 1982, Seismic velocity and postshot properties in and near chimneys, in Proceedings of Monterey containment symposium, Monterey, Calif., August 26-28, 1981: Los Alamos National Laboratory Report LA-9211-C (in press).
- Cook, J. C., 1965, Seismic mapping of underground cavities using reflection amplitudes: Geophysics, v. 30, p. 527-538.
- Dobrin, Milton B., 1976, Introduction to geophysical prospecting (3d ed.): New York, McGraw-Hill, 630 p.
- Ege, J. R., Carroll, R. D., Magner, J. E., and Cunningham, D. R., 1980a, U.S. Geological Survey investigations in the U12n.03 drift, Rainier Mesa, Area 12, Nevada Test Site: U.S. Geological Survey Open-File Report 80-1074, 29 p.
- Ege, J. R., Danilchik, Walter, and Feazel, C. T., 1980b, Geology of the U12n.02 (Midi Mist) drift, and postshot observations, Rainier Mesa, Area 12, Nevada Test Site: U.S. Geological Survey Report USGS-474-229, 21 p.; available only from U.S. Department of Commerce, National Technical Information Service, Springfield, VA 22161.
- Gibbons, A. B., Hinrichs, E. N., Hansen, W. R., and Lemke, R. W., 1963, Geology of the Rainier Mesa Quadrangle, Nye County, Nevada: U.S. Geological Survey Geologic Quadrangle Map GQ-215, scale 1:24,000.
- Hazlewood, R. M., 1961, Interim report on seismic velocities of the Oak Spring Formation, U12e and U12b tunnel systems, Nevada Test Site, Nye County, Nevada: U.S. Geological Survey Open-File Report TEI-795, 12 p.
- Maldonado, Florian, Steele, S. G., and Townsend, D. R., 1979, Supplementary lithologic logs of selected vertical drill holes in Area 12, Nevada Test Site: U.S. Geological Survey Report USGS-474-261, 61 p.; available only from U.S. Department of Commerce, National Technical Information Service, Springfield, VA 22161.
- Orkild, P. P., 1963, Geologic map of the Tippihah Spring Quadrangle, Nye County, Nevada: U.S. Geological Survey Geologic Quadrangle Map GQ-213, scale 1:24,000.
- Ostle, Bernard, 1960, Statistics in research: Iowa State University Press, 487 p.

Scott, J. H., and Cunningham, D. R., 1966, Seismic studies in the Red Hot and Deep Well cavities, Area 12, Nevada Test Site, Nevada: Unpublished data on file in Mercury, Nevada office of the U.S. Geological Survey.

U.S. Geological Survey, 1959, Geologic effects of the Rainier underground nuclear explosion: U.S. Geological Survey Open-File Report TEI-355.

____ 1978, U.S. Geological Survey investigations in connection with the Dining Car event, U12e.18 tunnel, Rainier Mesa, Nevada Test Site: U.S. Geological Survey Report USGS-474-246, 68 p.; available only from U.S. Department of Commerce, National Technical Information Service, Springfield, VA 22161.

____ 1979, U.S. Geological Survey investigations in connection with the Mighty Epic event, U12n.10 tunnel, Nevada Test Site: U.S. Geological Survey Report USGS-474-228, 191 p.; available only from U.S. Department of Commerce, National Technical Information Service, Springfield, VA 22161.

____ 1982, Geologic, geophysical, and in situ stress investigations in the vicinity of the Dining Car chimney, Dining Car/Hybla Gold tunnels, Nevada Test Site: U.S. Geological Survey Open-File Report 82-137, 121 p.